General Disclaimer

One or more of the Following Statements may affect this Document

- This document has been reproduced from the best copy furnished by the organizational source. It is being released in the interest of making available as much information as possible.

- This document may contain data, which exceeds the sheet parameters. It was furnished in this condition by the organizational source and is the best copy available.

- This document may contain tone-on-tone or color graphs, charts and/or pictures, which have been reproduced in black and white.

- This document is paginated as submitted by the original source.

- Portions of this document are not fully legible due to the historical nature of some of the material. However, it is the best reproduction available from the original submission.

NASA

Technical Memorandum 83816

Goddard Contributions to the La Jolla Workshop on Gamma-Ray Transients

AUGUST 1981

GODDARD CONTRIBUTIONS TO THE LA JOLLA WORKSHOP

ON GAMMA RAY TRANSIENTS

CONTENTS

GAMMA RAY LINES FROM SOLAR FLARES AND COSMIC TRANSIENTS

R. Ramaty
Laboratory for High Energy Astrophysics, NASA-Goddard
Space Flight Center, Greenbelt, MD 20771

R. E. Lingenfelter*
Center for Astrophysics and Space Sciences
University of California, San Diego, La Jolla, CA 92093
and
B. Kozlovsky**
Laboratory for High Energy Astrophysics, NASA-Goddard
Space Flight Center, Greenbelt, MD 20771

ABSTRACT

Gamma ray line emission processes in solar flares and cosmic transients are reviewed and implications of recent line observations are discussed. The gamma ray line emission from solar flares results from nuclear interactions of accelerated particles with the solar atmosphere. The observed line intensities give information on the total number and spectrum of particles accelerated in the flare, on the temperature and density in the interaction regions and on the time history of the interactions. Analysis of the line observations from the June 7, 1980, flare show that the number of protons accelerated in the flare exceeded the number observed in the interplanetary medium by a factor of ~100. The bulk of the accelerated protons, therefore, remained trapped in the solar atmosphere where they produced gamma ray line emission as they slowed down.

The gamma ray emission lines observed from gamma ray transients appear to result from both the annihilation of positrons produced in photon-photon interactions and from deexcitation of nuclear levels and capture of neutrons produced in nuclear interactions. The observed line intensity provides information on the temperature, density composition, magnetic field and redshift in the transient sources. Both the gravitational redshift and the iron enrichment implied by the gamma ray line observations strongly suggest that neutron stars are the source of the transients.

INTRODUCTION

Gamma ray lines are unique tracers of the high energy processes that dominate the physics of solar flares and cosmic transients. In solar flares the lines are produced by nuclear interactions of energetic protons and nuclei with the solar atmosphere. Similar interactions in high temperature plasmas may also produce gamma ray lines in cosmic transients. In addition, the extremely high photon densities, matter densities and magnetic fields expected in the sources of these cosmic transients should lead to gamma ray line production processes that have no counterparts in solar flares. Because of the high photon densities, photon-photon collisions can become a dominant line producing mechanism via e^+-e^- pair production. The high pair densities resulting from these interactions may also lead to pair degeneracy and to possible maser action. The ultra high magnetic fields produce cyclotron emission and absorption lines, and cool and confine the e^+-e^- plasma, a necessary ingredient for producing an observable annihilation line.

The strongest line in solar flares is at 2.223 MeV from neutron capture on hydrogen in the photosphere. This result, predicted by theory and now confirmed by many observations, is consistent with line production by accelerated particle interactions. Indeed, for particles with essentially cosmic abundances and energies around a few tens of MeV/nucleon, neutron production greatly exceeds the production of any single nuclear deexcitation line. The prompt deexcitation lines, such as the 4.44 MeV line of ^{12}C, do, however, provide a direct measure of the energetic particle reaction rate. This line as well as other prompt lines have been observed from several flares, revealing the time history of the nuclear interactions.

The strongest emission line, observed in gamma ray transients, is that in the energy range from 0.40 to 0.46 MeV. It is reasonable to associate this line with e^+-e^- annihilation. The redshift from a line energy of 0.511 MeV or more could be due to the gravitational redshift of a neutron star or to maser (grasar) action discussed elsewhere in this volume. Lines from nuclear reactions also seem to be present in cosmic transients. In addition to the gravitational redshift, the principal difference between these lines and the solar lines is the drastically different particle abundance needed to explain the cosmic transient lines. In particular, an enhanced abundance of ^{56}Fe is required to account for both a nuclear deexcitation line in a gamma ray burst and a neutron capture feature in a longer duration transient. This result also supports a neutron star origin for cosmic transients.

In the first part of this paper we review the theory of solar gamma ray line production and present results of new numerical calculations based on more detailed and accurate nuclear cross sections. We illustrate the application of the theory by considering the June 7, 1980, flare for which there are reasonably detailed gamma ray data from SMM and important supporting particle data from ISEE-3, Helios-1 and IMP-8.

In the second part of the paper we discuss the physical processes responsible for gamma ray line production in cosmic transients, in particular, positron production and annihilation and nuclear line emission. We also review the possible origin of the gamma ray lines observed in a longer duration transient which is a particularly strong gamma ray line emitter.

SOLAR FLARES

Nuclear interactions of flare-accelerated protons and nuclei in the solar atmosphere produce gamma ray lines from neutron capture, positron annihilation and nuclear deexcitation. The first solar gamma ray lines at 0.511, 2.22, 4.44, and 6.13 MeV, were observed by Chupp et al[1] with a NaI detector on the OSO-7 satellite during the August 4, 1972 flare. These and other lines have been observed from several subsequent flares by detectors on the HEAO-1[2], HEAO-3[3] and SMM[4] satellites. The relative intensities of these lines were consistent with earlier predictions.[5] A review of the observations is given by Chupp in this volume.

Neutron, Positron and Deexcitation Line Production

The strongest gamma ray line observed in nearly all of these flares is that at 2.223 MeV from neutron capture on hydrogen, $^1H(n,\gamma)^2H$. Several theoretical studies [5-10] have been made of neutron production, slowing down and capture in solar flares. Here we briefly review the interaction models used and we present results of new numerical calculations based on updated nuclear cross sections, which will be published elsewhere.

The instantaneous, or thin-target, neutron production rate is given by

$$q_n = n_H c \sum_i \sum_j a_i \int_0^\infty dE \beta \sigma_{ij}(E) N_j(E) \tag{1}$$

where n_H is the ambient hydrogen density, a_i is the relative number of target nuclei i with respect to hydrogen, and σ_{ij} is the neutron production cross section from the interaction of target nuclei i with accelerated particles j having velocity βc, energy per nucleon E, and energy dependent number $N_j(E)$.

The time-integrated, or total thick-target, neutron yield, is given by

$$Q_n = A_o \sum_i \sum_j a_i \int_0^\infty dE \ (dx/dE)_j \ \sigma_{ij}(E) \int_E^\infty dE' \ \bar{N}_j(E') \tag{2}$$

where A_o is Avogadro's number, $(dE/dx)_j$ is the energy loss rate per nucleon of accelerated particles j per unit path length of the ambient medium, and $\bar{N}_j(E)$ is the total number of accelerated particles j incident on the target. For more details see ref. (10).

Various forms of accelerated particle spectra were used in previous treatments[10-13] of neutron and gamma ray line production in energetic particle reactions. Two such forms, which also give[14] good fits to the particle data in interplanetary space, are exponentials in rigidity

$$N_j(E) \text{ or } \bar{N}_j(E) = A_j \exp(-P_j/P_0) \, dP_j/dE \qquad (3)$$

and Bessel functions,

$$N_j(E) \text{ or } \bar{N}_j(E) = A_j K_2\left[2(3p/m_p c\alpha T)\right] \qquad (4)$$

Here A_j is proportional to the abundance of the energetic particles j, $P_j = (A/Z)_j p$ is particle rigidity, $p = \sqrt{E(F + 2m_p c^2)}$ is particle momentum per nucleon, m_p is the proton mass, K_2 is the modified Bessel function of order 2, and P_0 (measured in MV) and α T(nondimensional) characterize the spectrum of the energetic particles.

Equation (4) was shown[13] to be the particle number spectrum that results from stochastic Fermi acceleration with no energy losses, an energy and charge independent acceleration efficiency α and an escape time T. Furthermore, for the June 7, 1980, flare which is the first SMM event with reasonably complete gamma ray line and interplanetary particle data, this Bessel function spectrum gives a very good fit to both the proton and alpha particle spectra with essentially the same αT.

The solar atmospheric abundances[15] and the energetic particle abundances, used in the present calculations, are listed in Table 1. The particle abundances, which show a substantial enrichment of heavy nuclei, are known (e.g. ref. 16) to vary from flare to flare.

The cross sections for neutron production in energetic particle reactions have been summarized in ref. (10). We have recently updated these cross sections and added many new reactions that involve all the isotopes listed in Table 1. These new cross sections, to be published elsewhere, are used in the present calculations.

The magnitude, spectral form and charge dependence of the energy loss rate $(dE/dx)_j$ have important consequences on the nuclear yields in thick targets.

The present calculations have been carried out for slowing down in a neutral medium. The expression

$$(dE/dx)_j = (Z^2_{eff}/A)_j \, 630E^{-0.8} \text{ (MeV/nucleon)}(g/cm^2)^{-1} \qquad (5)$$

where

$$Z_{eff} = Z \left[1 - \exp(-137\beta/Z^{2/3})\right] , \qquad (6)$$

gives a good fit to the tabulated[17] values of dE/dx for charged particles slowing down in neutral H. In an ionized medium the energy losses are higher[13] and hence the gamma ray yield per unit energy deposited is lower. We limit the present treatment, however, to a neutral medium.

TABLE 1 Abundances

| Isotope	Ambient Particles	Energetic Particles
^{1}H	1.	1.
^{4}He	0.07	0.15
^{12}C	4.15×10^{-4}	1.07×10^{-3}
^{13}C	4.64×10^{-6}	1.28×10^{-5}
^{14}N	9.0×10^{-5}	2.14×10^{-4}
^{15}N	3.46×10^{-7}	8.57×10^{-7}
^{16}O	6.92×10^{-4}	2.14×10^{-3}
^{18}O	1.38×10^{-6}	4.28×10^{-6}
^{20}Ne	9.0×10^{-5}	2.14×10^{-4}
^{22}Ne	1.0×10^{-5}	2.57×10^{-5}
^{23}Na	2.28×10^{-6}	$4.28 - 10^{-5}$
^{24}Mg	3.11×10^{-5}	6.42×10^{-4}
^{25}Mg	4.01×10^{-6}	8.14×10^{-5}
^{26}Mg	4.43×10^{-6}	8.49×10^{-5}
^{27}Al	3.18×10^{-6}	5.35×10^{-5}
^{28}Si	3.46×10^{-5}	6.42×10^{-4}
^{29}Si	1.80×10^{-6}	3.21×10^{-5}
^{30}Si	1.18×10^{-6}	2.14×10^{-5}
^{32}S	1.80×10^{-5}	1.07×10^{-4}
^{34}S	7.61×10^{-7}	4.71×10^{-6}
^{36}Ar	3.39×10^{-6}	2.14×10^{-5}
^{38}Ar	6.23×10^{-7}	4.28×10^{-6}
^{40}Ca	2.28×10^{-6}	4.28×10^{-5}
^{52}Cr	4.15×10^{-7}	2.14×10^{-5}
^{54}Fe	1.94×10^{-6}	6.85×10^{-5}
^{56}Fe	3.11×10^{-5}	1.07×10^{-3}
^{57}Fe	7.61×10^{-7}	2.57×10^{-5}
^{58}Ni	1.25×10^{-6}	2.14×10^{-5}
^{60}Ni	4.84×10^{-7}	8.57×10^{-6}
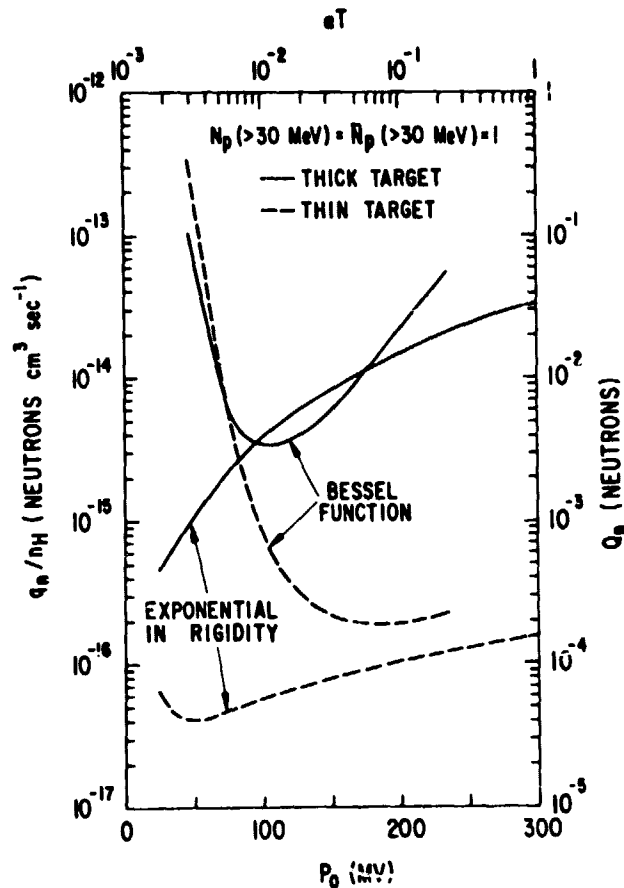
Fig. 1. Total neutron production in the thick-and thin-target interaction models with Bessel function (αT) and exponential (P_0) spectra.

The calculated neutron production rates and yields are shown in Figure 1 for energetic particle densities normalized to 1 proton above 30 MeV. For relatively flat energetic particle spectra, corresponding to large values of P_0 or αT, the bulk of the neutrons are produced in $p\alpha$ reactions. For steep particle spectra, given by the Bessel function at small αT, the large neutron yields result from reactions between α-particles and heavy nuclei. This effect is absent for the rigidity spectra because particles with $Z \geq 2$ have lower energies per nucleon at the same rigidity and hence produce less nuclear reactions. These effects were discussed in more detail in ref. (10) in connection with the comparison of neutron production by particles with spectra that were either power laws in energy or exponentials in rigidity.

The 2.223 MeV gamma ray line emissivity is equal to the neutron production rate times a quantity $\bar{f}$ which is the product of the fraction of neutrons that are captured on hydrogen in the photosphere and the probability of the resultant 2.223 MeV photon escaping from the photosphere. These neutron captures must compete with nonradiative

captures, as well as with neutron decay and escape from the sun. Non-radiative capture on ^{3}He is the most important competing reaction[8], even though ^{3}He is only a minor constituent of the photosphere, because the cross section for the reaction ^{3}He $(n,p)^3$H is about four orders of magnitude larger than that for the reaction ^{1}H $(n,\gamma)^2$H. Observations of the intensity of the 2.223 MeV line compared to that of other lines can limit the photospheric ^{3}He/^{4}He ratio. Calculations 8,10,18 assuming ^{3}He/^{1}H of 5×10^{-5}, isotropic neutron production above the photosphere and a flare site away from the limb, give $\bar{r}$ ranging from 0.1 to 0.14, depending on the energy spectrum and interaction model. In the thick target case, however, the neutrons could be produced in the photosphere which could increase $\bar{r}$ to as much as ~0.2.

The 0.511 MeV line from positron annihilation has been observed from several flares. A number of theoretical studies have been made of positron production 5,7,10 and on positron slowing down and annihilation 19,20. For this paper we give the results of new calculations of positron production based on much greater number of $\beta+$ emitters than were considered in the previous calculations. The results are given in Figure 2, where we show the ratio for thick and thin targets, Q_{e+}/Q_n and q_{e+}/q_n respectively.
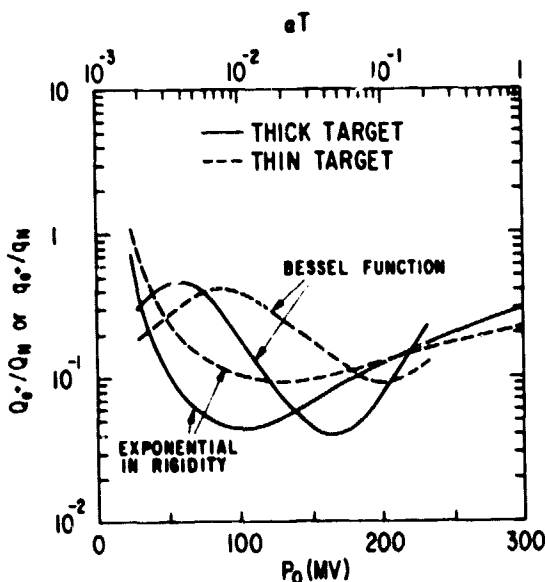

Figure 2. Ratios of the total position yield to the total neutron yield for the thick-and thin-target interaction models and Bessel function (αT) and exponential (P_0) spectra.

Q_{e+} and q_{e+} were calculated using the same equations, abundances and particle spectra as given above for the neutron calculation. The positron yields shown in this figure represent total yields. Because of the finite half-lives of the various $\beta+$ emitters in a short observation time of a transient event, fewer positrons than indicated in Figure 2 are available for 0.511 MeV line production.

Flare-accelerated particle interactions also lead to many other gamma ray lines from deexcitation of nuclear levels. The two strongest lines, at 4.44 and 6.13 MeV due to [12]C* and [16]O* deexcitation respectively, were first observed[1] from the solar flare of August 4, 1972. These and other nuclear lines have been seen in a number of subsequent flares, reviewed by Chupp elsewhere in this volume.

We have treated[12] in detail the production of gamma ray lines in energetic particle reactions. Using this treatment, we have evaluated the prompt gamma ray lines for the abundances, particle spectra and interaction models discussed above. Each of the resultant lines has two components: a narrow ($\Delta E/E \approx 2.5\%$) line component from deexcitation of the recoiling, ambient-gas nuclei and a much broader underlying component from deexcitation of the fast, accelerated-particle nuclei. The bulk of the gamma ray flux, observed from the August 4, 1972 flare at energies between 4 and 7 MeV, has been shown[11] to result from the superposition of broad and narrow nuclear lines rather than electron bremsstrahlung or other continuum emission processes. This energy band, now referred to in the SMM observations as the "main channel window", can thus provide a direct and sensitive measure of this interaction rate of flare accelerated nuclei.

Because the cross sections of nuclear excitation levels have different energy dependences from those of neutron and positron production, the calculated [5,10] ratios of nuclear deexcitation line emissivities to the neutron production rate depend strongly on the assumed spectra of the accelerated particles. One of the strongest nuclear deexcitation lines is that at 4.44 MeV.
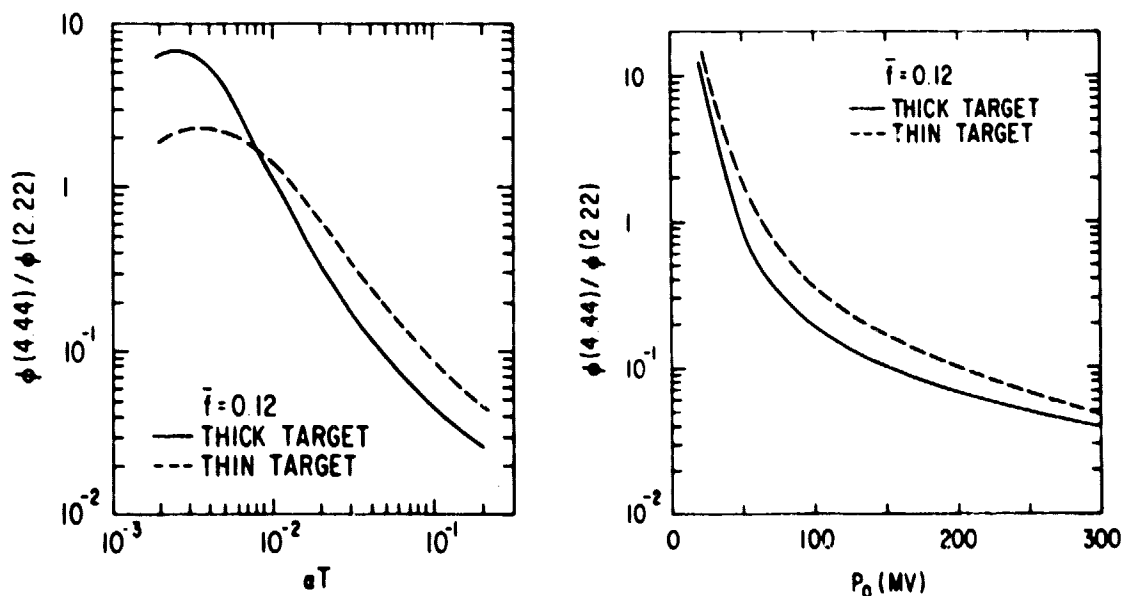
Figures 3 and 4. Ratios of the 4.44 MeV to the 2.22 MeV line intensity in the thick-and thin-target models with $\bar{r}$ = 0.12 for Bessel function (αT) and exponential (P_0) energetic particle spectra.

In Figures 3 and 4 we show ratios of the intensity of this line to the 2.223 MeV line intensity for the different interaction models and energetic particle spectra. As can be seen, these ratios generally decrease with increasing energetic particle spectral hardness reflecting an increased neutron production and decreased 4.44 MeV photon production by particles of high energies. Likewise $\phi(4.44)/\phi(2.22)$ is lower for thick targets than for thin targets (except for very steep Bessel function spectra) because the energy losses harden the particle spectra in the thick target. For very steep (small αT) Bessel function spectra, the thick target ratio exceeds that for thin targets, because of the suppression of the heavy particle fluxes by energy losses in the thick target. As mentioned above, the interaction of these particles with helium are the main neutron sources at low energies. This effect is not present for rigidity spectra, because, as explained earlier, the contributions of the heavy particles to the nuclear reaction rates is negligible for such spectra for both thick and thin targets.

Implications of Line Observations

The observations of the intensity, time history and relative strength of gamma ray lines from solar flares allow us to determine important properties of the flare accelerated particles, the interaction and emission region and the particle acceleration process.

Particle Spectrum and Number

In this paper we shall focus on the flare of June 7, 1980 for which there are both gamma ray line observations and interplanetary particle measurements. The combined analysis of these observations and measurements provide important new information. In particular we find that in this flare the bulk of the gamma ray line emission results from thick-target interactions of accelerated particles trapped and slowing down in the solar atmosphere and not from interactions of the particles during their acceleration. Moreover, for this flare the gamma ray line intensities require that the bulk of the flare accelerated particles remained trapped in the solar atmosphere and that only a very small fraction of the accelerated particles escaped into the interplanetary medium.

The June 7 flare was located at N12W74 and hence was well connected magnetically to Earth. Indeed, several observations of energetic particles have been reported[21-23]. Based on these, the number of protons of energies greater than 10 MeV released into the interplanetary medium, Nesc(>10MeV), has been estimated[21] to be ~10^{31}. Furthermore, the spectrum of these protons was well fit with the Bessell function of equation (4) with αT equal to 0.013 (R. McGuire, private communication 1981). This spectral form also fits the α-particle spectrum with essentially the same αT.

In the thin target model, the 2.22 MeV line fluence can be written[13] as

$$\phi\ (2.22) = T\ (q_n/n_H)\ n_H T\ Nesc\ (>30\ MeV)/4\pi d^2 \tag{7}$$

here T is the particle escape time from the thin-target interaction region and d is the distance to the sun. If this region is also the

acceleration region, the time T in equation (7) is the same as the time T in the parameter αT that defines the spectral hardness of the Bessell function.

Using the proton data ($\alpha T=0.013$, and $\text{Nesc}(>10\text{MeV}) \approx 10^{31}$ protons giving $\text{Nesc}(>30\text{MeV}) \approx 5\times10^{29}$) and the gamma ray data ($\phi(2.22) \approx 6.6$ photons cm^{-2} from Chupp in this volume), we obtain from Figure 1 and equation (7) that for a thin target $n_H T \approx 7 \times 10^{14}$ cm^3 sec^{-1}, or a matter traversal for 30MeV protons of $12 \rho m\text{cm}^{-2}$. The large abundances of spallation products (^{2}H, Li, Be, B) that would result from such a long path length are not observed in solar flares. We conclude, therefore, that the gamma ray lines observed from the June 7, 1980 flare were probably not produced in thin-target interactions. A similar conclusion has been reached[13] for the August 4, 1972 flare.

In the thick-target models, on the other hand, the spallation products, that accompany the production of gamma ray lines, are slowed down in the solar atmosphere and hence are not expected to be seen in the interplanetary medium. In this model the 2.22 MeV fluence is given by

$$\phi(2.22) = \bar{f} Q_n \bar{N}_p(>30\text{MeV})/4\pi d^2 \tag{8}$$

where Q_n is calculated from equation (2).

If we assume that the same process accelerates both the particles, $\bar{N}_p$, that interact at the sun to produce the gamma ray lines and the particles, Nesc, that are observed in the interplanetary medium, and that both populations therefore have essentially the same energy spectrum, then $\bar{N}_p$ should be approximately equal to Nesc $(1-F)/F$, where F is the fraction of particles escaping into the interplanetary medium. From the Q_n calculated for $\alpha T=0.013$ (Figure 1) and the observed $\phi(2.22) \approx 6.6$ photons cm^{-2}, we then find that $\bar{N}_p (>30\text{MeV}) \approx 4.5\times10^{31}$ protons or $\bar{N}_p (>10\text{MeV}) \approx 10^{33}$ protons. This exceeds $\text{Nesc}(>10\text{MeV})$ by a factor of ~ 100, implying that $F \approx 10^{-2}$ or only $\sim 1\%$ of the accelerated protons escaped from the June 7 flare and that the rest remained trapped in the solar atmosphere where they produced the observed gamma ray line emission by nuclear interactions while they slowed down.

Analysis of the prompt gamma ray line emission from the June 7 flare also suggest that the observed emission was produced in thick-target interactions, not thin target. In particular, we consider the ratio of the combined line fluence in the 4 to 7 MeV band to the fluence in the 2.22 MeV line, which in this flare was found to be 1.74 ± 0.27 (from Chupp in this volume).

Using the methods and nuclear data of ref. (12) with the Bessel function spectrum of equation (4) and the abundances given in Table 1, we calculate for $\alpha T=0.013$ that $q(4-7)/n_H = 4.4\times10^{-16}N_p(>30\text{MeV})$ cm^3 sec^{-1} for the thin-target model and $Q(4-7)=1.1\times10^{-3}\bar{N}_p(>30\text{MeV})$ for the thick-target model. Comparing with the neutron production rates (Figure 1), taking $\bar{f} = 0.12$, we calculate $\phi(4-7)/\phi(2.22) \approx 2.6$ for the thick target and ~ 7.5 for thin target. The observed ratio of 1.74 ± 0.27 is in much better agreement with the thick-target model than with the thin-target. Moreover, since in the thick-target model the neutrons may be produced in the photosphere where $\bar{f}$ could be as much as ~ 0.2, the calculated $\phi(4-7)/\phi(2.22)$ could be as low as ~ 1.6 and

thus be in excellent agreement with the observations. Other effects, such as some beaming of the charged particles, could also produce similar agreement in the thick-target case.

Structure of the Interaction Region

Theoretical studies [5,8-10] of the solar flare gamma ray line emission processes suggest that the prompt, deexcitation line emission, the subsequent positron annihilation and the eventual neutron capture emission should each occur at successively deeper mean depths in the solar atmosphere. This results from two effects. First, the range of the ~10MeV protons primarily responsible for the excitation of nuclear levels is only about 1/5th of that of the ~30MeV protons that produce the bulk of the positrons and neutrons. Thus, if these particles are accelerated high in the solar atmosphere and travel down the magnetic field lines into the deeper atmosphere where they lose their energy and are eventually stopped, the bulk of the nuclear line excitation should occur at a higher altitude than the neutron and positron production. Second, since the range of the secondary positrons is less than that of the ~30 MeV protons which produced them, the positrons should annihilate at a depth close to that at which they were produced. But the neutrons on the other hand have a slowing down and capture mean free path that is greater than that of their proton pregenitors, so they can propagate to significantly greater depth before they are captured. On the average, therefore, those neutrons that are captured will do so at a greater average depth than that at which they were produced, since those neutrons which move upward to shallower depths are more likely to escape or decay before they can be captured.

Strong observational evidence for such differences in the mean emission depths of the deexcitation and capture lines appear in the gamma ray line observations of the limb flares of June 21, 1980 and April 27, 1981, described by Chupp in this volume. In these flares the observed ratio of the deexcitation line fluence at 4-7 MeV to that of the 2.22MeV neutron capture line was roughly a factor of 40 times and 10 times that of the average disk flares, respectively. This is clear observational evidence that the 2.22 MeV line is produced in the photosphere with differential attenuation, or limb darkening, of the 2.22 MeV line corresponding to column density differences between the nuclear deexcitation region and the neutron capture region of $(2 \text{ to } 3) \times 10^{25} \text{H cm}^{-2}$. The exact longitudes of these limb flares are not known but these differences probably correspond to radial column depth differences of a few times 10^{24}H cm^{-2}. Such a value for the depth of the mean neutron capture region is also consistent with the average density of $~10^{17} \text{H cm}^{-3}$ in the neutron capture region for the June 7, 1980 flare implied by the $~10^2$ sec decay time of its 2.2 MeV line emission. Detailed studies of the time dependence of the positron annihilation and neutron capture line emission in all of these flares should provide much more information on the structure of the flare emission region.

GAMMA RAY BURSTS

Observations of emission lines and absorption features, seen in the spectra of many gamma ray bursts and transients, are reviewed by Teegarden in this volume.

The absorption features are observed[24] at energies below about 100 keV in the spectra of 20 bursts. If tnese are due to cyclotron absorption, they require very strong magnetic fields of the order of 10^{12} gauss, such as those expected around neutron stars. The most commonly observed emission line falls in the range from 0.4 to 0.46 MeV, as observed[24] by low resolution NaI detectors in seven gamma ray bursts. In the spectrum of one of these bursts, that of November 19, 1978, a small Ge detector has resolved[25] two lines at ~ 0.42 MeV and ~0.74 MeV, which the NaI detectors have seen as one broad emission feature from 0.3 to 0.8 MeV. Line emission in the range of 0.4 to 0.46 MeV is most likely due to gravitationally redshifted e^+-e^- annihilation radiation, while the line at 0.74 MeV could be either collisionally excited and gravitationally redshifted 0.847 MeV emission from ^{56}Fe, an abundant constituent of the crusts of neutron stars, or gravitationally redshifted single photon e^+-e^- annihilation[26,27] radiation at 1.022 MeV in a very strong (~10^{13} gauss) magnetic field. In all cases, the implied redshifts of 0.1 to 0.3. are consistent with those expected from neutron star surfaces. Thus, the magnetic fields, the redshifts and the surface composition indicate that the sources of the bursts with observed lines are probably neutron stars.

Positron Annihilation

The principal positron producing mechanism in gamma ray bursts is likely to be pair production in photon-photon collisions. This follows from the enormous photon densities in the burst sources deduced[28,29] from the observed luminosities, likely source distances and sizes. The latter probably are of the dimensions of neutron stars or smaller.

The production of a relatively narrow e^+-e^- annihilation line requires[30] that the pairs annihilate at a temperature which is substantially lower than the burst temperature deduced from the observed continuum spectrum or the temperature required to produce the pairs. A promising cooling mechanism[31,32] is synchrotron radiation in strong magnetic fields ($B>10^{11}$gauss). The radiation produced by this cooling could be responsible[31,32] for the continuum emission of the bursts at energies below ~300 keV.

This synchrotron cooling model was specifically applied[31,32] to the March 5, 1979 transient. Although the observation of a ~0.43 MeV emission line from this transient suggests that its source was a neutron star, the origin of this spectacular event remains unresolved. The position of the burst has been determined by triangulation (see review by Cline in this volume) leading to an error box of size less than an arc minute within the supernova remnant N49 in the Large Magellanic Cloud (LMC). Nevertheless, the question remains whether the burst did indeed originate in the LMC or whether its source was much closer. The probability for chance coincidence between the March 5 burst source position and N49 has recently been estimated[33] to be <10^{-3}.

The synchrotron cooling model removes one of the principal difficulties posed by a burst source in the LMC, namely that of the very high brightness temperature (~1MeV) of the observed radiation. For this model, the bulk of the observed continuum emission, rather than being thermal radiation of particles with $kT \lesssim 100$ keV, is optically thin synchrotron emission of the ~MeV electrons and positrons. These particles, after losing their kinetic energy by synchrotron radiation, annihilate and produce the observed ~0.43 MeV line. The minimum magnetic field required for a cooling time shorter than the annihilation time is of the order of a few times 10^{11} gauss. This value turns out, also, to be the minimum B required to confine the e^+-e^- plasma that produces the observed annihilation line. This confinement is crucial, because otherwise the super-Eddingtonian burst luminosity would cause relativistic expansion of the emission region in clear conflict with an observed redshifted line.

An important addition has been recently proposed[34] to the synchrotron model for the March 5 transient. The MeV e^+-e^- pairs, in addition to producing synchrotron radiation, could also Compton scatter their own synchrotron photons and thus produce the observed continuum above ~0.5 MeV. Since both the synchrotron and Compton components of the observed spectrum depend linearly on the same relativistic pair density, the model allows a distance determination. The distance d depends only on B, the mean relativistic particle energy, γmc^2 and the area of the emitting region, A. For B~2×10^{11} gauss, γmc^2 ~ 1 MeV, and A of the order of a neutron star surface area, d turns out to be approximately the distance to the LMC. If the source were much closer, Compton scattering of the synchrotron photons could not explain the high energy continuum unless the emitting area were very small. For example if d ~ 100 pc, A would have to be only a few millionths of the neutron star surface.

In a separate paper in this volume, by Ramaty, McKinley and Jones, the possibility of gamma ray amplification through stimulated annihilation radiation (grasar) has been proposed. This process could produce a narrow annihilation line without requiring a low temperature annihilation region. Grasar action requires an e^+-e^- pair density which substantially exceeds the thermodynamic equilibrium density at the temperature of the burst source (~10^{30} cm^{-3} at T~3×10^9 K). This is equivalent to the population inversion of a regular maser. But it is not clear yet how such an inversion could be produced in a gamma ray burst source. If an inversion can be produced, however, grasar action would lead to a narrow emission line at ~0.43 MeV without the requirement of a large gravitational redshift. One strong observational argument for grasar action would be the detection of narrow annihilation lines of width less than about 0.1MeV.

Nuclear Line Emission

At least one gamma ray burst, that of November 19, 1978 also shows[25] evidence of possible nuclear line emission. Its spectrum, reviewed by Teegarden in this volume, shows a strong narrow line at about 0.74 MeV, and other features at higher energies. The continuum spectra of gamma ray bursts are suggestive of optically thin bremsstrahlung emission of electrons with temperatures $\gtrsim 10^9$ K.

Calculations[35-37] of the expected nuclear deexcitation and radiation capture line emissivities from thermonuclear reactions in high temperature plasms have been made for a temperature range of 10^8 to 10^{12}K.
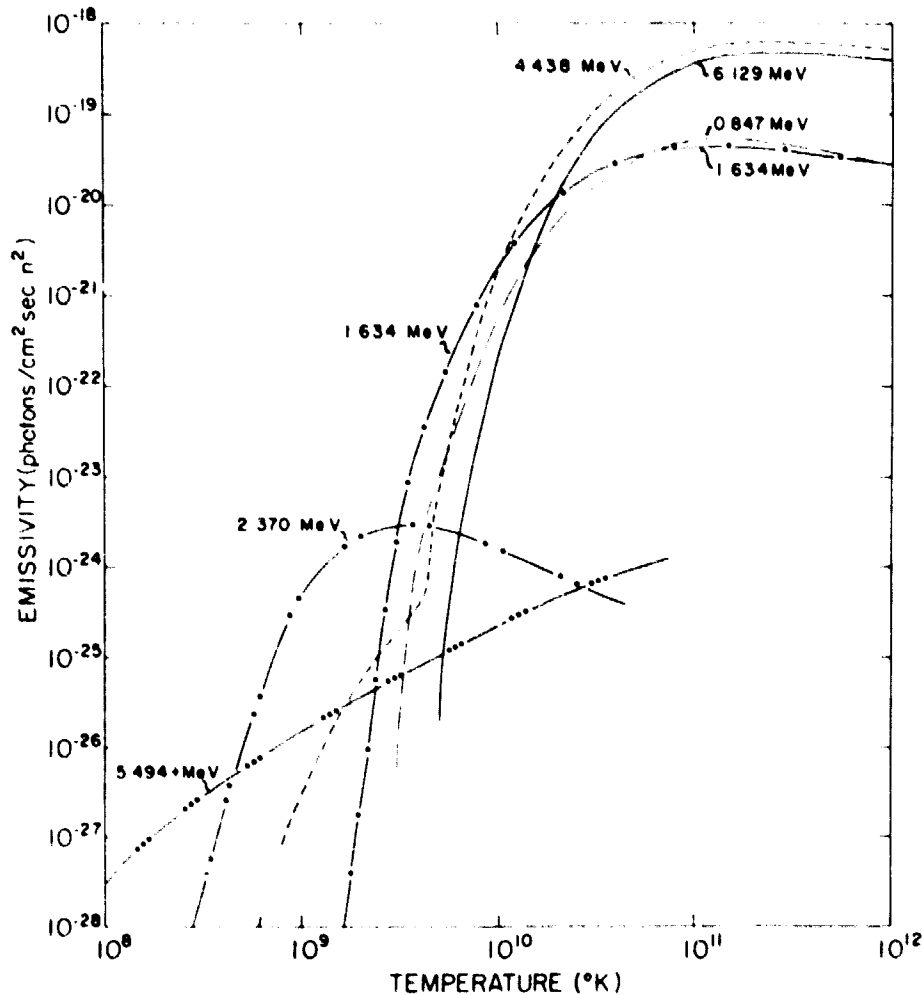

Figure 5. The emissivities of the principal nuclear deexcitation and proton radiative capture lines resulting from thermonuclear reactions in a plasma of local interstellar composition. These lines result from the following reactions: 5.494+ MeV from $^2H(p,\gamma)^3He$; 2.370 MeV from $^{12}C(p,\gamma)^{13}N$; 1.634 MeV from $^{20}Ne^*$; 4.438 MeV from $^{12}C^*$, 6.129 MeV from $^{16}O^*$; and 0.847 MeV from $^{56}Fe^*$.

The calculated emissivities of these lines from a plasma of local interstellar composition are shown in Figure 5. As can be seen, the strongest lines for such abundances at temperatures of 10^8 to $\sim 3 \times 10^9$K are radiative capture lines from $^2H(p,\gamma)^3He$ and $^{12}C(p,\gamma)^{13}N$. Proton capture on ^2H leads to a line at the reaction $Q \sim 5.494$ MeV plus the kinetic energy available in the center of mass of the interaction which depends directly on the ion temperature. Proton capture on ^{12}C is dominated by a strong, narrow resonance in the capture cross section at about 0.46 MeV/nucleon, leading to a line at ~ 2.37 MeV whose energy is relatively independent of the ion temperature.

For ion temperatures of about $\sim 3 \times 10^9$ to 3×10^{10}K nuclear deexcitation lines should be the most intense. The principal lines from a plasma of local composition are those at 6.129 MeV from $^{16}O^*$, 4.438 MeV from $^{12}C^*$, 1.634 MeV from $^{20}Ne^*$ and 0.847 MeV from $^{56}Fe^*$. These lines should be relatively narrow, thermally broadened to widths FWHM at $\sim 10^{10}$K of about 140, 120, 30 and 10 KeV respectively.

At ion temperature $\geq 3 \times 10^{10}$K neutron production exceeds the emissivity of the deexcitation lines and neutron radiative capture lines could become the most intense. If the capture occurs in the hot plasma($\geq 3 \times 10^{10}$K) in which the neutrons are made, however, the capture lines would be greatly shifted and broadened by the large available energy in the center of mass. In particular the 2.223 MeV capture line from $^1H(n,\gamma)^2H$ and the 7.632 and 7.646 MeV lines from $^{56}Fe(n,\gamma)^{57}Fe$ could be shifted by a few MeV or more and broadened to a width of more than an MeV.

The ~ 0.74 MeV line and a possible line at ~ 1.1 MeV, reported by Teegarden in this volume, in the spectrum of the November 19, 1978 burst could be nuclear deexcitation lines at 0.847 MeV and 1.238 MeV from the first and second levels of ^{56}Fe, redshifted by $z \sim 0.14$. Such a redshift is also implied by the broad feature at ~ 0.42 MeV, if it is redshifted e^+-e^- annihilation radiation. This redshift is within the range of gravitational redshifts expected at the surface of neutrons stars.

But the high relative luminosity of the ~ 0.74 MeV line, $\sim 9\%$ of the total burst luminosity observed above 200 KeV, puts strong constraints on a nuclear origin of the line. In particular, if this line is redshifted 0.847 MeV emission accompanied by an optically thin, thermal bremsstrahlung continuum, then the line-to-continuum luminosity ratio requires that the emission come from an iron-enriched, two-temperature plasma with Fe/H $\approx 10^{-2}$, an ion temperature $T_{ion} \geq 2 \times 10^{10}$K and an electron temperature $T_e \leq 2 \times 10^9$K. Such a plasma of unit optical depth on the surface on a neutron star at a nominal distance of 100 pc, emitting $\sim 10^{38}$ erg sec^{-1} in bremsstrahlung and $\sim 10^{37}$ erg sec^{-1} in ^{56}Fe deexcitation lines, could produce the observed burst spectrum.

An alternative suggestion[27] that the ~ 0.74 MeV line is a strongly redshifted (~ 0.38) line at 1.022 MeV from single photon annihilation of e^+-e^- pairs in very strong magnetic fields ($\sim 10^{13}$gauss) has not been studied in any detail but such a process could not account for a possible line at ~ 1.1 MeV or higher energy features.

GAMMA RAY LINE TRANSIENTS

There is apparently another class of gamma ray transients in which essentially all of the observed radiation is in the form of line emission. Such a gamma ray line transient was discovered by Jacobson et al.[38] with a high resolution Ge detector on June 10, 1974 from an unknown source. This event, lasting about twenty minutes, was characterized by strong emission in four relatively narrow energy bands at 0.40-0.42 MeV, 1.74-1.86 MeV, 2.18-2.26 MeV, and 5.94-5.96 MeV with no detectable continuum. A detailed description of this observation is given by Ling et al. elsewhere in this volume.

As pointed out by Jacobson et al.[38] the line identification alone appears to require strongly redshifted emission, since the lines at ~0.41 MeV and ~5.95 MeV cannot be identified with any unshifted lines that would not be accompanied by much stronger companion lines which were not observed. All of these lines however can be identified with lines from the most intense nuclear emission processes expected in nature, positron annihilation and neutron capture on hydrogen and iron, if we assume that the emission comes from a gravitationally redshifted region with a z ranging from ~0.2 to 0.285. In particular the 5.94-5.96 MeV line can be identified with the two strongest lines from neutron capture on the iron crust of a neutron star having a surface gravitational redshift of $z = 0.285$. Since ^{56}Fe is expected to be the dominant constituent of neutron star crusts this line alone strongly suggests a neutron star source for the transient emission on June 10, 1974.

The 0.40-0.42 MeV and the 1.74-1.86 MeV lines can similarly be identified as the positron annihilation and neutron capture in a hydrogen atmosphere of density $n_H > 10^{16}$ H cm^{-3} extending from the surface z of 0.285 up to an altitude corresponding to a z of about 0.2. Such an atmosphere is presumably a temporary feature perhaps formed by infall of gas from an accretion disk. This minimum hydrogen density is required in order that a significant fraction of the neutrons are captured before they decay. The width of the ~0.4 MeV line also places a limit on the average temperature of this atmosphere of $<2 \times 10^6$ K. The unshifted ($z = 0+.02$) line at 2.22 MeV requires a comparable high density region well above the neutron star surface and can be understood as neutron capture in the atmosphere of a binary companion.

A surface redshift of ~0.285 implies a neutron star mass of about 1.4 to 1.8 M and a radius of 10 to 13 km, depending on the assumed equation of state. The observed 25 keV full width of the ~5.95 MeV line reduced by the instrumental broadening of 5 keV and the redshifted ^{56}Fe doublet separation of 10 keV gives an emitted width of 10 keV. If the line were produced unformly over the surface of the neutron star, this width would give a lower limit for the rotation period

$$P > \frac{E_\gamma}{\Delta E_\gamma} \cdot \frac{4\pi r \sin\theta}{c} = \frac{\sin\theta}{4} \text{ sec,}$$

where θ is the angle between the rotation axis and the direction of observation.

If the lines do result from neutron capture near the surface of a neutron star, however, the observed line fluences would then require either rapid mixing or rapid break up of the resultant ^{2}H and ^{57}Fe formed by the capture since these nuclei would quickly accumulate to many optical depths for any reasonable source distance. The column density of ^{2}H and ^{57}Fe, produced at the surface of a neutron star during the June 10, 1974 transient, would amount to $~3 \times 10^{30} D^2_{100}$ ^{2}H cm^{-2} and $~10^{30} D^2_{100}$ ^{57}Fe cm^{-2} where D_{100} is the assumed distance in units of 100 pc.

But even assuming such an identification for the lines, the origin of the neutrons and positrons required to produce them is still problematical. Although one might imagine that it should not be hard to find ways of generating neutrons directly on the surface of a neutron star, the observation of the unshifted neutron capture line on hydrogen would require that the average energy of the neutrons produced at the neutron star surface must be $~150$ MeV, equal to the escape energy from the star, so that a significant fraction could escape to a lower z region to be captured. There is no obvious process for generating such energetic neutrons. It also seems unlikely that the neutrons and positrons could have been produced in nuclear reactions in a flare on the binary companion because of energetic considerations. One possibility, however, would appear[36] to be that the neutrons and positrons which were captured and annihilated in the vicinity of the neutron star and its binary companion were all produced by nuclear reactions occurring when gas, flowing episodically from the companion, was gravitationally accelerated to an energy of > 1 MeV and collided with gas in the outer part of the accretion disk around the neutron star. In addition to the observed lines we would also expect other lines and continuum emission, but the expected intensities are not necessarily inconsistent with observations.

Lastly, since the sum of the neutron-capture gamma-ray line intensities for the transient event of June 10, 1974 was $~3 \times 10^{-7}$ erg cm^{-2} sec^{-1}, the neutron capture line luminosity of the source $L_{n,\gamma}$ $= 3 \times 10^{35} D^2_{100}$ erg sec^{-1}. Assuming a maximum neutron yield of $< 2 \times 10^3$ neutrons erg^{-1}, see ref.(36), and an average neutron capture photon energy of $~3$ MeV, the total source luminosity L must have been $\geq 10^{38} D^2_{100}$ erg sec^{-1}.

REFERENCES

1. E.L. Chupp et al., Nature, 241, 333 (1973).

2. H.S. Hudson et al., Astrophys. J. Lett., 236, L91 (1980).

3. T.Prince et al., paper presented at Conf. on Cosmic Ray Astrophys. and Low Energy Gamma Ray Astronomy, U. of Minn., Sept. 1980.

4. E.L. Chupp et al., Astrophys. J. (in press 1981).

5. R.E.Lingenfelter and R.Ramaty, in High Energy Nuclear Reactions in Astrophysics, ed. B.S.P.Shen (Benjamin, N.Y., 1967) p.99.

6. R.E.Lingenfelter et al., J. Geophys. Res., 70, 4077 (1965).

7. R.Ramaty and R.E. Lingenfelter, in High Energy Phenomena on the Sun, ed. R. Ramaty and R.G. Stone (NASA SP 342, 1973) p. 301.

8. H.T. Wang and R. Ramaty, Solar Phys. 36, 129 (1974).

9. H.T. Wang, Ph.D. Thesis, Univ. of Maryland (1975).

10. R. Ramaty, B.Kozlovsky and R.E.Lingenfelter, Space Sci. Rev. 18, 341 (1975).

11. R. Ramaty, B.Kozlovsky and A.N.Suri, Astrophys.J. 214, 617 (1977).

12. R. Ramaty, B.Kozlovsky and R.E.Lingenfelter, Astrophys. J. Supp. 40, 487 (1979).

13. R.Ramaty in Particle Acceleration Mechanism in Astrophysics ed. J.Arons et al. (Am. Inst. Phys., N.Y., 1979) p. 135.

14. R.E.McGuire, T.T. vonRosenvinge and F.B.McDonald, 17th Cosmic Ray Conf. Papers, 3, 65 (1981).

15. A.G.W.Cameron in A Festschrift in Honor of Willy Fowler's 70th Birthday (1980)

16. G.M.Mason et al., Astrophys.J., 239, 1070 (1980).

17. L.C. Northcliffe and R.F. Schilling, Nuc.Data Tables, 7, 233 (1970).

18. G.Kanbach et al., 14th Internat. Cosmic Ray Conf. Papers, 5, 1644 (1975).

19. C.J. Cranell et al., Astrophys. J., 210, 582 (1976).

20. R.W.Bussard, R.Ramaty and R.J.Drachman, Astrophys.J., 228, 928 (1979).

21. T.T.vonRosenvinge, R.Ramaty and D.V.Reames, 17th Internat.
     Cosmic Ray Conf. Papers, 3, 28 (1981).

22. P. Evenson, P. Meyer and S. Yanagita, 17th Internat. Cosmic
     Ray Conf. Papers, 3, 32 (1981).

23. M.E.Pesses et al., 17th Internat. Cosmic Ray Conf. Papers, 3,
     36 (1981).

24. E.P. Mazets et al., Nature 290, 378 (1981).

25. B.J.Teegarden and T.L.Cline, Astrophys.J.Lett., 236, L67 (1980).

26. J.K. Daugherty and R.W.Bussard, Astrophys.J., 238, 296 (1980).

27. J. Katz, preprint (1981).

28. W.K.H.Schmidt, Nature, 271, 525 (1978).

29. G. Cavallo and M.J. Rees, M.N.R.A.S., 183, 359 (1978).

30. R. Ramaty and P. Meszaros, Astrophys. J., 250, (in press 1981).

31. R. Ramaty, R.E.Lingenfelter, and R.W.Bussard, Astrophys. and
     Space Sci,75, 193 (1981).

32. R. Ramaty et al., Nature 287, 122 (1980).

33. J.E. Felten, 17th Internat. Cosmic Ray Conf. Papers, (in press 1981).

34. E.P.T.Liang, Nature 292, 319 (1981) and paper in this volume.

35. J.C. Higdon and R.E. Lingenfelter, Astrophys.J., 215, L53 (1977).

36. R.E.Lingenfelter, J.C.Higdon and R.Ramaty in Gamma Ray Spectro-
     scopy in Astrophysics, ed. T.L.Cline and R. Ramaty (NASA,1978)
     p. 252.

37. W.A. Fowler, G.R. Caughlan and B.A.Timmerman, Ann. Rev. Astron. and
     Astrophys., 13, 69 (1975).

38. A.S. Jacobson et al., in Gamma Ray Spectroscopy in Astrophysics,
     ed. T.L. Cline and R. Ramaty (NASA, 1978) p. 228.

A REVIEW OF THE 1979 MARCH 5 TRANSIENT

T. L. Cline
Laboratory for High Energy Astrophysics
NASA/Goddard Space Flight Center, Greenbelt, MD   20771

ABSTRACT

The understanding of the 1979 March 5 event remains a problem of central importance for researchers in gamma ray transient astronomy. Efforts in the study of the observational results and in the development of interpretations regarding the nature of this event and its relationship to the variety of other gamma ray burst phenomena have continued through the past 2 years. A consensus of opinion has not yet been reached regarding its possible origin in N49 at 55 kpc distance, versus in an invisible source 3 or 4 orders of magnitude closer, although interpretations favoring N49 appear to be presently gaining momentum. This presentation outlines the existing data in a review of what remains the most singular high-energy astrophysical phenomenon of the space age.

INTRODUCTION

I assume that most of the persons interested in this subject are familiar with the March 5, 1979 gamma ray transient; since the bulk of the observational data has been published for some time this review seems at first unnecessary. However, progress has been and continues to be made in both the experimental and the interpretative reanalyses of the measurements. Thus, although the event remains an historic fact, its study is very much a current activity; in fact, the 'correct' interpretation is undoubtedly yet ahead of us. I personally have found this event to be fascinating, both because of its apparent observational rarity and because of its role as a generator of theoretical ideas and related calculations. Will we see a gamma ray transient like this again in our research lifetimes? Probably not, at least, probably not when we shall be as prepared with third-generation instrumentation as we happened to be with second generation instrumentation on March 5th of 1979. However, if detector sensitivity and resolution can be sufficiently improved, March 5-like events of much weaker visual magnitude may be observable and capable of detailed study, whether arriving from more distant stellar or from extragalactic sources. Will an entirely new modelling (such as the grasar, to be unveiled at this conference[1]) be found to be applicable? If so, some new experimental approach involving the measurement of, for example, polarization, or submillisecond oscillations, or gamma ray coherence, may provide another observational breakthough, in addition to that which gamma ray line spectroscopy now provides.
We can first review the question of whether the 1979 March 5 event is so different from other gamma ray bursts as to be termed 'unique', which I have described it to be in an earlier review.[2]

The variety of gamma ray burst data we have been shown at this conference, in fact, leads one to believe that every gamma ray burst is unique! However, the first basic difference that appears to confront us is that while the typical or so-called 'classical' gamma ray bursts seem generally to have time histories of random structure, with randomly evolving spectral features, the March 5 event appears to be especially ordered, with a singularly fast rise time, a single very intense peak, and a subsequent, well-defined
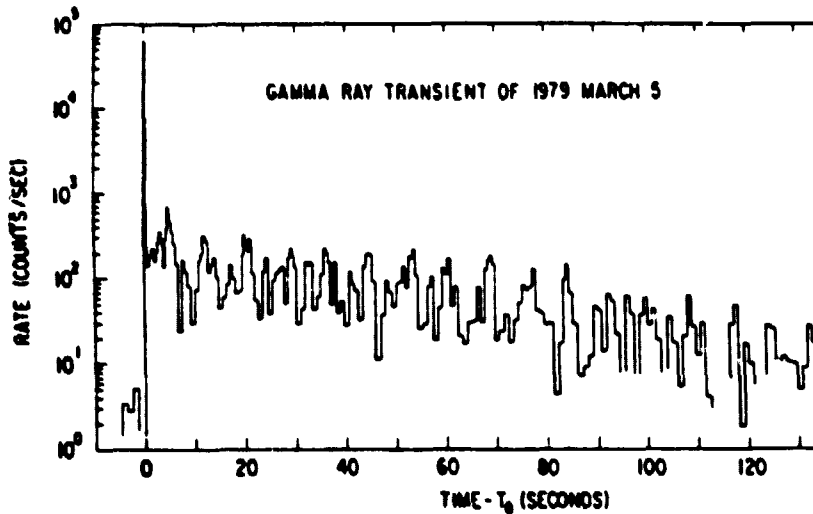
GAMMA RAY TRANSIENT OF 1979 MARCH 5

Fig. 1. Time history of the 1979 March 5 transient as observed with the ISEE-3 space probe[3].

oscillation. The other basic difference is the fact that the March 5 event is the only one with a candidate source object. Of course, its features may only seem to be atypical due to their greater resolution afforded by the great apparent brightness of the event; also, its source identification could be a cosmic accident. To 'write off' the event in this manner would be to completely ignore a possibility of great value to astrophysics, in my opinion.

The March 5 event possesses a 420-keV spectral feature[4] in common with some other classical bursts[5,6]; this, together with the regular oscillation (which is not clearly exhibited by classical events) has prompted the general belief that both originate in neutron star phenomena. However, they may of course originate by means of two or more entirely differing mechanisms. In fact, the 420-keV feature also has a novel and entirely differing implication: as we shall hear later in this conference[1], the neutron star redshift explanation is no longer the only possible interpretation of the 420 keV feature. Thus either the March 5 or the classical event connections to neutron star redshifts or both may yet be found to be incorrect or imprecise.

It is a fair statement, unfortunate though it may be, that no mathematical treatment has yet been evolved to systematically classify or categorize gamma ray bursts; thus, the probability of uniqueness of the March 5 event has not been quantitatively estimated. To pursue this, we can look at some of its features in greater detail.

OSCILLATIONS

Of the several unusual features of the March 5 event, including the rise, the intensity, the oscillations, the spectrum and the direction, the oscillations were invoked first as providing basically new information.[7] Except for a weak but suggestive ~
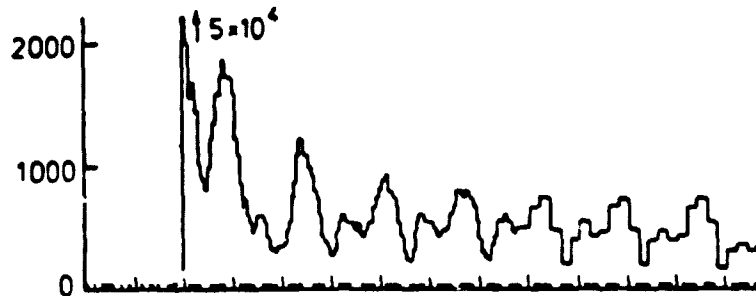

Fig. 2. (Above) Venera-11 observations of the March 5 event (horizontal scale = 5 seconds/mark), indicating the first clear evidence for periodicity in a gamma ray transient (from Mazets et al.[4]).
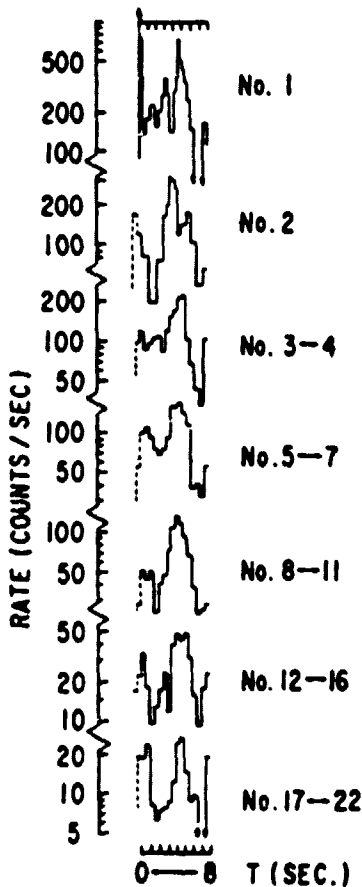
Fig. 3. (Left) ISEE-3 observations of the first 22 cycles of the March 5 event, plotted on an 8-second per period basis folded with an increasing number of cycles per plot, to compensate for the decreasing statistical validity per cycle. The large pulse and the secondary features remain constant in time, yielding an average period of 8.00 ± .05-second.[3]

4-second, ~ 5 cycle long, periodic effect in the time history of the 29 October 1977 gamma ray burst event,[8] no evidence is known for any cyclic features in classical gamma ray bursts. The clear 8-second periodicity in the March 5 event provided the first evidence of that

kind for the neutron star origin model of a gamma ray transient.
(Spectral evidence existed before that time for one very slow gamma
ray transient[9,10] although it was not then and still is not clear
what relationship that isolated phenomenon has to classical gamma
ray bursts. Of course, it also is not clear what relationship the
March 5 event has to classical events.) Figure 2 shows the results
from the spaceprobe Venera-11 as published by Mazets and his
colleagues of the Leningrad group.[6,7] Both the general 8-second
repetition and the ~ 4-second modulation are clear. Similar time
histories were exhibited by a companion sensor on Venera-12. The
oscillations were tracked for about 3 minutes with the Goddard
experiment on ISEE-3, as seen in the time history in Figure 1, but
of course suffered from decreasing statistical significance as a
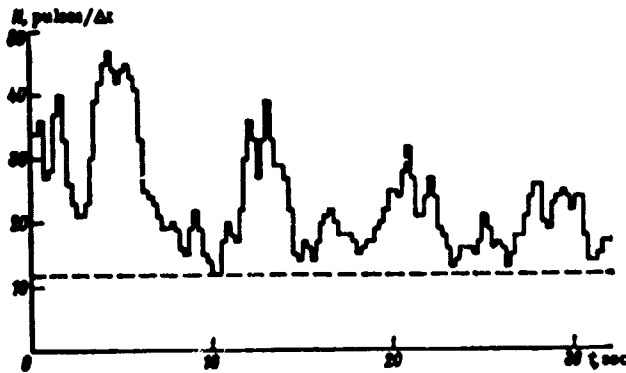
Fig. 4. The time history
as observed with the
Franco-Soviet instrument on
Venera-12, indicating
evidence for ~ 1-second
features.[12]

function of time. This effect is compensated for in the presen-
tation of Figure 3, in which an increasing number of cycles are
included per plot. Here the constant phase of the compound
structure is evident, providing a period of 8.00 ± 0.05 second.[3]
This periodicity is clearly not a fluctuation but very definite
evidence for a cyclic phenomenon; whether the 8-second feature is
rotational, precessional or radial is another question. The fact
that the main and secondary pulses decay differently has been
invoked as evidence for a directional emission from a rotating
neutron star.[11]

Weak evidence also exists for features of time structure finer
than the 4-second interpulse. Figure 4 shows the Venera-12 data as
published by Vedrenne and his colleagues of Toulouse and Estulin and
his colleagues of Moscow.[12,13] Here, as in earlier figures,
suggestive fluctuations are evident on a shorter time scale. The
spectral power as a function of period derived from these results,[13]
shown in Figure 5, and the power spectrum as a function of frequency
of 3 minutes of Pioneer-Venus Orbiter data[14] of Evans and his
colleagues at Los Alamos, shown in Figure 6, both indicate second-
order structure in the ~ 0.7 to 1.1-second region. (The ISEE-3
results do show some detail but its time history may be somewhat
spin-modulated, although not severely, since the source direction is
only 3.5 degrees from the ISEE-3 spin axis.) Finally, one can
suspect that even finer time variations could exist within the first

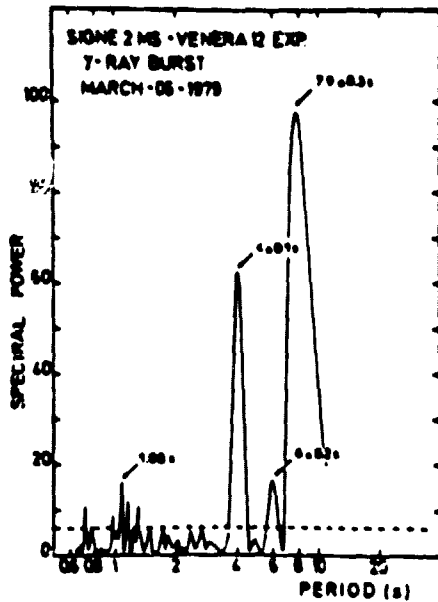oscillation. In Figure 7 the Leningrad Venera-11 data hint at a ~
0.2-second fluctuation.

Fig. 5. Spectral power
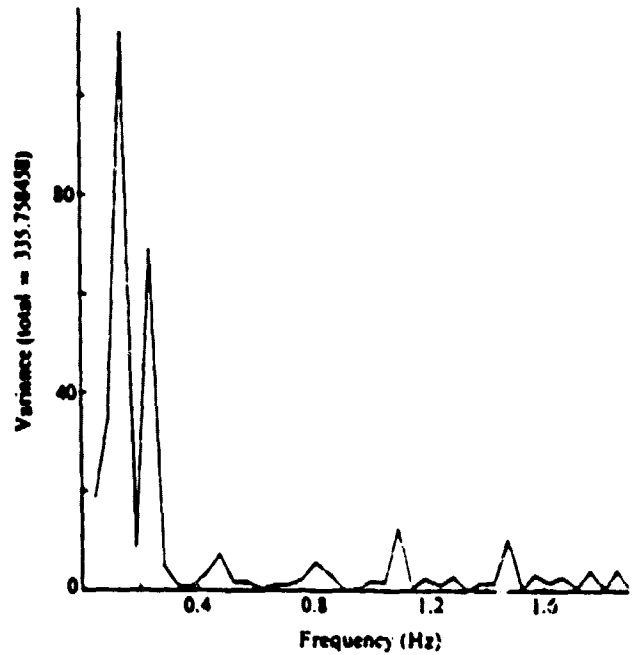evidenced in the Franco-
Soviet Venera-12 results.[13]

Fig. 6. Power spectrum from
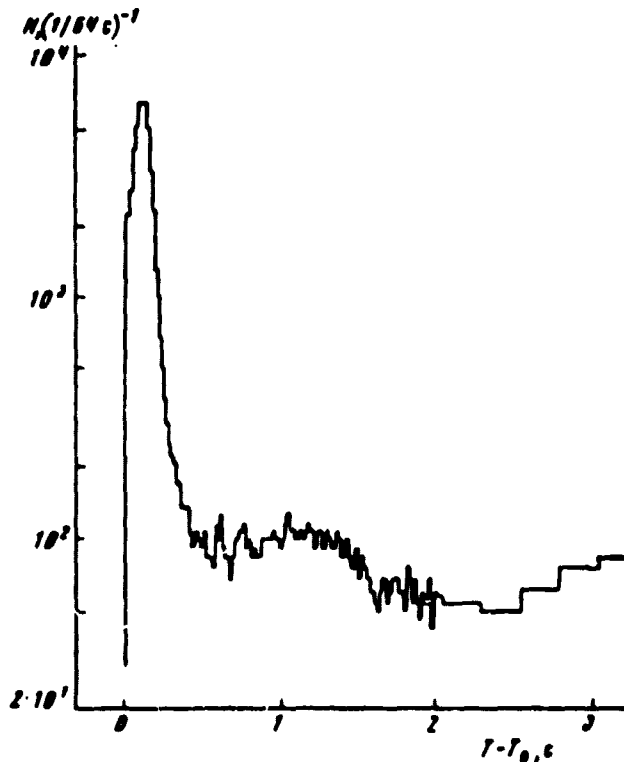the Pioneer-Venus-Orbiter
measurements.[14]

Fig. 7. Detailed Venera-11
time history of the early
part of the event,
including the first intense
peak, its decay and the
buildup of the first
oscillation.[4,7]

BURST TIME HISTORY

The initial high-intensity burst of radiation in itself may be even more anomalous than the oscillating portion of the March 5 event. Its features, not shared by the general population of classical gamma ray bursts, are a fast rise, a single peak, a smooth decay and an instantaneous intensity near detector-saturation for most of the instruments (of the order of one count per 10 microseconds). In fact, the unknown spectrum of hard X-rays below detector threshold for these gamma ray detectors presents some uncertainity of possible measurement distortion; it is hoped that the effect is not major, a belief supported by the fac. that the observations generally mutually agree. For example, the onset rise is faster than can be measured with every instrument, yet the peak counting rate is seen to occur usually about 20 milliseconds into the event. (Unfortunately the ISEE-3 γ-ray spectrometer failed 2 months earlier, depriving us of a comparison measurement made with germanium rather than with scintillators.) This onset consists of a sudden increase of several orders of magnitude within the resolution time of, for example, 1 millisecond in the ISEE-3 Goddard/MPI scintillator,[3] as shown in Figure 8. The exponential time constant of intensity increase is therefore less than 200 microseconds, implying a light travel distance of less than 60 km.
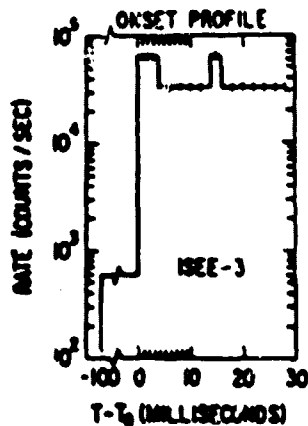

Fig. 8. (a) Onset of the high-intensity portion of the 1979 March 5 transient.[3] A time constant of less than 0.2 ms is inferred from the increase of two orders of magnitude from near background to essentially full intensity within a resolution time of 1 ms. (In this instrument the time to accumulate 64 photons is recorded to 1 ms accuracy; the first several readings are in fact 1 ms and 2 ms accumulations.) This < 1 ms full rise in the onset shape is also seen with Pioneer-Venus-Orbiter.[3,14]

No other gamma ray transient exhibits as brief a rise time, within a factor of 10 to 30 depending on the various detector limitations considered. (For example, the Goddard Helios-2 detector is instrumented with slower, 4 millisecond temporal resolution; the entirety of the fast spike as observed with that instrument[3] is shown in Figure 9. Four years of gamma ray bursts were monitored before the Helios-2 spacecraft was turned off; only the March 5 event produced a trigger response in the 4-ms circuits; all other events triggered in its 32 or 250-ms modes.) However, other events have been observed that are briefer than the 150-millisecond total duration observed here. Two events of moderate intensities were detected in 1979 with Venera and PVO, one of which was also observed with Venera-12 giving a directional determination at high galactic and celestial latitude (K. Hurley, R. Klebesadel, private communication). The question of whether such fast, single-spike

events occasionally detected, including perhaps 3 more in the archived Vela data (R. Klebesadel, private communication), are merely the tips of more complex classical-event icebergs or are March 5-like events, cannot yet be answered.
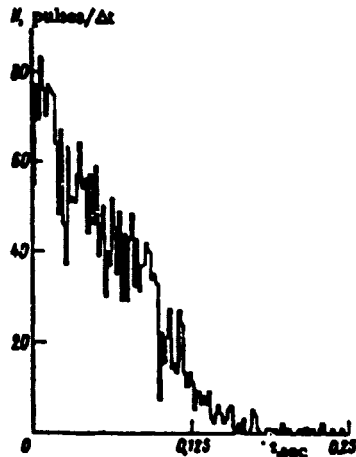

Fig. 9. The 150-millisecond wide initial burst. A transition from a slow decay of ~ 150 ms time constant to a steeper decay of ~ 35 ms time constant is seen about 100 ms into the event. These data are plotted on a ~ 4 ms per accumulation time basis.[3]
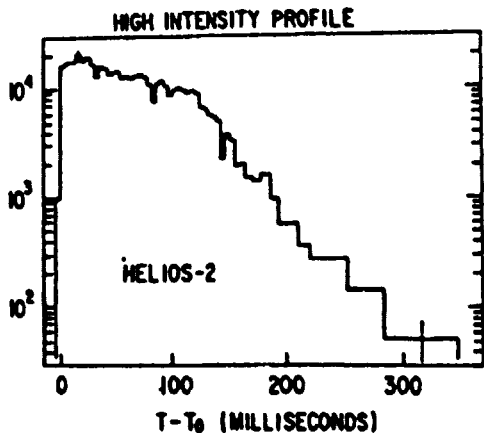

Fig. 10. The data, on a ~ 2 ms per accumulation basis, from the Franco-Soviet experiment on Venera-11, collected during the initial one-quarter second of the March 5 event.[12]

The question of very fine time variations in the March 5 event time history is interesting for several reasons. (These range from the existence of 0.1 to 100 ms oscillations, due either to an inherently fast neutron star spin period or to model-dependent transition damping vibrations,[15] to the possible existence of a very short duration nonrandomicity in the counting rate that would relate to a possible coherence, as in certain other models.[1]) Detailed studies of the first 125 milliseconds of the event, examples of which are shown in Figures 9 and 10, have been carried out using data from all available high time resolution sources, including the Einstein Observatory X-ray monitor. The Venera time histories hint at a ~ 25 msec effect with marginal statistical accuracy (K. Hurley, private communication) and the Einstein time history, of only 55 msec duration, can be interpreted to be consistent with two 27 msec features (M. Weisskopf, private communication); these departures from randomicity appear to be tantalizing but inconclusive.

INTENSITY AND SPECTRUM

The total intensity of this burst is that of a typical, strong gamma ray burst, but the instantaneous intensity of the peak is by far the greatest yet observed. Figure 11 shows a scatter plot of event total intensity versus maximum instantaneous intensity, using the sample of Helios-2 events detected from January 1976 to the
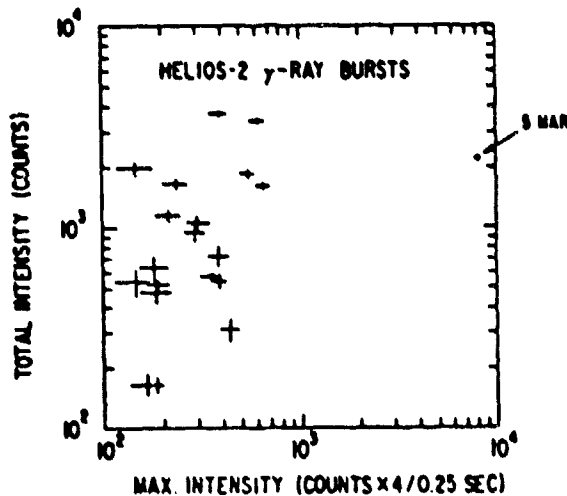

MAX. INTENSITY (COUNTS×4/0.25 SEC)

Fig. 11. Diagram of total versus maximum intensity for the gamma-ray bursts observed with Helios-2 from 1976 up to the 1979 March 5 event. The more extensive burst observations of the Vela system cannot be used for this purpose since they employ a geometrically lengthening time base whereas bursts do not always have maximum intensity near onset. If a search is made for Vela transients of March 5-like character, however, a comparison of total versus onset intensity gives a similar result.

March 5 event. It is also the case that this is the most intense event monitored with the Vela satellites for the decade beginning in 1969 (R. Klebesadel, private communication). The observed intensity is at least several times 10^{-3} erg cm^{-2} sec^{-1}, a lower limit due to the unknown fluxes below the 30 to 50-keV instrument thresholds and to the unknown effects of pulse pile-up at these energies (considering that most instruments were running near saturation). The intensity of the oscillating portion is $\sim 10^{-2}$ that of the peak; since this event is so intense relative to most gamma ray bursts, it is possible that some of the classical events of average or weak intensity could possess an analogous but unobservable periodic decay component.

The spectrum of the March 5 event is another of its anomalies. Although both this event and some classical events have the famous 420-keV feature,[4,5,6] this event has a considerably softer spectrum below ~ 100 keV than do typical classical bursts. Figure 12 illustrates the spectra of the peak of the March 5 event and of the oscillating portion,[4] compared with that of a typical classical event. The 420-keV feature is clearly evident in the intensity peak (the loss of the ISEE-3 germanium spectrometer, 2 months earlier, deprived us of a knowledge of the inherent width of this peak). Besides the excess in the 30 keV region and the 420-keV feature, the other well-known aspect of this spectrum is the lack of
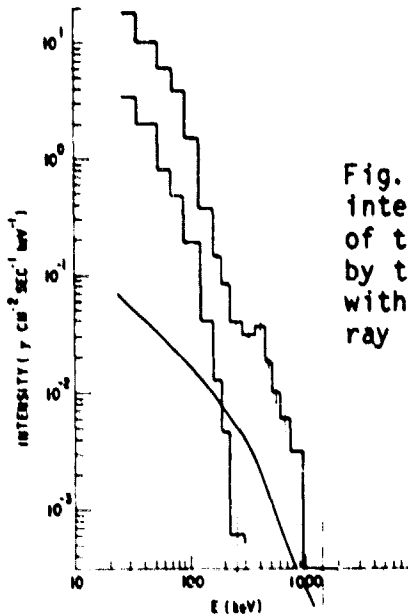
Fig. 12. The photon number spectra of the intensity peak of the March 5 event and of the oscillating portion, as observed by the Leningrad group,[4] as compared with that of a typical 'classical' gamma ray burst.
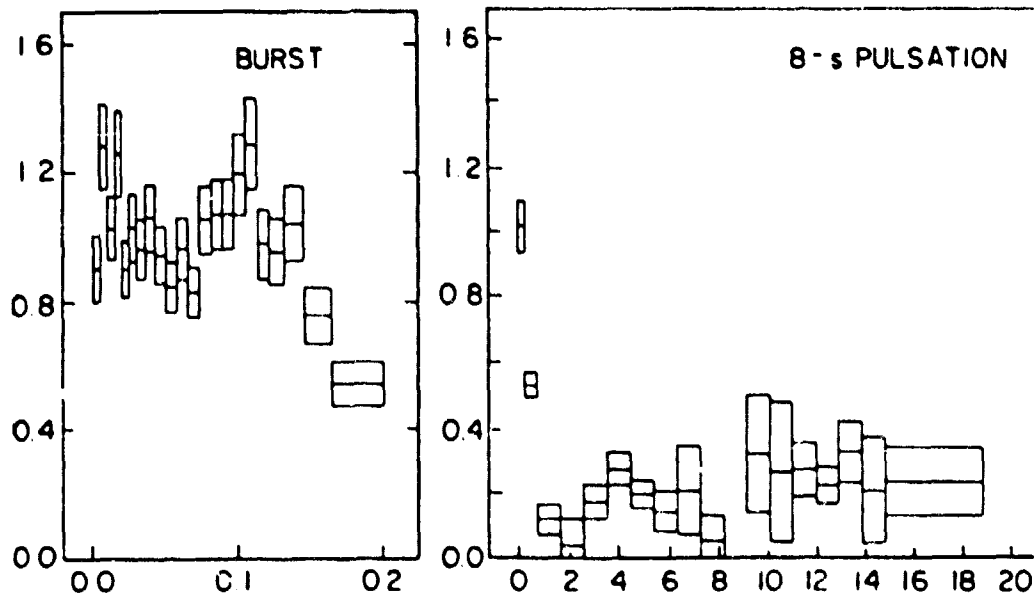

Fig. 13. Pioneer-Venus-Orbiter measurements of the spectral hardness of the March 5 event (in the above/below 100-keV region), illustrating variable behavior at the onset and shoulder of the intensity spike, and ■ in phase with the first two oscillations.

higher energy photons, particularly above 1 MeV. This deficiency is probably due to the fact that photons above the pair production

threshold energy would be, of necessity, removed by that process due to the extreme density at the source, particularly if the source is very distant.[16] The spectrum of the oscillating portion of the event is even softer than of the onset, with no detectable counts as high in energy as 400 keV. The only other published spectral observations of this event are shown in Figure 13, illustrating a spectral hardness factor (counts > 100 keV/50-100 keV) as a function of time.[11] The hardness is maximum at the onset and at the time of the change of rate of intensity decay, or shoulder, at ~ 100 msec into the event. As shown in the second illustration, the spectral hardness in the periodic portion is less than in the onset, in agreement with the Leningrad results, but is shown to vary in phase with the 8-second oscillation, with higher energy photons in greater quantity during the times of greater intensity.[11]

RECURRENT EVENTS

The March 5 event was the first gamma ray transient to exhibit recurrent events, i.e., to be associated with repeated bursts having a common source direction. Three events of very weak intensity, detected only with the Leningrad experiments on Venera-11 and -12, were observed to follow the March 5 event by delays of ~ 0.60, 29 and 50 days with intensities ~ 3, 1 and 0.5 percent that of the March 5 intensity, respectively.[15] Their time histories, shown in Figure 14, are not the same (on a reduced scale) as the March 5 profile but generally slower, although their spectra, as seen in
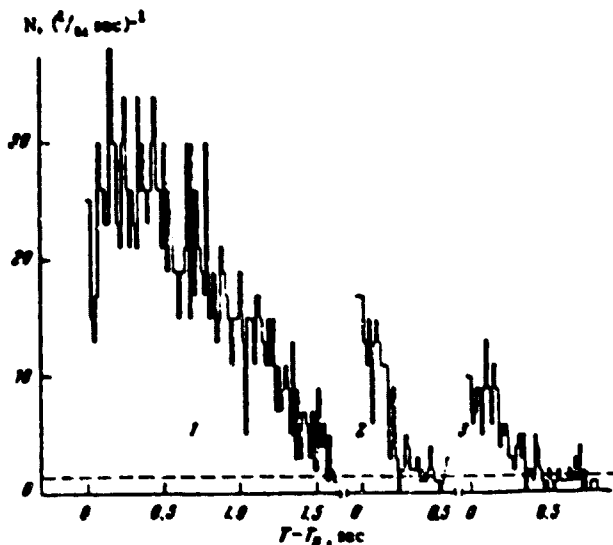

Fig. 14. Counting rate histories of the delayed March 6, April 4 and April 24 events, found to have source directions consistent with that of the March 5 event.[15]
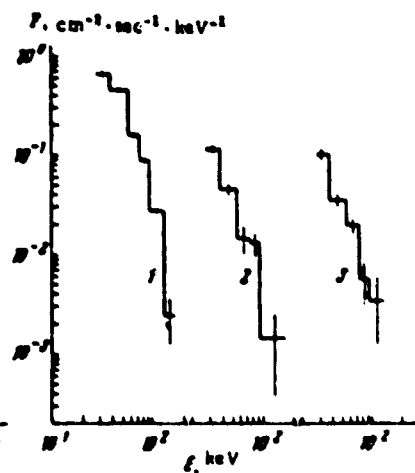
Fig. 15. Spectra of the events of the previous figure, seen to be not unlike that of the decay portion of the March 5 event.[15]

Figure 15, are similar to that of the softer, oscillating portion although statistically limited due to their very low intensity. Their directions agree with that of the March 5 event (the Venera-11 to Venera-12 time delays provide an accurate one-dimensional source measurement in conjunction with a rough source direction estimated from the directional count rate characteristics). Given their sequential connection to each other and to the March 5 event, it is entirely reasonable to assume this to be the discovery of a common burst source emitter. Only one other series having a common source direction has been detected;[17] however, that 3-event series does not follow any intense primary or 'parent' gamma ray transient. Its source direction is in the galactic plane at ~ 45 degrees galactic longitude, consistent with either a nearby or a very distant galactic source object.

DIRECTION

One remarkably fortuitous historic accident was that of the occurrence of the March 5 event during the October 1978 to December 1979 time frame. This is the interval when the interplanetary gamma ray burst network possessed its full instrument complement and was positioned in trajectories far from the Earth for their maximum interspacecraft event timing resolution. The identification of the supernova remnant N49 in the neighboring galaxy of the Large Magellanic Cloud as a possible source object was made as one of the first accomplishments of that network.[18,19] This measurement made possible the enlarged scientific controversy over the nature of the physical process involved by immediately creating the distinct possibility that the source object was at a 55-kpc distance, two to three orders of magnitude farther than would have been assumed had the directional information consisted instead of the formerly available resolution. That would have been several square degrees, providing only rough overlap of the LMC and various stellar regions in the constellation of Dorado at 30-odd degrees negative galactic latitude. Figure 16 illustrates the source location, and shows the extent of the densest optical part of N49. Another aspect of this identification is that,by contrast, high-precision directional studies of classical gamma ray bursts made with this network have provided source fields that are optically empty down to at least the 18th magnitude.[20,21] An additional factor is the fact that N49 is an X-ray emitter, strengthening the case for its identification, since one might assume there would be some X-ray/gamma-ray correlation. Finally, it is also the case that not only other precise burst source locations but previous larger source field determinations also found no correlation with either transient or steady X-ray sources or other objects that could be obvious source candidates[22,23]. Figure 17 shows the source position plotted on the X-ray contours of N49 measured (quite accidentally) within a few days of the event with the Einstein Observatory.[24] A remarkable aspect of this X-ray survey, however, is the fact that no point source was found: this does not necessary provide a weakening of the association of the event with N49 since it yields an upper limit

(at   10-9) to the ratio of point source X-ray strength to burst
strength independent of source distance. (The X-ray measurements
also included a comparison, made by chance before and after the

Fig. 16.   Source location of the
March 5 event shown on a reproduction
of optical field, in which the
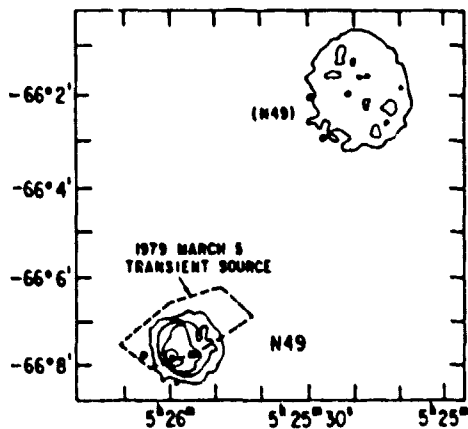densest portion of the N49 snr
nebula is visible.[19]

Fig. 17.   Source location of the
event[19] plotted on the X-ray
surface brightness contour map of the
N49 and (N49) region, as observed
with the Einstein Observatory high-
resolution imager.[24] Here the
nebula is seen as 2 arc minutes wide,
and the nearest neighboring nebula,
(N49), is resolved at the weakest
intensity level. No point X-ray
source was resolved. No change in
X-ray intensity above ~ 2×10^{-12}
erg cm-2 s-1 was observed from
shortly before to several days after
the event. A comparison X-ray study
with Einstein has been recently made
to search for a slow, delayed effect,
but the results are not available at
this time.

burst, showing again an upper limit of ~ 10-9 to the intensity
change ratio.) Thus, the fact that N49 is an extended object,
suggesting a greater likelihood of chance association, is contrasted
by the facts, supporting its identification, that it is a supernova
remnant - an object associated with neutron star phenomena, and that
it is an X-ray emitter. Further, the visible stars in the source
field have been determined to be also at the same distance as the
LMC,[25] thereby removing their distraction from this association. Of

course, the argument for chance association is only a factor of two larger than if the candidate object were a point object, since the error box and N49 consist of about the same solid angle. That probability, considering the total solid angle of extended X-ray emitters and the total number of point X-ray sources (times the source box size) is between 10^{-5} and 10^{-6}, too small to be a strong argument against the identification. The basic argument against N49 is of course its distance and the $\sim 10^{45}$ erg sec^{-1} emission implied if the radiation in this event is isotropic.

DISCUSSION

The observations of the March 5 event, although inconclusive regarding the question as to whether this event is so different (that it must have been produced by an entirely different mechanism), clearly provides support for the hypothesis that its nature and possible origin at N49 are phenomena so unusual that they deserve critical study per se (rendering the question as to whether its understanding will enlighten us as to the nature of 'classical' gamma ray bursts, or vice versa, as secondary). A variety of early papers concerning this event tended to dismiss the N49 association as chance, avoiding the very real problems in the theoretical contortions necessary to get around the photon self-absorption inherent in fitting a physically possible mechanism to the 10^{45} erg sec^{-1} luminosity required by an isotropic N49 emission.[4,24,26,27,28] It had been known for some time that gamma ray burst intensities implied a several hundred pc source distance if treated at face value, given that the spectra entended beyond the pair production threshold;[16,29] recent updates show that, given nearby classical burst source distances,[30] the March 5 event source distance would be accordingly only ~ 2 pc, keeping the optically thin Bremsstrahlung treatment.[31] Creative treatments of the March 5 issue, taking the N49 association as a serious and possibly fruitful possibility, have only recently started to gain momentum.

The first detailed calculations of the March 5 event spectrum, treating the process of pair production, annihilation and scattering with an optically thin synchrotron mechanism (in the intense magnetic field of a neutron star requiring a ~ 20 percent gravitational redshift), fit the observations surprisingly well. Figure 18 shows the calculations of Ramaty and his coworkers, as outlined in a November 1979 gamma ray burst conference.[32] The low energy excess emission, the position and width of the line and the general shape of the continuum are all seen to be duplicated, in essence. The more worrisome problem of the source mechanism was first addressed in a sequel to this work, in which the same group showed that an earlier model of the storage of energy in neutron star vibrations, involving the release of (undetectable) gravitational radiation, provided a good fit of the vibrational damping time to the 150 msec width of the initial burst (see Figure 19). This model provided the necessary storage mechanism that made the 55-kpc distance physically
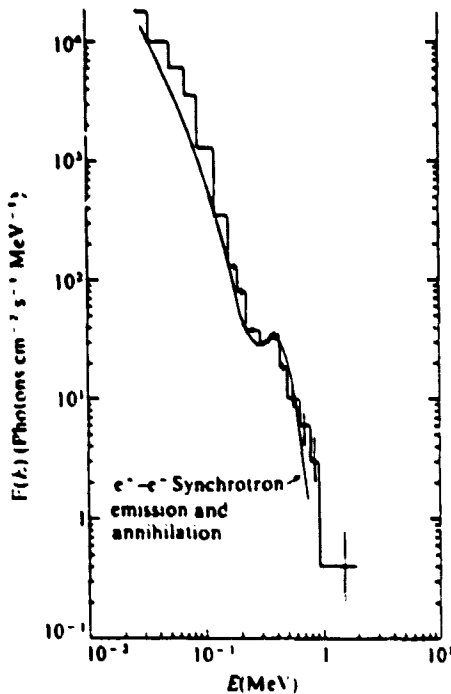
Fig. 18. The calculated spectrum of the intense portion of the March 5 event, based on an annihilation-creation model incorporating synchrotron losses and a redshift effect in a neutron star environment,[32] compared with the observations.[4]
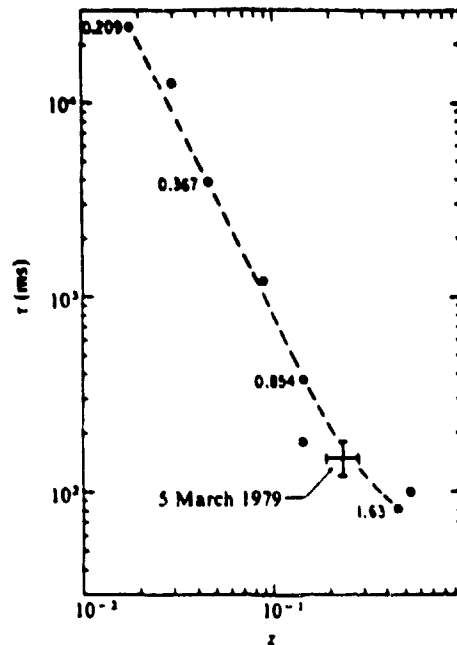
Fig. 19. The quadrupole gravitational radiation damping time versus gravitational redshift for neutron stars, with the dashed line connecting calculated values having the same equation of state, compared with the March 5 event.[15]

possible, and linked the internal, gravitational process to the external, magnetospheric, observable phenomenon. More recently, the Ramaty model has been extended by Liang to include the higher energy effects of the inverse Compton process.[33] These calculations not only fit the observed spectrum a little better, but also provide a derivation, from first principles, of the luminosity at ~ 10^{44} erg sec^{-1}, giving an order-of-magnitude fit to the N49 source. I do not illustrate it here since it is presented in this Conference.[33] Given that these calculational exercises provide consistency, or better, with the N49 source association, we are freed from the necessity of assuming that it must be a chance association. Final proof of which view may be correct is quite possibly a long way off, however.

An ongoing reanalysis of the March 5 event directional data has provided a more precise source location;[34] this new error box is inside N49 although not at its center (see Figure 20). The 0.1 arc min^2 size of this source field is only about 5 percent that of the original conservative treatment of essentially the same data, making searches for point objects possibly a lot easier, but reducing the
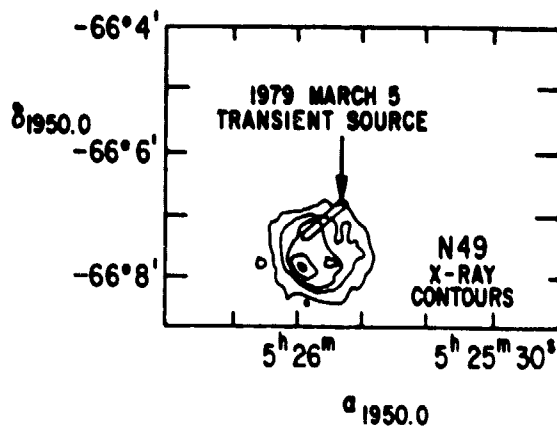
Fig. 20. The revised 1979 March 5 event source location, entirely consistent with N49 but in an eccentric location, 15 to 55 arc seconds from its center.[34] Given an unknown radial component, a possible location of the source may even be at the edge of the shell. This is the most precisely determined gamma ray source location in existence.

probability of chance identification with N49 by only a factor of two (since the N49 solid angle remains 2 arc min^2). This result would imply a motion of the neutron star from the center of the remnant, assuming N49 to be source, of ~ 900 ± 400 km sec^{-1}, if the age of the remnant is 10,000 years. This is probably not an entirely unreasonable value. Of course the neutron star involved in the March 5 emission may not be the parent neutron star of the N49 snr itself, given the snr and neutron star density in the LMC.

What then is the relationship of this event to the bulk of gamma ray bursts - why is there a gap in the size spectrum? No one would extend the N49 association to the point of attributing the March 5 event, as the brightest of all bursts, to an LMC origin because that galaxy is the nearest of the external galaxies that, in turn, produce the weaker, isotropically distributed, classical bursts. This size spectrum difficulty is avoided in one way by assuming that March 5-like events are rare, either intrinsically rare, as are supernovae themselves (perhaps for reasons that are related), or apparently rare, because of a beamed emission anisotropy (or a mixture of both); in this case the detection of one event in a decade from the neighboring galaxy LMC is not really less likely than from our own galaxy.[35] (The nearby origin model has no corresponding way out of the size spectrum difficulty, other than to invoke a simple accident of proximity, like the accident of coincidence with the direction of N49 itself.) Continuing this speculative notion, a possible link between the March 5 event and the other bursts is the series of three weak, delayed events, compared with the existence of another series of three small common-origin events that does not itself follow any identifiable large event. The source direction of that series, as noted above, is in the galactic disk at ~ 45 degrees galactic longitude.[17] That direction is consistent with a galactic source distance of up to perhaps 20 kpc, half the distance to the LMC, putting those events into a model of consistency with an N49 origin for the delayed March 6--April series, except that any primary or 'parent' event in this case was invisible, due perhaps to an anisotropy of emission. Are, in fact, the larger 'classical' gamma ray bursts also 'secondary,

delayed' emissions, but with repetition times outside the presently measurable several-year extents, perhaps linked to their greater intensity, relative to the March 6--April series? This would imply the existence of many apparently invisible March 5-like events, i.e., of the requirement of a narrow solid angle of emission, perhaps several hundred square degrees. Yet some link surely exists, defining the occurrence rate of the various kinds of transient events from each neutron star source. Finally, one can question the basic assumption of the neutron star gamma ray transient source concept, accounting for the 420 keV lines as evidencing a ~ 20 percent redshift, gravitationally required for a 1.4 M_0 neutron star, of the 511-keV line. The stimulated emission concept is shown in this conference to produce a 420-keV feature without the presence of a gravitational redshift.[1] Clearly a great deal of research is needed to investigate the emission characteristics implied, such as the amount of coherent beaming, that may clarify, eliminate or unify these ideas in terms of the relationship to gamma ray phenomenology of the 1979 March 5 event.

I wish to point out that I have not treated some very recently published theoretical studies of the March 5 event, but I do wish to refer them to your attention.[36,37,38,39,40]

Acknowledgements

REFERENCES

1. R. Ramaty, J. McKinley and F. C. Jones, Proceedings of this Symposium

2. T. L. Cline, Comments Ap. 9, 3 (1980).

3. T. L. Cline et al., Ap. J. (Letters) 237, L1 (1980).

4. E. P. Mazets, S. V. Golenetskii, V. N. Il'inskii, R. L. Aptekar' and Yu. A. Gur'yan, Nature 282, 587 (1979).

5. B. J. Teegarden and T. L. Cline, Ap. J. (Letters) 236, L67 (1980).

6. E. P. Mazets, S. V. Golenetskii, R. L. Aptekar', Yu A. Gur'yan and V. N. Il'inskii, Nature 290, 378 (1981).

7. E. P. Mazets et al., P.T.I. (Leningrad) preprints 599 and 618 (1979).

8. G. Pizzichini, Ap. Space Sci. 75, 205 (1981).

9. A. S. Jacobson, J. C. Ling, W. T. Mahoney and J. B. Willett, "Gamma Ray Spectroscopy in Astrophysics", NASA TM-79619, ed. T. L. Cline and R. Ramaty., p. 228 (1978).

10. R. E. Lingenfelter, J. C. Higdon and R. Ramaty, "Gamma Ray Spectroscopy in Astrophysics", NASA TM-79619, ed. T. L. Cline and R. Ramaty, p. 252 (1978).

11. E. E. Fenimore, W. D. Evans, R. W. Klebesadel, J. G. Laros and J. Terrell, Nature 289, 42 (1981).

12. G. Vedrenne, V. M. Zenchenko, V. G. Kurt, M. Niel, K. Hurley and I. V. Estulin, Soviet Astron. Letters 5, (6), 314 (1979).

13. S. Barat et al., Astr. Ap. 79, L24 (1979).

14. J. Terrell, W. D. Evans, R. W. Klebesadel and J. G. Laros, Nature 285, 383 (1980).

15. R. Ramaty, S. Bonnazzola, T. L. Cline, D. Kazanas, P. Mészáros and R. E. Lingenfelter, Nature 287, 122 (1980).

16. W. K. H. Schmidt, Nature 271, 525 (1978).

17. E. P. Mazets and S. V. Golenetskii, P.T.I. (Leningrad) Preprint 632 (1979).

18. W. D. Evans, R. Klebesadel, J. Laros, T. Cline, U. Desai, B. Teegarden and G Pizzichini, I.A.U. Circular # 3356, May 11 (1979).

19. W. D. Evans et al., Ap. J. (Letters) 237, L7 (1980).

20. J. G. Laros et al., Ap. J. (Letters) 245, L63 (1981).

21. T. L. Cline et al., Ap. J. (Letters) 246, L133 (1981).

22. T. L. Cline et al., Ap. J. (Letters) 229, L47 (1979).

23. T. L. Cline et al., Ap. J. (Letters) 232, L1 (1979).

24. D. S. Helfand and K. S. Long, Nature 282, 589 (1979).

25. G. J. Fishman, J. G. Duthie and R. J. Dufour, 1981, Ap. Space Sci. 75, 135 (1981).

26. F. A. Aharonian and L. M. Ozernoy, Astron. Tsirkulyar # 1072, 1 (1979).

27. G. S. Bisnovaty-Kogan and V. M. Chechetkin, S.R.I. (Moscow) preprint # 561 (1980).

28. I. I. Kumkova and I. G. Mitrofanov, 1980, Pis'ma Astr. Zh., 6, (4), 213 (1980).

29. G. Cavallo and M. J. Rees, Mon. Not. R. Astron. Soc., 183, 359 (1978).

30. D. Gilman, A. E. Metzger, R. H. Parker, L. G. Evans and J. I. Trombka, Ap. J. 236, 951 (1980).

31. M. Ruderman, Erice reprint (1981).

32. R. Ramaty, R. E. Lingenfelter and R. W. Bussard, Ap. Space Sci., 75, 193 (1981).

33. E. P. T. Liang, Nature 292, 319 (1981).

34. T. L. Cline et al., in preparation.

35. T. L. Cline, U. D. Desai and B. J. Teegarden, Ap. Space Sci 75, 93 (1981).

36. J. I. Katz, preprint (1981).

37. R. Hoshi, C.F.A. preprint 1495 (1981).

38. Qu Qin-yne, Wang De-Yu, Xu Ao-Ao, and Li Ze-qing, Proceedings of the 17th Cosmic Ray Conference, Paris, 1981, Paper XG 2.2-4 (1981).

39. A. K. Drukier, Proc. 17th Cosmic Ray Conference, Paris 1981, Paper XG 2.2-11 (1981).

40. T. M. K. Marar, A. K. Jain, D. P. Sharma, K. Kasturirangan and U. R. Rao, Proc. 17th Cosmic Ray Conference, Paris 1981, Paper XG 2.2-3 (1981).

GAMMA-RAY BURST SPECTRA

B. J. Teegarden
NASA/Goddard Space Flight Center
Greenbelt, MD 20771

ABSTRACT

A review of recent results in gamma-ray burst spectroscopy is given. Particular attention is paid to the recent discovery of emission and absorption features in the burst spectra[10,11,13,14]. These lines represent the strongest evidence to date that gamma-ray bursts originate on or near neutron stars. Line parameters give information on the temperature, magnetic field and possibly the gravitational potential of the neutron star. The behavior of the continuum spectrum is also discussed. A remarkably good fit to nearly all bursts is obtained with a thermal-bremsstrahlung-like continuum. Significant evolution is observed of both the continuum and line features within most events.

INTRODUCTION

This paper is intended as a review of the measurements to date of the spectral characteristics of gamma-ray bursts (GRB). It will also cover to a certain extent the theoretical interpretation of these results where it relates in a direct way to the understanding of the observations. Within recent years GRB spectral measurements have begun to reveal a very rich phenomenology and to make a major contribution to the understanding of the origin and physics of GRB's.

Early measurements[1-8] were made with instruments designed for some other purpose than the detection of gamma-ray bursts. With the launching of instruments specifically designed to study the spectral characteristics of GRB's[9-14] a great variety of new observations have significantly extended our knowledge of the spectral behavior of GRB's. In particular the work of Mazets and his colleagues at the A.F. Ioffe Physical-Technical Institute[9-12], Leningrad, represents the most comprehensive study of GRB spectra presently available. Their data have among other things revealed the repeated presence of absorption and emission lines in GRB spectra. "Cyclotron" absorption features are very probably present in a major fraction of the events measured[10]. In addition, lines at 400-450 keV are seen in a smaller number of events that are probably from redshifted annihilation radiation[10]. Taken together these results are strong, if not compelling, evidence for the neutron star origin of GRB's.

In this paper the early spectral results are first briefly reviewed. Then the behavior of the GRB continuum spectrum, its form, variability, and evolution, is treated. Finally the absorption

and emission features, their relationship to other spectral
parameters and physical interpretation are discussed.

HISTORICAL OVERVIEW

Early results on GRB spectra[1-8,15] generally suffered from a
number of problems; e.g., poor statistics due to small detector
area, inadequate time resolution and variable intensity modulation
due to spacecraft rotation. The first published GRB spectra[1] were
derived from a small instrument on the Imp-6 spacecraft intended to
measure solar flare X-rays and interplanetary positrons. Spectra
from six events were reported covering the energy range from 0.1-1.2
MeV. The spectral form for all events was consistent with a simple
exponential form $\exp(-E/E_O)$ with $E_O = 150$ keV. In a subsequent
paper[2] using data from the Imp-7 spacecraft they presented further
evidence that event-integrated GRB spectra could be represented by a
single functional form. This time the original 150 keV exponential
was modified by the addition of a power-law high energy tail
$(E^{-2.5})$. The Imp-7 spectra of Cline and Desai[2] are reproduced in
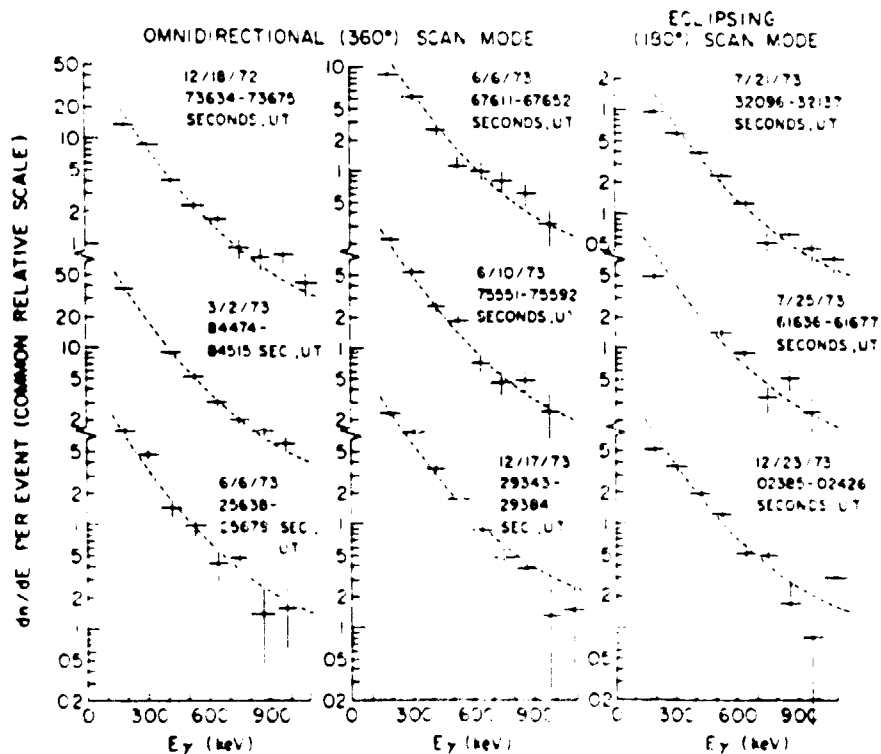Figure 1. Other contemporaneous results[3,4,6,15] were consistent

Figure 1. GRB spectra from the Imp-7 experiment of Cline and co-
workers[2]. A single functional form consisting of a 150 keV
exponential with a power-law tail appears to fit all the events.

with this picture. We shall see later, however, that this simple
picture was, in fact, not correct and that spectral variability from
event-to-event and evolution within individual events are, in fact,
typical characteristics of GRB's.

Of the early GRB spectral results, the most precisely
determined spectrum was that of the event of 1972 April 27 as
measured by the γ- and X-ray spectrometers on Apollo 16[6]. This
spectrum is shown in Figure 2. A combination of two detectors, (1)
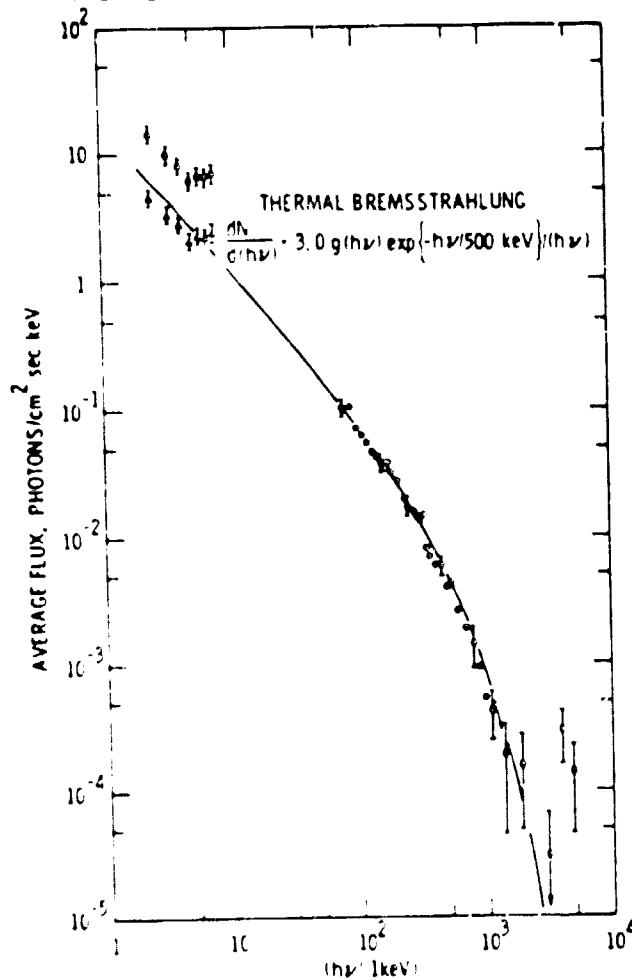an X-ray proportional counter and (2) an NaI γ-ray spectrometer,

Figure 2. Spectrum
of the Apollo 16
GRB[16] averaged over
the entire event.

gave the widest energy coverage (2 keV to 5 MeV) of any GRB thus far
recorded. An unfortunate gap between the coverage of the two
instruments in the 10-60 keV range may have precluded them from
making the first discovery of cyclotron lines in GRB's. In a
subsequent paper Gilman et al.[16] showed that the Apollo 16 data
could be fit remarkably well by a thermal-bremsstrahlung spectrum
with a temperature of 500 keV. It should be noted that this fit to
the data was quite good over a range of three decades in energy.
The authors naturally assumed that the burst source was, in fact, a
hot optically thin plasma. To maintain the observed spectral shape,
the source must be optically thin to Compton scattering. In

addition, it is possible to place a limit on the size of the emitting region the Apollo 16 event based on the most rapid time variations observed during the event. Variations as fast as 110 msec were seen, which imply a source size $\lesssim$ 3000 km. These assumptions taken together allow one to place a limit on the distance to the source of $\lesssim$ 50 pc. This early result did, in fact, establish a correct spectral form for GRB's (i.e., a thermal-bremsstrahlung-like spectrum). The interpretation, however, in the light of more recent data[10,11] is almost certainly not correct. Later results will show that the emitting region is probably not optically thin and dominated by free-free emission.

THE CONTINUUM SPECTRUM

The KONUS experiment of E. P. Mazets and coworkers at the A. F. Ioffe Institute, Leningrad has yielded by far the most comprehensive set of data on the spectra of gamma-ray bursts[9,10,11]. Their relatively simple instrumentation consists of six NaI scintillators each of ~ 50 cm^2 area arranged to provide complete sky coverage. The spectrum is measured over the 30 keV-1 MeV interval in 16 channels. Identical instruments were carried on board the Venera-11 and -12 spacecraft. The fortunate combination of all-sky coverage, absence of earth occultation and magnetospheric background effects and a 1 1/2-year active lifetime has produced a data sample of ~ 150 GRB's. The spectrum of the 1970 April 19 GRB as measured by the KONUS experiment[10] is reproduced in Figure 3. As was true with the
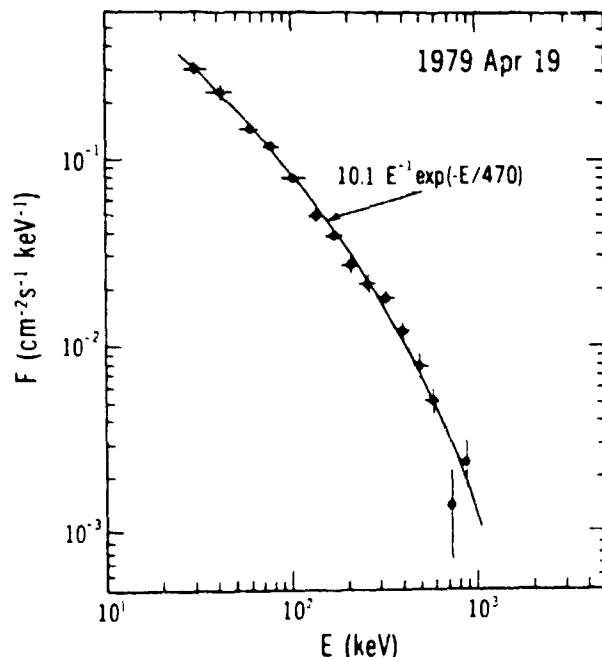

Figure 3. Spectrum of the 1979 April 19 GRB from the KONUS experiment at the maximum of the event.

Apollo 16 event, this GRB is well fit by a thermal bremsstrahlung-like spectrum. In fact, the radiation temperature of 470 keV is close to that of Gilman et al.[16]. However, it should be pointed out that Gilman et al.[16] incorporated a Gaunt factor into their fit and

Mazets et al.[10] did not. This leads to somewhat higher radiation
temperatures than otherwise. Of the published spectra of Mazets and
coworkers, nearly all can be fit with a spectral form
$dN/dE \propto \frac{1}{E} \exp(-E/E_o)$. The observed range of radiation temperatures
E_o is quite broad--from ~ 30 keV to more than 1 MeV. That a single
spectral form provides an excellent fit to the great majority of
events over such a broad range of radiation temperature is a remarkable
and significant feature of GRB's and one that GRB models must now
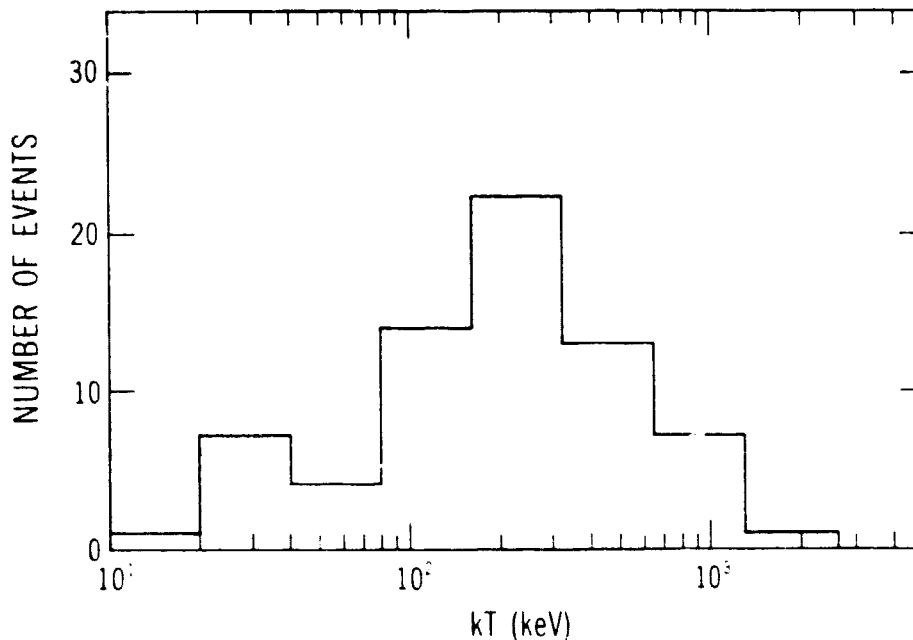incorporate. In Figure 4 the distribution of the number of events

Figure 4. Number of events vs. maximum radiation temperature[11].

versus maximum radiation temperature is plotted[11]. The distribution
is broad with a maximum at 200-300 keV.

Recently the first results from the γ-ray spectrometer on the
Solar Maximum Mission (SMM) have been reported by Share et al.
1991[17]. In slightly more than a year the instrument has detected 17
events in the energy range 300 keV to 8 MeV. The large volume of
NaI detectors make this the most sensitive instrument for GRB
spectroscopy thus far flown. Unfortunately however, the low energy
threshold is at ~ 300 keV. They find in at least one case (1990
April 19) that the spectrum is consistent with an $E^{-2.5}$ power law in
the .3-8 MeV interval. Since their energy window is different from
that of Mazets et al.[10,11], it is not clear that this conflicts with
the Mazets observations. It may be, however, that they have found
evidence for a high energy tail that departs from the thermal
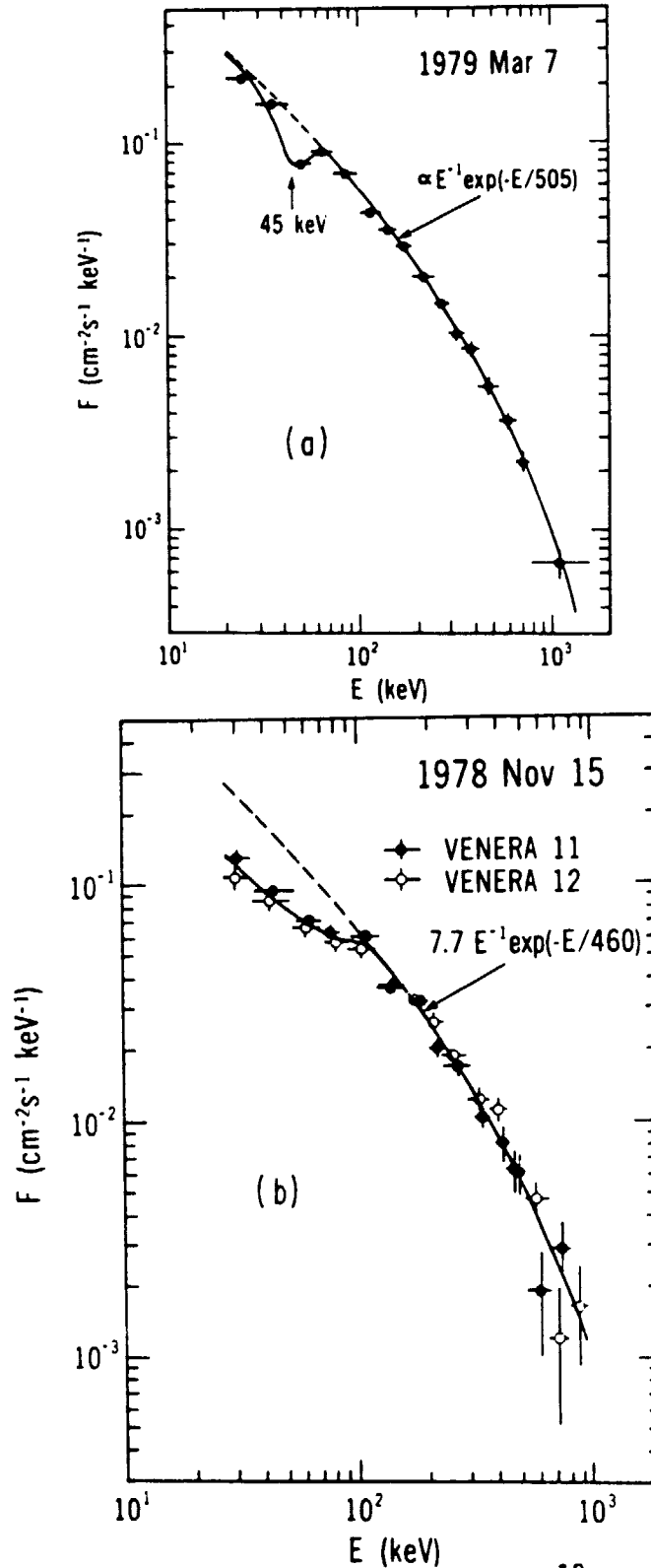bremsstrahlung-like spectrum.

Figure 7. (a) Spectrum of the 1979 Mar 7 GRB[10] showing a "cyclotron" absorption line. (b) Spectrum of the 1978 Nov 15 GRB[11] showing a broad absorption band extending from ~ 30 to 100 keV.
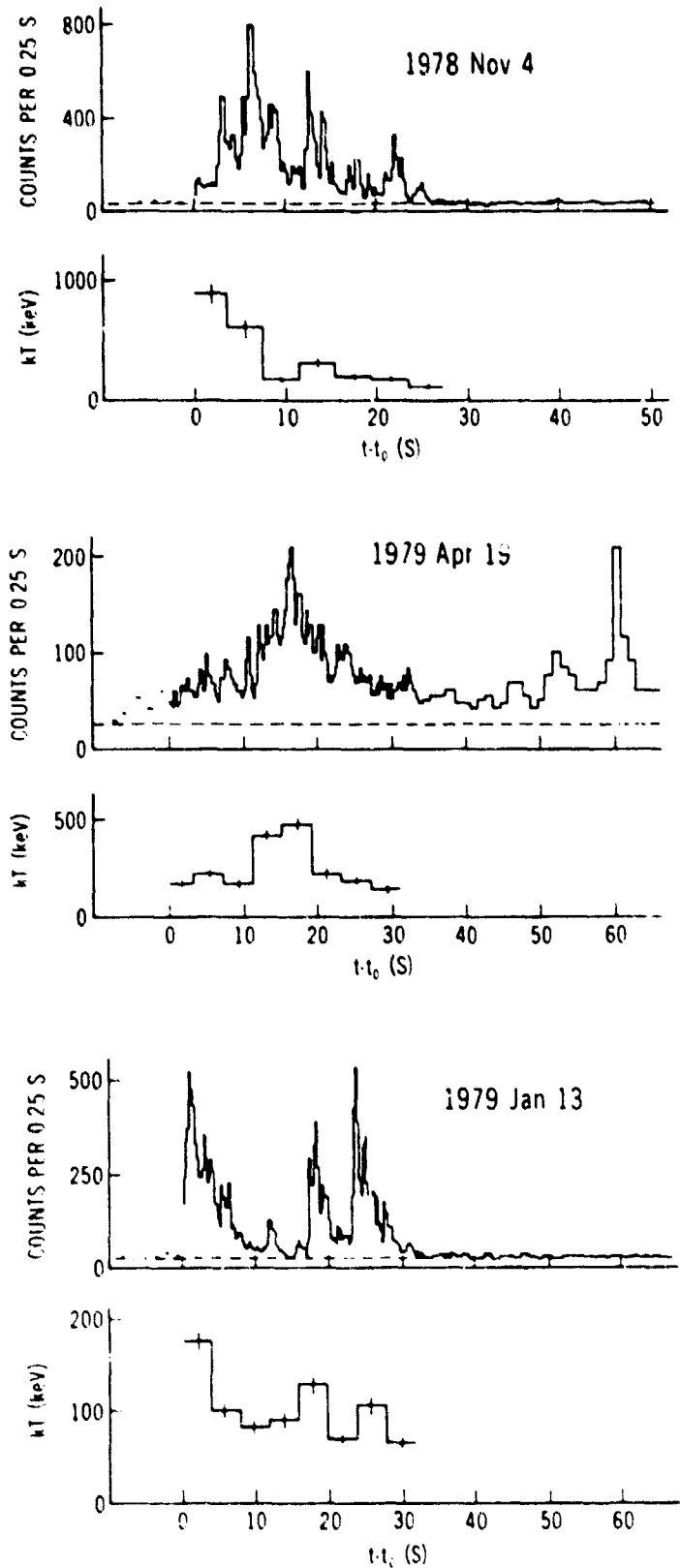
Figure 6. Time histories of the intensity and radiation temperature for 3 separate events[11].

and 1979 January 13 do appear to display a correlation between radiation temperature and intensity. The former shows a radiation temperature that peaks well into the event, and the latter shows a definite correlation of the temperature with subsidiary peaks in the count rate. It is evident that there is a rich variety of behavior present in the continuum spectra of GRB's. Some of the implications of this behavior will be discussed later in this paper.

EMISSION AND ABSORPTION LINES IN GAMMA-RAY BURST SPECTRA

a) Cyclotron Emission and Absorption Features

During the past year it has become apparent that emission and absorption features are common occurrences in the spectra of GRB's[10,11,13,14,18]. The most prevalent type of spectral feature that is seen is either an absorption line or broad absorption band in the 30-70 keV range[10,11]. Of the ~ 150 events recorded by the KONUS experiment, such features are seen in at least 30[10]. The proportion of events containing lines may, in fact, be even larger since the poor statistics of the smaller events may be masking the presence of these features. Two examples of "cyclotron" absorption features are given in Figure 7a,b[10]. The spectrum of the 1979 March 7 event (Figure 7a) clearly exhibits an absorption feature at ~ 45 keV having a FWHM of 15-20 keV and an equivalent width of 7 ± 0.6 keV[10]. The 1978 November 15 event[11] (Figure 7b), on the other hand displays a broad absorption band extending from ~ 100 keV down to at least the 30 keV threshold of the instrumnent. Note that there is excellent agreement between the spectra measured on the two different spacecraft. Evolution of the "cyclotron" absorption feature during an event is shown in Figure 8[10]. The first 8 sec. of the event plotted in the left panel of the figure clearly shows an absorption line at 65 keV superimposed on a thermal-bremsstrahlung-like continuum spectrum having a radiation temperature of 240 keV. The right hand panel shows the subsequent 24 sec where the line feature has completely disappeared. Furthermore, the radiation temperature has increased to 480 keV. In nearly all of the events studied by Mazets et al.[10,11] the absorption features are present for less than the total duration of the event. Furthermore, they are always strongest during the initial phase and tend to decay away more rapidly than the overall burst intensity. In general the behavior of the absorption feature is not well correlated with the behavior of the continuum spectrum of the burst[11].

At the present time, only one possible confirmation of the presence of cyclotron absorption features in GRB's is known to us. This is the event of 1980 April 19 as recorded by the Hard X-Ray Burst Spectrometer on SMM[18]. The general character of the absorption feature as well as its time variability appear to be consistent with the behavior of the events reported by Mazets et al.[10,11]. The issue, however, is somewhat confused by the fact that a solar origin cannot be ruled out. It should be pointed out that solar origin any of the Mazets events is ruled out since directions are determined for each event by the KONUS experiment.
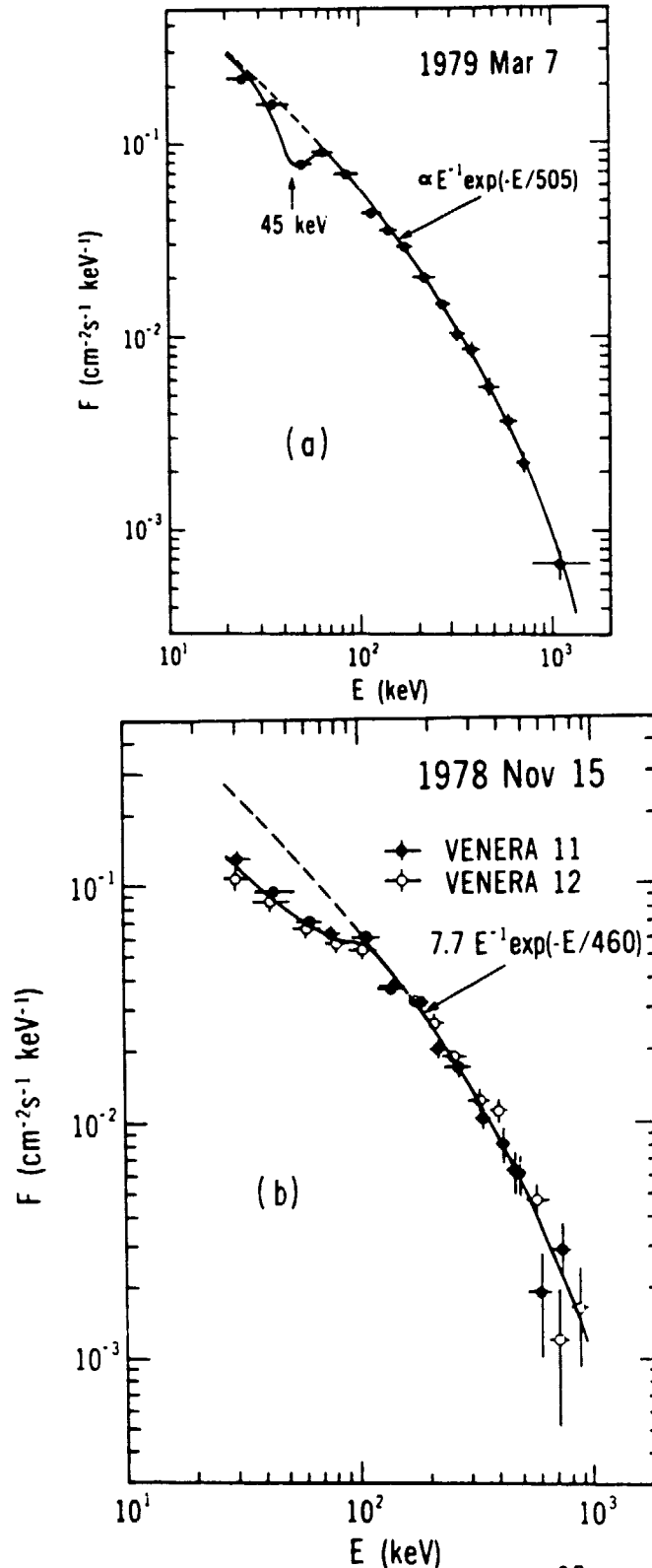
Figure 7. (a) Spectrum of the 1979 Mar 7 GRB[10] showing a "cyclotron" absorption line. (b) Spectrum of the 1978 Nov 15 GRB[11] showing a broad absorption band extending from ~ 30 to 100 keV.
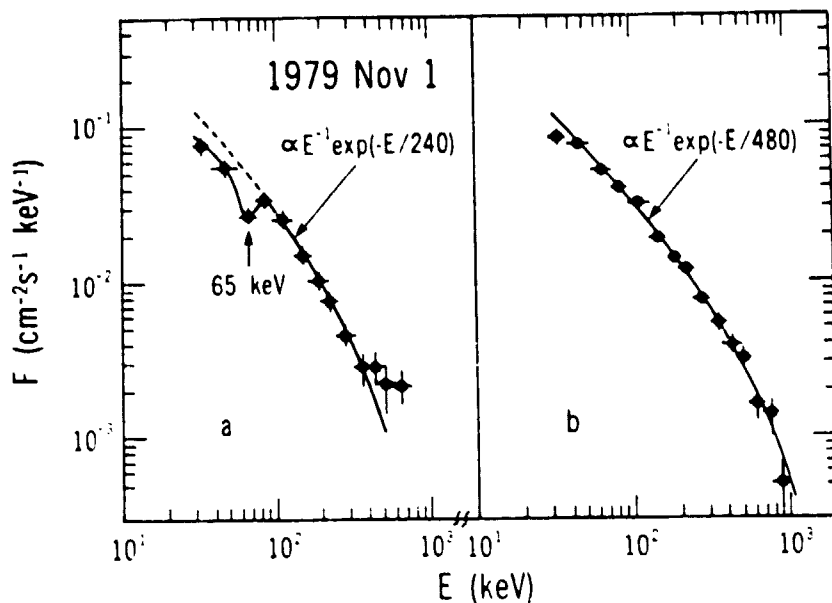
Figure 8. Spectrum from the 1979 Nov 1 GRB from the KONUS experiment. Left hand panel is the first 8 sec. of the event. Right hand panel is the subsequent 24 sec.

A very striking example of spectral evolution during a burst is given in Figure 9 where the usual "cyclotron" absorption feature is seen during the early phase of the event superimposed on a 400 keV continuum spectrum[10]. Note, however, that the lowest energy point at $\sim$ 20 keV departs significantly from the thermal-bremsstrahlung representation, indicative of the possible presence of a separate soft component. A second spectrum is plotted that was taken during a minimum intensity period of the event occuring at an intermediate time within the burst. The two lowest energy data points have not changed. The hard 400 keV spectrum previously present above $\sim$ 70 keV has, however, now completely disappeared. Only a very soft spectrum, which appears as a continuous extension of the unchanged low energy data points, now remains. This event seems to have two components, a soft one that remains more or less constant and a hard one that is time-variable. We shall return to this point later as a number of other observations suggest that a two-component model is appropriate.

The detailed characteristics of the "cyclotron" features appear to bear little or no relationship to the properties of the continuum spectrum. One can use the Mazets et al.[10], published data to calculate an effective "FWHM" by dividing the equivalent width by the depth of the absorption feature. For the broad band features this "FWHM" should be interpreted as a lower limit on the true width since the features generally extend below the instrumental threshold.

1979 Mar 29

- • - 1
- ○ - 2

$\propto E^{-1} \exp(-E/400)$

50 keV

$2'$

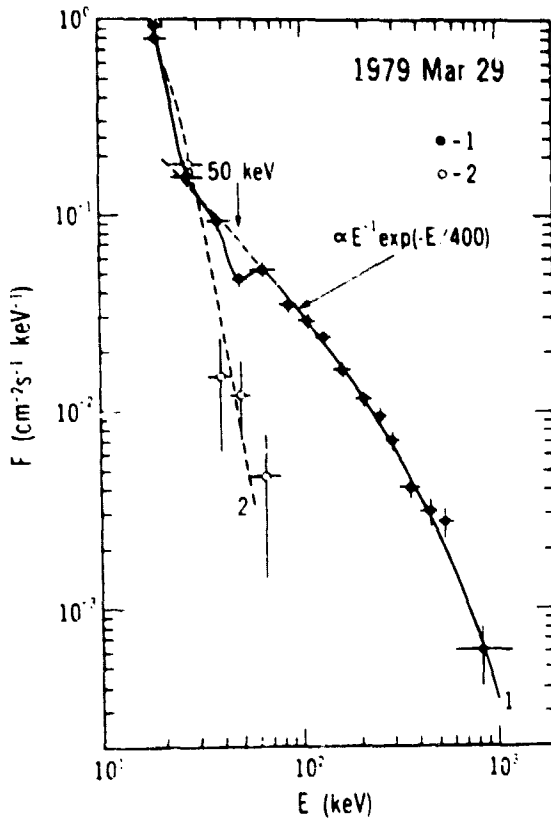1

F $(cm^{-2}s^{-1} keV^{-1})$

E (keV)

Figure 9. Spectra from the 1979 Mar 29 GRB from the KONUS experiment. Solid line is from the initial stage. Dashed line is from a deep minimum between burst peaks.

"FWHM" = 938 W/h

W = EQUIV WIDTH
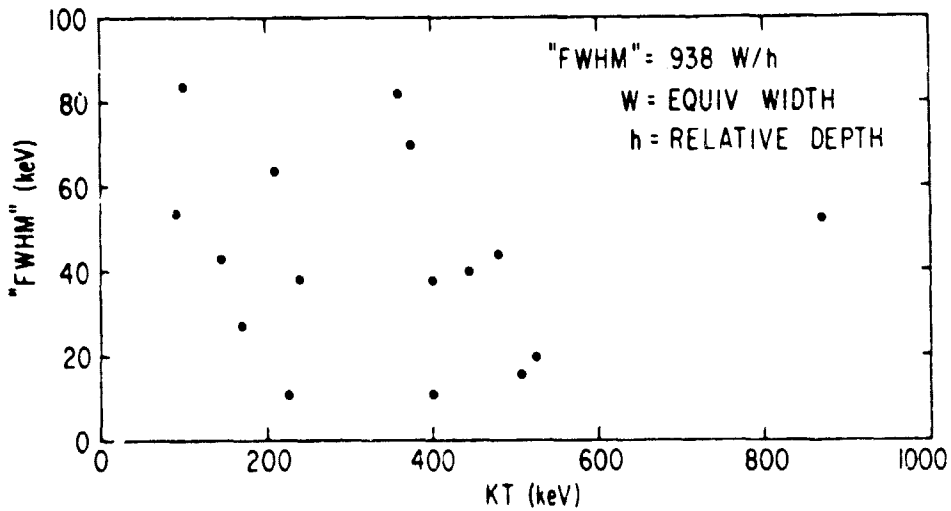
h = RELATIVE DEPTH

"FWHM" (keV)

KT (keV)

Figure 10. "FWHM" of cyclotron features vs. continuum radiation temperature for a sample of the KONUS events.

This effective "FWHM" is plotted in Figure 10 versus the continuum radiation temperature for the Mazets events where data are available[10]. There is obviously no evidence here for any correlation between the line width and the continuum temperature. This can be taken as further evidence that two different processes or regions are responsible for the line and continuum behavior.

One final example of a "cyclotron" feature is given in Figure 11[10]. This is the 1979 May 26 event which is the only published
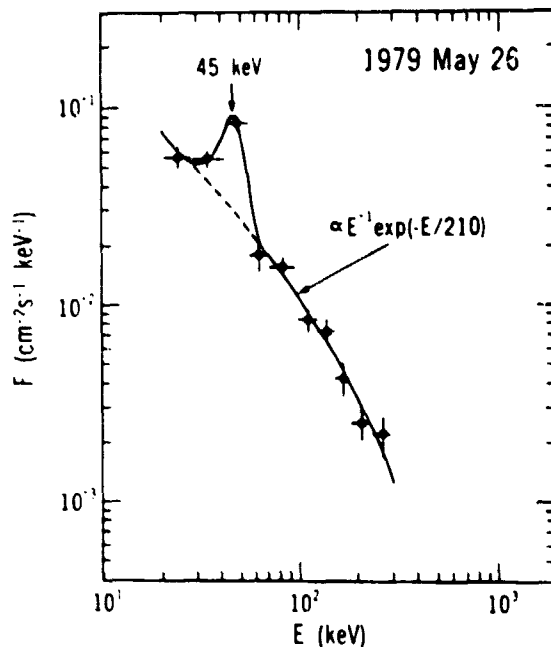

Figure 11.
Spectrum of the 1979 May 26 GRB from the KONUS experiment[10]. A "cyclotron" emission feature appears at ~ 45 keV.

example of a "cyclotron" emission feature. It appears at an energy of 45 ± 5 keV and has a width of ~ 20 keV.

The persistent presence of these absorption and emission features in the 30-70 keV range of GRB spectra is strong evidence for a neutron star origin. In the intense (10^{12}-10^{13} gauss) magnetic fields that are expected to be present near the surfaces of neutron stars, the cyclotron frequency corresponds to photons in the hard X-ray range. The fact that such lines exist superimposed on a very hot continuum spectrum poses a problem. To produce a cyclotron absorption line requires that the electron temperature be smaller than the energy of the line (first Landau level). If the temperature were comparable to or higher than this, one would expect to see the line in emission. The one example of "cyclotron" emission (1979 May 26) may, in fact, be a case where the temperature in the emission region is higher than the first Landau level. The width of the line (in some cases $\lesssim$ 20 keV) imposes a further constraint on the temperature of the absorbing region. The Doppler broadening of the line is given by Trumper[19]:

$$\frac{\Delta E}{E} = \sqrt{8\ln2} \; \overline{\frac{kT}{mc^2}} \cos \theta$$

where θ is the angle between the line of sight to the observer and the magnetic field. Taking $\frac{\Delta E}{E} = 0.3$ and $\theta = 45^\circ$ gives $kT = 16$ keV for the electron temperature. To account for these observations it appears that one must postulate that the cyclotron absorption takes place in a relatively cool (< 20 keV) layer that overlies the hot region which produces the continuum spectrum.

We return now to the question raised in the previous chapter of whether optically thin thermal bremsstrahlung can be a realistic physical description of the radiation process during a GRB. The presence of cyclotron features in the 30-70keV range implies that 10^{12}-10^{13} gauss fields are present in the emission region. It is then extremely unlikely that free-free transitions will be the dominant mode of radiative transport. It is much more likely in this intense field that synchrotron radiation and related processes will dominate.

b) Emission Lines > 400 keV

Emission lines > 400 keV in GRB spectra have been reported by Mazets et al.[10,11] and Teegarden and Cline[13,14]. The former, as mentioned earlier used NaI scintillators, whereas the latter employed a radiatively-cooled Germanium detector. This instrument, launched on the ISEE-3 spacecraft, had a resolution of 8 keV at the time of launch. Unfortunately, after only 4 months of operation , an electronics failure disabled that portion of the memory in which GRB spectra were stored. As a result, high-resolution Ge spectra are available for only two events.

An example of an emission line at ~ 400 keV is given in Figure 12 for the event of 1978 September 18[10]. The line appears quite pronounced and is superimposed on a 185 keV thermal-bremsstrahlung-like continuum. As was the case with the "cyclotron" lines, the 400 keV features do not appear to bear any correlation with the continuum radiation temperature. Of the 150 events recorded by the KONUS experiment, 11 display emission features in the 400-460 keV range. These featur have been interpreted as redshifted annihilation radiation. Redshifts in the 15-20 percent range are expected for radiation produced near the surface of a 1 $M_\odot$ neutron star. This would shift the 511 keV annihilation line into the 400-460 keV range. There are, unfortunately, a number of factors that complicate this interpretation. First, for high electron temperatures the energy of the line will be blueshifted since all of the energy of the electrons (kinetic + rest mass) is converted into photon energy[20,21]. It is not clear, however, that electron temperatures high enough for this effect to be significant are consistent with the observations. In addition, the possibility of stimulated e^+-e^- annihilation exists if one is dealing with a cool dense electron plasma (Ramaty, private communication). It turns out
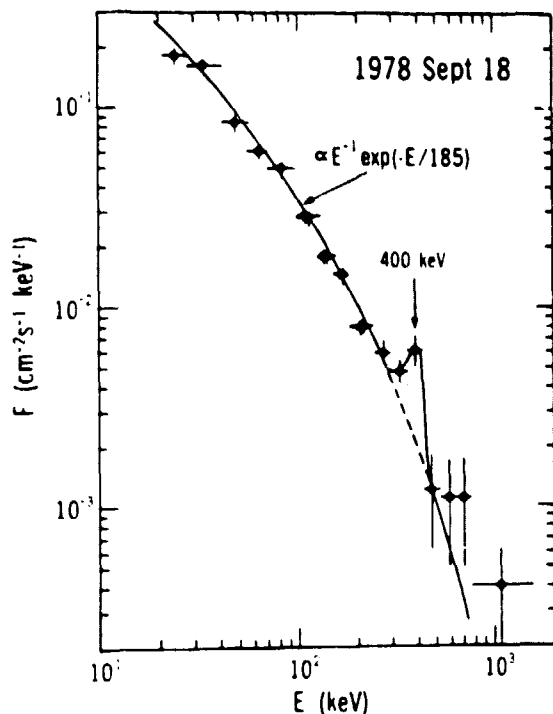
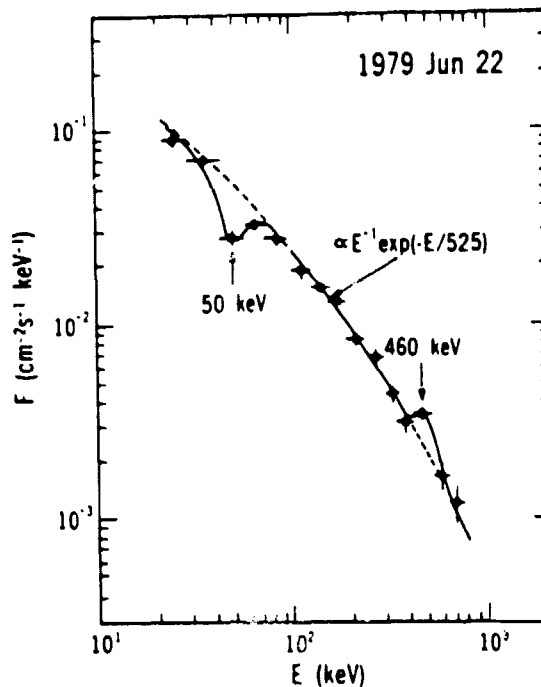Figure 12. Spectrum of the 1978 Sept 18 GRB from the KONUS experiment.[10]

Figure 13. Spectrum of the 1979 June 22 GRB from the KONUS experiment[10]

that the energy dependence of the photon absorption coefficient is such that a peak in the 400-460 keV range can be produced.

Figure 13 is an example of an event where both a "cyclotron" absorption feature and a 460 keV emission line are observed[10] simultaneously. There is only one other such example that has been published by Mazets and coworkers[11]. This is the event of 1979 November 1 which is reproduced in Figure 14. This single figure displays much of the rich phenomenology tnat has manifested itself in the spectra of GRB's. The left panel of the figure shows the first 8 sec of the event where both a ~ 65 keV absorption line and a broad emission feature in the 350-650 keV interval are seen. These lines lie on top of a 280 keV continuum. A profile of this emission band with the continuum subtracted is also shown. Typically, the ~ 400 keV emission features have widths of ~ 250 keV. In the right hand panel two spectra in the later portion (respectively ~ 16 sec and ~ 24 sec after the onset) of the event are displayed. Both the absorption and emission lines have disappeared. In fact, the typical behavior for the ~ 400 keV features is appearance at the onset of the event and a lifetime shorter than that for the total intensity. Such behavior, as was seen earlier, is also commonplace with the "cyclotron" features. During the intermediate porunion of the event, the radiation temperature rises to a value of 800 keV and
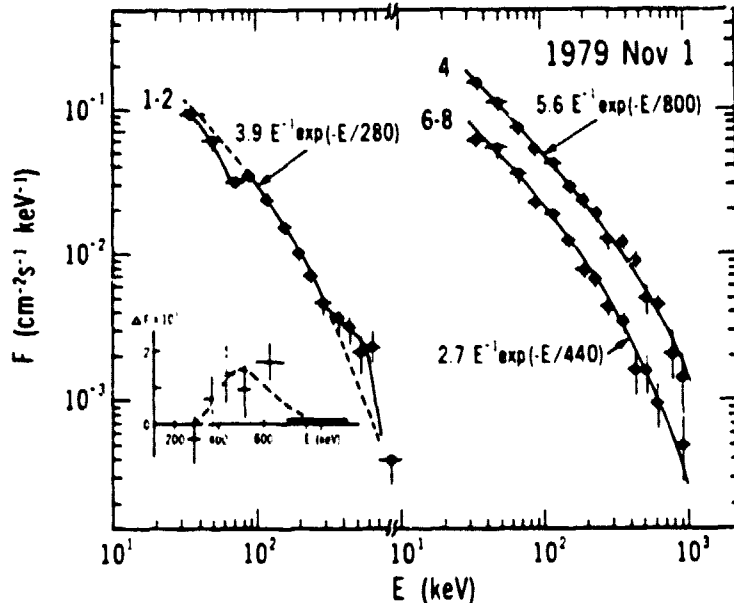
Figure 14. Spectra of the 1979 Nov 1 GRB from the KONUS experiment[11]. (1-2) first 8 sec of the event; (4) 4th 4-sec interval; (6-8) 6th, 7th and 8th 4-sec intervals.

then decays to a value of 440 keV in the latter portion. Curiously enough, the disappearance of the lines is accompanied by a heating of the continuum temperature. The general lack of correlation between the ~ 400 keV emission features and the continuum temperature can be taken as further evidence for the existence of two components in the GRB source. Furthermore, the observed broadening (~ 250 keV) of the annihilation line requires that the electron temperature be low. If the line width were entirely due to Doppler broadening, we would have $kT \approx 15$ keV. Furthermore, as pointed out by Daugherty and Bussard[22] and Mazets et al.[11], the radiation produced by pair annihilation in strong magnetic fields will be broadened by the presence of the field itself. In fact, this broadening mechanism in a field of 5×10^{12} gauss could account for the full observed width of the 400 keV lines.

Ramaty and coworkers[23,24] have proposed a model for the 1979 March 5 event where the radiation originates in a thin (~ 10^{-2} cm) surface layer that overlies a hot MeV plasma. They point out that electron cooling by synchroton radiation in a $\geq 10^{11}$ gauss field will generally take place more rapidly than e^+-e^- annihilation. In their model the continuum spectrum is therefore produced by the synchroton emission from the rapidly cooling electrons and positrons which subsequently annihilate and produce observable lines whose width is characteristic of the low temperature in this thin surface layer. The 1979 March 5 event is unique in a number of ways: (1) its luminosity is brighter than any other recorded event, (2) eight-

second oscillations were observed superimposed on a slowly decaying tail, (3) it has been identified with a supernova remnant, N49, in the Large Magellanic Cloud and (4) its continuum spectrum is very soft. These unique features may point to different physical conditions at the source of this event. It is nonetheless true that the Ramaty et al.[23,24] model for the 1979 March 5 event may be applicable to other GRB's.

A cool layer that is optically thin to Compton scattering appears to be required to explain the spectral behavior that has been recently observed. The fact that in many events $\gtrsim$ 1 MeV photons are present would imply that γ - γ pair production in the region immediately above the absorption layer is not an important process. Schmidt[24] has used this argument to place a limit on the distances of GRB sources. He assumed an emitting region of 10^9 cm extent and obtained a distance limit of $\lesssim$ 2 kpc for events in which MeV photons are present. The weight of recent evidence is towards a much smaller size ($\sim 10^5$ cm) for the emission region which in turn may lead to a smaller distance limit for the burst sources. The problem is, however, complicated by the strong energy and angular dependence of the cross-sections[25] so that detailed calculations will be necessary to establish a true distance limit.

Figure 15 shows the spectrum of the 1978 November 19 GRB as measured by the Germanium spectrometer onboard the ISEE-3 spacecraft[13,14]. A broad marginally significant feature is present at $\sim$ 400 keV that is consistent with the spectral feature reported by Mazets et al.[10] during this same event. In addition, the ISEE-3 data show a second line at an energy of 740 keV having a width of $\sim$ 40 keV. This line is significant at the 99 percent confidence level[13]. Teegarden and Cline[13] pointed out that the energy of this line is consistent with that expected if the 847 keV first excited level of iron is redshifted by the same amount as the $\sim$ 400 keV feature. It is perhaps significant that this event has the hardest spectrum of any thus far recorded and is one of the few that apparently cannot be fit with a thermal-bremsstrahlung function. The continuum spectrum for energies $\sim$ 200 keV-2 MeV best fit with an $E^{-1.3}$ power law[13].

If the assumption of a redshifted iron line is correct. then conditions at the source are probably such that other nuclear levels can be excited. We do not a priori know the composition of the source region. If it is pure iron, then we would see only higher levels of Fe nuclei, but if it is, for example, the same as the solar system composition, then excited levels of other nuclei would probably produce significant radiation. Ramaty et al.[26] have calculated the production of gamma-rays by cosmic rays interacting with the interstellar medium. We have normalized their iron line intensity to that of our 740 keV line and then plotted the most prominent lines > 740 keV normalized by the same factor and redshifted by the same amount as the Fe line. The Ramaty et al.
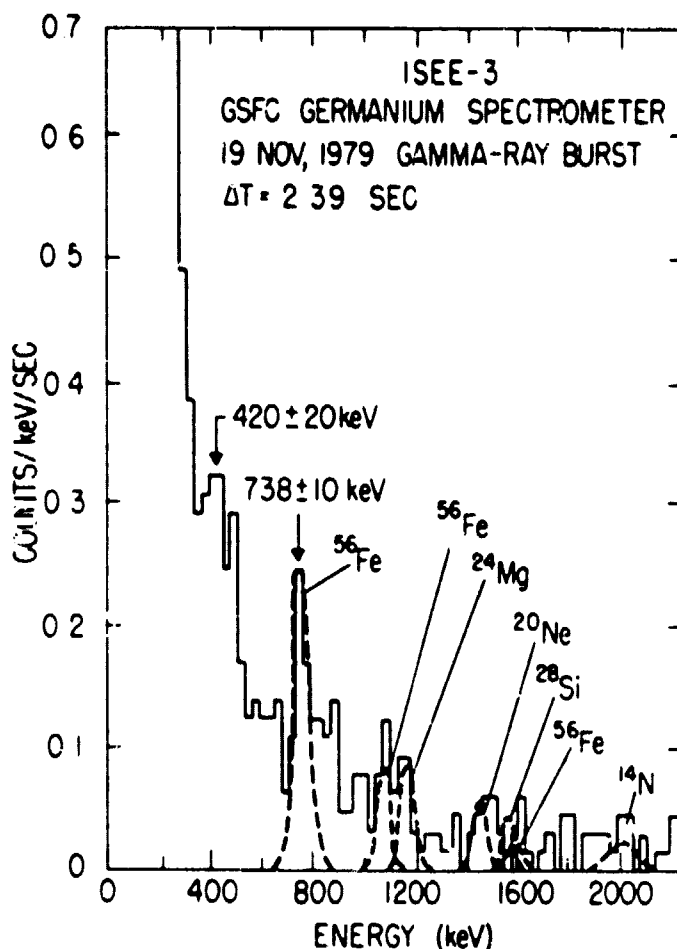
Figure 15. Spectrum of the 1978 Nov 19 event from the ISEE-3 Gamma Ray Burst Spectrometer[13,14].

calculations[26] that we used assumed an E^{-3} power law proton spectrum which may not be a good representation of the spectrum at the site of the GRB. The relative line strengths, however, are not strongly dependent on the shape of the proton spectrum but rather on the relative abundances and excitation cross-sections. It is evident in Figure 15 that these higher energy lines could make a signficant contribution to the > 1 MeV portion of the spectrum and that they might, in fact, account for the unusual hardness of the spectrum of this event.

Katz (1931) has put forth an alternate explanation for the 740 keV line. He has pointed out that for sufficiently high magnetic fields ($\gtrsim 10^{13}$ gauss) single photon annihilation will become the dominant mode. In this mode a single photon with energy 1.022 MeV is emitted so that the ratio of the two lines should in this simple-minded picture be a factor of two. The actual ratio in the data are ~ 1.76, but the peaks are broad enough so that a factor of two cannot be ruled out. Ramaty et al.[27] have pointed out that a

mechanism exists which can effectively shift the annihilation peaks toward lower energies and in general the one- and two-photon peaks will not be shifted by the same amount. It therefore remains unclear whether this can serve as an adequate explanation of the spectral features in the 1978 November 19 event.

SUMMARY AND CONCLUSIONS

The most important characteristics of GRB spectral behavior are summarized as follows:

1) The continuum spectrum is well represented by a thermal bremsstrahlung function with kT ranging between 30 keV and $\gtrsim$ 1 MeV. Possible evidence exists for a power-law high energy tail.

2) Significant evolution of the continuum sprectrum during the event is commonplace. The most typical behavior is a higher temperature during the early part followed by "cooling" or softening of the spectrum. There are, however, many examples of events where the temperature appears to be correlated with the intensity which may in turn possess complex structure.

3) "Cyclotron" absorption features in the 30-70 keV range are frequent, if not typical, occurrences in GRB's. At least 30 out of the 150 events recorded by the KONUS experiment display such features. Line widths vary from as small as ~ 20 keV (the probable instrumental limit) to broad absorption bands extending over more than 80 keV. "Cyclotron" features are normally present during the early part of the event and disappear before the event is finished. Little or no correlation exists between the continuum radiation temperature and the properties of the absorption lines.

4) Emission lines in the energy interval 400-460 keV are present in at least 7% of the GRB's. The features apparently are broad ($\Delta E \gtrsim$ 200 keV) and uncorrelated with the continuum temperature. As with the cyclotron features they appear at the onset and disappear before the event is over.

5) A narrow (~ 40keV) line has been reported in the 1978 November 19 event at 740 keV. This event has the hardest spectrum of any thus far recorded and is one of the few that apparently cannot be fit by the thermal-brehmsstrahlung expression.

The principal conclusions that can be drawn from these observations are summarized as follows:

1) The "cyclotron" and 400-460 features can be taken as strong evidence for a neutron star origin for GRB's. The 400-460 keV lines are interpreted as redshifted annihilation radiation. The redshift is consistent with that expected from a 1-1.5 $M_\odot$

neutron star.

2) The presence of absorption features <70 keV and ~ 400 keV lines with $\Delta E/_E \sim 0.5$ appears to require the existence of a cool layer overlying the hot plasma in which the continuum is produced. Rapid synchrotron cooling is a possible mechanism for the production of such a layer.

3) The presence of ~ 1 MeV photons in many events requires that the distance to the source $D \leq 1$ kpc. At larger distances γ-γ absorption would strongly suppress the high energy photons.

4) Optically thin thermal-brehmsstrahlung is probably not a viable description of the radiation mechanism at the source. In the strong magnetic fields in the source region synchrotron emission and absorption are almost certainly much stronger processes. Any theory, however, must account for the fact that the continuum spectra of nearly all GRB's are extremely well fit by a thermal-brehmsstrahlung expression over a wide range (30 keV - 2 MeV) in energy.

5) The 740 keV line could be explained either by a redshifted iron line or single-photon annihilation.

REFERENCES

1. T. L. Cline, U. D. Desai, R. W. Klebesadel and I. B. Strong, Ap. J. (Letters), 185, L1 (1973).
2. T. L. Cline and U. D. Desai, Ap. J. (Letters), 196, L43, (1975).
3. W. A. Wheaton, M. F. Ulmer, W. A. Baity, D. W. Datlowe, M. J. Elcan, L. E. Peterson, R. W. Klebesadel, I. B. Strong, T. L. Cline and N. D. Desai, Ap. J. (Letters), 185, L57, (1973).
4. C. Pizzichini, G. G. C. Palumbo and A. Spizzichino, Ap. J. (Letters), 195, L1, (1975).
5. W. L. Imhof, G. H. Nakano, R. G. Johnson, J. R. Kilner, J. B. Reagan, R. W. Klebesadel and J. B. Strong, Ap. J., 191 L7, (1974).
6. A. E. Metzger, R. H. Parker, D. Gilman, L. E. Peterson and J. I. Trombka, Ap. J. (Letters) 194, L19, (1974).
7. S. R. Kane and K. A. Anderson, Ap. J., 210, 875, (1976).
8. S. R. Kane and G. H. Share, Ap. J., 217, 549, (1977).
9. E. P. Mazets and S.V. Golenetskii, Astrophys. Space Sci., 75, 47, (1981).
10. E. P. Mazets, S. V. Golenetskii, R. L. Aptekar, Yu. A. Guryan and V. N. Ilyinskii, Nature, 290, 378, (1981).
11. E. P. Mazets, S. V. Golenetskii, V. N. Ilyinskii, Yu. A. Guryan, R. L. Aptekar, V. N. Panov, I. A. Sokolov, Z. Ya. Sokolova and T. V. Kharitonova, A. F. Ioffe Institute preprint No. 719, Leningrad, (1981).
12. E. P. Mazets, S. V. Golenetskii, V. N. Ilyinskii, V. N. Panov,

R. L. Aptekar, Yu. A. Guryan, A. V. Dyatchkov, M. P. Proskma, I. A. Sokolov, Z. Ya. Soklova, N. G. Khavenson and T. V. Kharitonova, A. F. Ioffe Institute preprint No. 712, Leningrad (1981).

13. B. J. Teegarden and T. L. Cline, Ap. J. (Letters), $\underline{236}$, L67, (1980).

14. B.J. Teegarden and T. L. Cline, Astrophys. Space Sci., $\underline{75}$, 181, (1981).

15. G. G. C. Palumbo, G. Pizzichini and G. R. Vespignani, Ap. J. (Letters), $\underline{189}$, L9, (1974).

16. D. Gilman, A. E. Metzger, R. H. Parker, L. Evans and J. I. Trombka, Ap. J., $\underline{236}$, 951, (1980).

17. G. H. Share, M. S. Strickman, R. L. Kinzer, E. P. Chupp, D. J. Forrest, J. M. Ryan, E. Rieger, C. Reppin and G. Kanbach, to be published in the Proceedings of the 17th International Cosmic Ray Conference, Paris, France, (1981).

18. B. R. Dennis, K. J. Frost, A. L. Kiplinger, L. E. Orwig, U. D. Desai and T. L. Cline, proceeds of this conference, (1981).

19. J. Trumper, in Gamma Ray Spectroscopy in Astrophysics, NASA Technical Memorandum No. 79619, (1978).

20. F. A. Aharonian, A. M. Aloyan and R. A. Sunyaev, Yerevan Physics Institute preprint 432(39)-80, (1980).

21. R. Ramaty and P. Mészáros, Ap. J., in press, (1981).

22. J. K. Daugherty and R. W. Bussard, Ap. J., $\underline{238}$, 296, (1980).

23. R. Ramaty, S. Bonazzola, T. L. Cline, D. Kazanas, P. Mészáros and R. E. Lingenfelter, Nature $\underline{287}$, 122, (1980).

24. R. Ramaty, R. E. Lingenfelter, R. W. Bussard, Astrophys. Space Sci., $\underline{75}$, 193, (1981).

25. W. K. H. Schmidt, Nature $\underline{271}$, 525, (1978).

26. J. I. Katz, preprint, (1981).

27. R. Ramaty, B. Kozlovsky and R. E. Lingenfelter, Ap. J., (Supplement Series), (1979).

SEARCH FOR TIME VARIATIONS IN 511 KeV FLUX BY ISEE-3 GAMMA-RAY SPECTROMETER

Jay P. Norris
University of Maryland, College Park, MD 20742

Thomas L. Cline and Bonnard J. Teegarden
NASA/Goddard Space Flight Center, Greenbelt, MD 20771

ABSTRACT

The ISEE-3 gamma-ray spectrometer has provided nearly continuous monitoring of the cosmic gamma-ray background in the energy regime 125 keV to 6.5 MeV since launch of the satellite in August 1978. The data has been analyzed for possible variations in the cosmic 511 keV line flux. The detector is an unshielded, radiatively-cooled, high-purity germanium crystal with a sensitive volume 33 cm^3. At energies > 100 keV the detector has a field-of-view of > 2π steradians which includes the galactic center. The detector resolution was degraded continuously by exposure to high-energy charged particles in the interplanetary space environment; consequently, only the first 500 day sample of data is usable. Proton and electron flux rates available from a cosmic-ray experiment aboard ISEE-3 were used to eliminate all periods during which solar energetic particles contributed significantly to our counting rate. We are able to place upper limits on the variability of the cosmic 511 keV flux of < 2.2 x 10^{-2} and < 1.3 x 10^{-2} photons cm^{-2} s^{-1} for $\approx$ 20 day and $\approx$ 60 day integrations, respectively, for the period October 1978 to February 1980. Comparison is made with the HEAO-3 511 keV observations of the galactic center.

INTRODUCTION

During the past decade several observations of the galactic center region have produced positive detections of emission in the vicinity of the 511 keV annihilation line [1, 2, 3, 4, 5, 6, 7]. The observed fluxes range from 0.8 x 10^{-3} up to 4.2 x 10^{-3} photons cm^{-2} s^{-1}. The first observations from a satellite-borne experiment appear to support the interpretation that the emission may originate from a time-varying "point" source. Since the available data have been sporadic, it would be desirable to have a continuous record of observations over an extended period. We report here upper limits to the variation of galactic 511 keV flux as observed by the ISEE-3 gamma-ray spectrometer for 500 days of nearly continuous observation.

INSTRUMENTATION

The ISEE-3 (Third International Sun-Earth Explorer) spacecraft is in a halo orbit about the Lagrangian point on the earth-sun line

230 earth radii (4.5 light-seconds) inward towards the sun. This location is particularly advantageous; the time-varying exposure to trapped radiation within the magnetosphere and the earth-albedo problem are completely avoided.

The spectrometer is approximately aligned with the spacecraft spin axis, that is, normal to the ecliptic plane. The instrument is recessed within the lower body of the spacecraft, preventing direct sunlight from destroying the thermal performance of two nested radiatively-cooled stages. The detector is housed in the inner stage. The outer stage is conically shaped to define a 126° (thermal) field-of-view for the inner stage. This field-of-view does not contain the sun, earth, or any significant portion of the spacecraft[6].

The detector is an unshielded p-type co-axial high-purity germanium crystal, 4 cm diam. x 3 cm depth, with an active volume of 33 cm³. Pre-launch tests measured an energy resolution of 3-3.5 keV at 1 MeV. A higher temperature (130 K) than the predicted equilibrium temperature of 100 K for the crystal was reached when the spacecraft was placed in orbit. Consequently, the initial operating resolution of a calibration line at 570 keV from a [207]Bi source was ≈ 8 keV (FWHM).

OBSERVATIONS AND ANALYSIS

The experiment was intended to monitor the celestial sphere for gamma-ray bursts, providing information on any narrow spectral features within the energy range 125 keV to 6.5 MeV. In the absence of a burst trigger, a background mode operates, permitting spectral analysis of the diffuse gamma-ray background radiation. The background mode has functioned successfully since September 1978. Because of the extremely low bit rate allocated to this experiment, the instrument analyses only one photon of ≈ 550 detected in the background mode. Hence, in order to accumulate a sufficient number of counts to constitute an observation, the spectra must be accumulated for a minimum of several days.

Energy calibration was achieved by monitoring two background lines at 570 keV and 1064 keV. For the purpose of rebinning counts into fiducial channels, it was assumed that the gain was a linear function of energy. The positions and widths of the lines in accumulated spectra were fit both manually and by an automatic gaussian line fitting routine. The gain (channels/keV) decreased very nearly linearly by about 10% during the first 650 days of experiment operation. Also, significant deterioration of the energy resolution occurred: the 570 keV line broadened from the initial 8 keV FWHM to ≈ 50 keV in 600 days (Figure 1). After this period, the 511 keV and 570 keV lines began to overlap significantly. The relative magnitudes of the gain and resolution changes are consistent with a decreasing charge collection efficiency, evidently caused by detector radiation damage from high-energy charged particles and fast neutrons.

Time variation in the interplanetary charged particle flux due to solar modulation and other effects will produce variations in
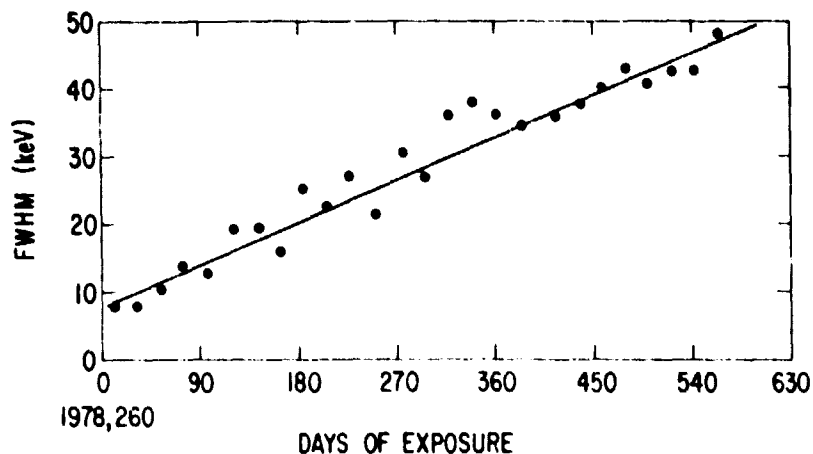
Fig. 1.- Resolution of 570 keV calibration line for 600 days from start of experiment.

the detector background that must be evaluated. Particle fluxes for several different proton energy ranges and for electrons were independently recorded by a cosmic-ray experiment aboard ISEE-3 and these data were kindly made available to us [9]. Those particles (energies $\simeq$ 14 MeV to 18 MeV) which deposit energy in the detector within the PHA energy range originate primarily from solar flares. Therefore, to calculate the actual particle rate contribution, a canonical solar flare energetic particle spectrum proportional to $E^{-3.0}$ was assumed and the required rates extrapolated from the available data. Periods for which the calculated particle rate exceeded one-tenth of the random error for given spectral accumulation intervals were eliminated from the data base. From late 1978 to 1980 the sun was especially active. Consequently, the requirement for non-contaminated spectra resulted in eliminating up to 60% of the data.

Extraction of the astrophysical 511 keV flux from the "cleaned" data was complicated by two effects. First, a large fraction of the detected flux is instrumental in origin and its contribution is difficult to estimate. Furthermore, the capability to point the spectrometer does not exist; hence an on-source minus off-source type of observation cannot be conducted. At energies > 100 keV, the cooler stages and the spacecraft well into which the spectrometer is recessed are virtually transparent, affording the detector an effective field-of-view > 2π steradians. The galactic center region, from which a variable 511 keV flux may emanate, is constantly within the detector field-of-view. Assuming the galactic center is the most intense 511 keV source, for a galactic center observation it is sufficient to distinguish a variation in the total 511 keV flux. This subject will be addressed in the Discussion section of this paper. A second complication results

from the broadening instrumental resolution due to detector
exposure to particle radiation. Because of the low statistical
significance of the accumulated spectra, it was not acceptable to
employ a straightforward technique of fitting a gaussian line to
the 511 keV feature and subtracting a continuum. Instead, to
accumulate counts of ≈ 511 keV energy, an automatic "window"
spectra program was employed which appropriately gain-adjusted the
spectra and summed counts in four energy windows of widths 38, 50,
60, and 70 keV, centered at 511 keV. This treatment results in a
systematic decrease of counts with time in a given energy window
due to the broadening resolution. Therefore, a reduction technique
was employed for each accumulated 511 keV window spectrum in
which 1) an adjusted continuum computed from a window spectrum of
width 40 keV, centered at 450 keV, was subtracted from the line
plus continuum spectrum (the continuum above 511 keV was not used
due to the presense of the strong calibration line at 570 keV); 2)
a gaussian-shaped line which broadened with time commensurate with
the observed broadening of the calibration lines was assumed for
the 511 keV line, and normalized model curves were constructed
which accounted for the systematic loss of counts from the energy
windows; 3) the observed count rates and the models were
subtracted to yield relative 511 keV count rate variations as a
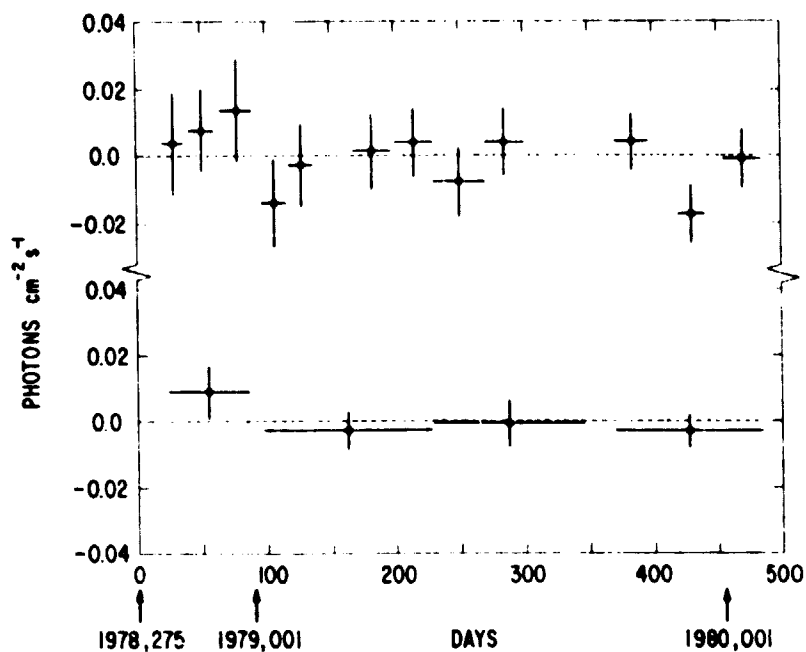function of time. The count rates were then converted to fluxes by

Fig. 2.- One sigma upper limits on variation of 511 keV flux. The
integration intervals (live times) are approximately 20 days (top)
and 60 days (bottom). The data are plotted with respect to the mean
values (dotted lines).

dividing by the effective area of the detector. The wider energy windows have an inherently poorer sensitivity due to the inclusion of more background counts. For the narrowest (38 keV) window, the sensitivity decreases more rapidly with time as the 511 keV line progressively broadens, leaving less counts within the static window. The sensitivity is effected more drastically by the use of wider energy windows. The resulting fluxes for the 38 keV window are shown in Figure 2 for $\simeq$ 20 day and $\simeq$ 60 day integrations (live times). The two sigma upper limits are 2.2×10^{-2} (20 day) and 1.3×10^{-2} (60 day) photons cm^{-2} s^{-1} on the 511 keV flux variation from $> 2\pi$ steradians for the period September 1978 to February 1980. During the same period, the (> 60 MeV) particle flux determined from the ISEE-3 cosmic-ray experiment was practically constant ($\pm < 4\%$) for the intervals of retained data. The instrumental background results primarily from illumination of the spacecraft and activation of the detector crystal by this radiation. The percentage particle flux variation for any given spectral accumulation interval accounts for a maximum of less than one-fourth of the quoted limits on the 511 keV flux variation. No correlation is apparent between the (> 60 MeV) particle rate and our final results.

DISCUSSION

The galactic center observations performed with the HEAO-3 gamma-ray spectrometer support the interpretation that a time-varying source of 511 keV emission lies near the galactic center[7]. Several balloon experiments[1,2,3,4,5,6] indicate that the source flux may range from 0.8×10^{-3} up to 4.2×10^{-3} photons cm^{-2} s^{-1}. The ISEE-3 upper limits for the 511 keV flux may be examined in two ways. First, since the spectrometer field-of-view includes more than half of the galactic plane, the $\simeq$ 20 day observations exclude transient galactic sources ($\tau \gtrsim$ one month) with fluxes $> 2.2 \times 10^{-2}$ photons cm^{-2} s^{-1} (95% confidence). If sources similar to the galactic center source were distributed uniformly thoughout the galaxy, a source within 2 – 3 kpc could have been detected by the ISEE-3 spectrometer. The lack of detection is evidence that the galactic center source is unique within our galaxy. Second, the $\simeq$ 125 day observations (60 day live time) constrain the peak galactic center source flux to $< 1.3 \times 10^{-2}$ photons cm^{-2} s^{-1} during a period of 500 days from October 1978 to February 1980.

REFERENCES

1. W. N. Johnson, III, F. R. Harnden, Jr., and R. C. Haymes, Ap. J. (Letters), 172, L1 (1972)

2. W. N. Johnson, III, and R. C. Haymes, Ap. J., 184, 103 (1973).

3. R. C. Haymes, G. D. Walraven, C. A. Meegan, R. D. Hall, F. T. Djuth, and D. H. Shelton, Ap. J., 201, 593 (1975).

4. M. Leventhal, C. J. MacCallum, and P. D. Stang, Ap. J. (Letters), 225, L11 (1978).

5. M. Leventhal, C. J. MacCallum, A. F. Huters, and P. D. Stang, Ap. J., 240, 338 (1980).

6. F. Albernhe, J. F. Leborgne, G. Vedrenne, D. Boclet, P. Durouchoux, and J. M. da Costa, Astron. Astrophys., 94, 214 (1981)

7. G. R. Riegler, J. C. Ling, W. A. Mahoney, W. A. Wheaton, J. B. Willett, A. S. Jacobson, and T. A. Prince, submitted to Ap. J. (Letters).

8. B. J. Teegarden, G. Porreca, D. Stilwell, U. D. Desai, T. L. Cline, and D. Hovestadt, Gamma Ray Spectroscopy in Astrophysics, NASA TM79619, eds. T. L. Cline and R. Ramaty, 516 (1978)

9. T. von Rosenvinge, personal communication

TIME VARIATIONS OF AN ABSORPTION FEATURE IN THE

SPECTRUM OF THE GAMMA-RAY BURST ON 1980 APRIL 19

B.R. Dennis, K.J. Frost, A.L. Kiplinger, L.E. Orwig
Laboratory for Astronomy and Solar Physics

U. Desai and T.L. Cline
Laboratory for High Energy Astrophysics
NASA/Goddard Space Flight Center, 20771

ABSTRACT

A short but intense γ-ray burst was observed on 1980 April 19 at $01^h \cdot 9^m 46^s$ with the Hard X-ray Burst Spectrometer on the Solar Maximum Mission. The event lasted for a total of 10 s and consisted basically of three 200 - 300 ms wide spikes with significant variability on a time scale of 20 - 40 ms. The photon number spectrum integrated over the impulsive part of the event fits a thermal bremsstrahlung function with a temperature of (330 ± 70) keV at energies from 151 to 487 keV. At lower energies the data points lie considerably below this function suggesting a broad absorption feature extending down to < 28 keV, the lowest energy measured. The upper energy of this absorption feature varies between 100 and 150 keV on a time scale of < 0.5 s. This event is interpreted as a typical gamma ray burst although it is still remotely possible that it is of solar origin. The spectral features and their variability are interpreted in terms of electron interactions at the cyclotron resonance frequency in magnetic fields of $10^{12} - 10^{13}$ gauss close to the surface of a neutron star.

INTRODUCTION

Absorption and emission features in the high energy X-ray spectra of compact astrophysical objects are believed to result from magnetic bremsstrahlung in intense fields of the order of $10^{12} - 10^{13}$ gauss. At these intense field strengths the plasma cyclotron frequencies are in the 10 to 100 keV energy range. Emission and absorption at such frequencies create spectral features that can be used to determine magnetic and plasma conditions in the vicinity of the compact object.

The first observation of such a feature was made by Trümper et al.[1] in the spectrum of Her X-1. This feature, now confirmed by Gruber et al.[2], can be interpreted either as a cyclotron emission line at ~ 58 keV or as an absorption dip at ~ 42 keV. Such emission and absorption features have also been detected in the spectra of some gamma-ray bursts by Mazets et al.[3,4] They observed absorption features extending below ~ 100 keV in the spectra of 20 out of ~ 150 gamma ray bursts detected on the Venera 11 and 12 space probes,

and they observed an emission feature at 45 keV in the spectrum of one burst. They obtained spectra every 4s throughout the events and in some bursts observed large variations in the observed features. Their observations of absorption and emission lines interpreted as cyclotron features provide the most convincing evidence to date that gamma ray bursts are produced by neutron stars.

In this letter we present high energy X-ray spectral data for a gamma-ray burst with over an order of magnitude finer time resolution than that obtained by Mazets et al.[3] The measured photon number spectrum can be interpreted as showing a broad absorption feature at energies below ~ 100 keV similar to the features reported by Mazets et al.[3,4] for other events. These observations support the idea that gamma-ray bursts are produced in the vicinity of neutron stars.

OBSERVATIONS

The gamma ray burst was detected on 1980 April 19 at 01^h 19^m 46^s with the Hard X-ray Burst Spectrometer (HXRBS) on the Solar Maximum Mission (SMM). The HXRBS is an actively shielded and collimated CsI(Na) scintillation spectrometer designed primarily to detect high energy X-rays from solar flares[5]. Although the instrument is pointed at the sun at all times, any off-axis source is detectable within a 40° FWHM circular field of view. Outside this field of view the central detector is shielded by a minimum of 1" of CsI(Na) operated in anti-coincidence.

The arrival direction of the burst was determined to be ~ 18° from the sun using the detection times at SMM, Vela 5 and Vela 6 in earth orbit, at ISEE-3 located 4.5 light seconds away in the solar direction, and at the Pioneer-Venus Orbiter[6]. There is still a remote possibility, however, that the source was of solar or near-solar origin. Nevertheless, it is clear that the source was well within the field of view of the HXRBS, and no significant spectral distortions should have occurred. We also know that, at the time of the event, the Earth was well out of the HXRBS field of view, the horizon being > 50° off axis. Thus, fluorescence from the earth's atmosphere could not have contributed to the source spectrum measured during the burst.

The time profiles of the event in several different energy bins covered by the HXRBS are shown in Figures 1 and 2. The event is typical of many gamma-ray bursts and consists basically of three sharp, 200 - 300 ms wide spikes separated by 500 - 600 ms. Significant variations in flux are evident on time scales as short as 20 - 40 ms. A gradual flux increase precedes the first spike by 1 to 2 s and a general decay is evident for several seconds after the third spike. The fluctuations in the decay phase of the event do not show significant power at any frequency from 0.5 to 10 Hz.

The time profiles in the different energy ranges plotted in Figure 2 show clearly that the spectrum changes significantly throughout the event. The first spike is barely visible above a general plateau at energies below 126 keV but it shows up clearly in the 126
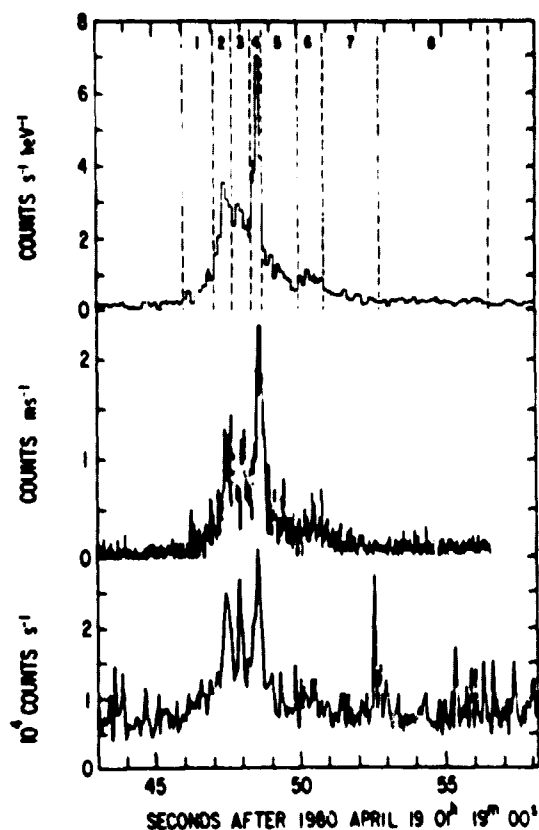
FIGURE 1 : Time profiles of the gamma-ray burst in different energy ranges and with different time resolutions. (a) Counting rate in the central detector for the energy range from 28 to 487 keV with a time resolution of 128 ms. The time intervals used for the energy spectra in Figures 3, 4 and 5 are indicated. (b) Counting rate in the central detector for the same energy range but with a time resolution of 20 ms. This data has not been corrected for instrument dead time, which changed from ~ 5% before and after the burst to ~ 15% at the time of the biggest spike in interval #4. (c) Counting rate in the CsI(Na) shield crystal for all energies $\gtrsim$ 200 keV with a time resolution of 64 ms. The spike at 01^h $19m$ $53s$ and all fluctuations below ~ 1200 counts s^{-1} are variations in the background rate.

to 151 keV and the 203 to 232 keV energy ranges and also in the shield data at $\gtrsim$200 keV shown in Figure 1. The second spike is clearly resolved only in the shield data. The third spike is also not well resolved at energies below 78 keV but shows up strongly at higher energies.

The photon number spectrum for the impulsive part of the event (intervals 2, 3 and 4 as indicated in Figure 1) is plotted in Figure 3. The spectral points were obtained iteratively by de-

PHOTONS cm^{-2} s^{-1} keV^{-1}

232-487 keV

203-232 keV

151-203 keV

126-151 keV

78-126 keV

28-78 keV
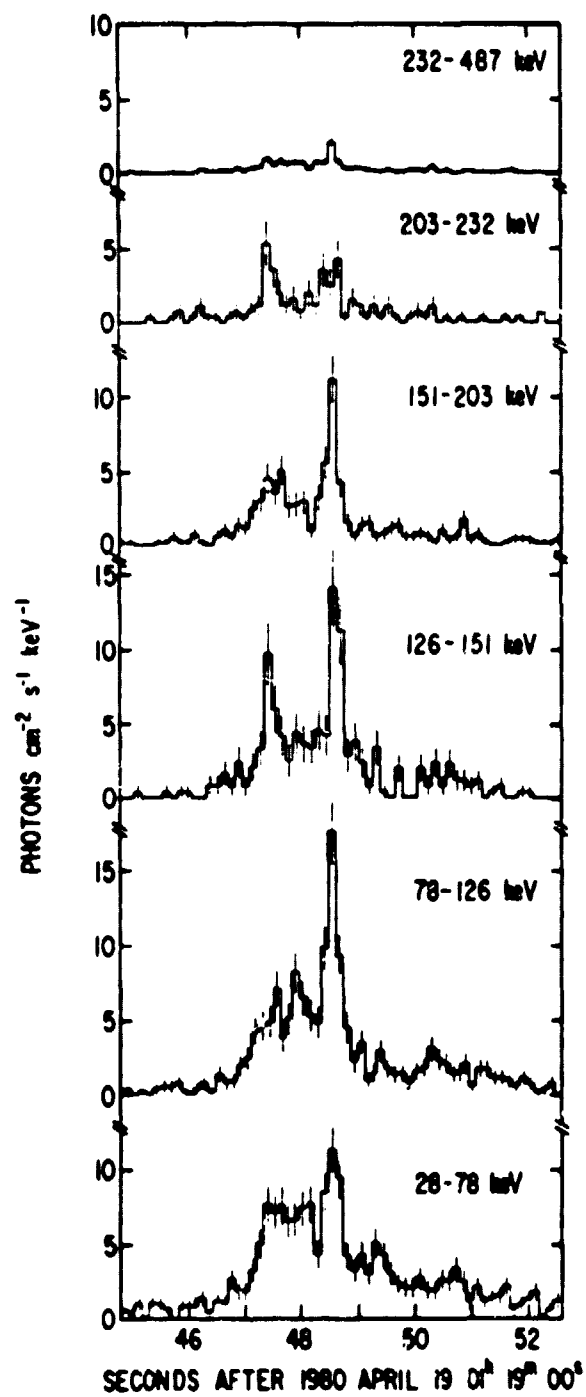
SECONDS AFTER 1980 APRIL 19 01^h 19^m 00^s

FIGURE 2 : Time profiles of the gamma-ray burst for the indicated energy ranges all with a time resolution of 128 ms.

convolving the observed 15-channel counting rate data through the instrument response matrix for an assumed incident spectrum equal to the least-squared fit exponential function indicated in Figure 3. The instrument response matrix was computed for different incident spectral shapes using the energy calibration determined for pre-launch data and in-orbit data from the the on-board Am^{241} source[5]. The computations take into account the detector efficiency and resolution, X-escape and Compton scattering using the results of pre-launch source calibrations and Monte Carlo simulations. To determine the accuracy of the calculations, comparisons were made of HXRBS spectra for several solar flares with spectra of the same flares obtained with the Gamma Ray Experiment (GRE) on SMM (Ryan, private communication), and with the hard X-ray detector on ISEE-3 (Kane, private communication). These comparisons suggest that systematic uncertainties are less than ± 30% for any of the 15 channels although all of the flare spectra are considerably steeper (E^{-4}) than the spectrum of the gamma ray burst. An additional systematic uncertainty arises from the probable 18° off axis position of the source. This results in a reduction in sensitive area by a factor of ~ 2 below the 68.6 cm^2 for an on-axis source, with the consequent increase in the calculated photon fluxes by the same factor. As indicated in Figure 3, an exponential spectrum of the form

photon flux = A exp(-E/E$_0$)
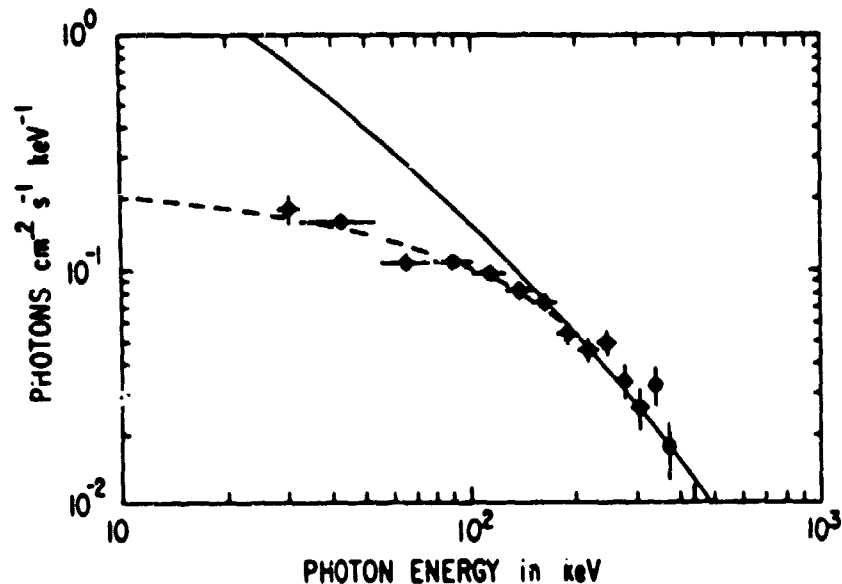
is an acceptable fit to all the data points. Here E is the photon

FIGURE 3 : Photon number spectrum for the intervals 2, 3 and 4 indicated in Figure 1 (impulsive part of the event). The error bars are ± 1σ based on the square-root of the observed number of counts in each energy interval. The solid curve represents the thermal bremsstrahlung function with kT = 330 keV, which gave the least-squares fit to the data points above 151 keV (channels 7-15). The broken curve represents the exponential function giving the best fit to all the data points.

energy and A and E_0 are free parameters determined in the fitting procedure. The value of E_0 obtained is 159 ± 8 keV and χ^2 is 13.5 for 13 degrees of freedom with the counting rate statistics alone used to weight the points. A double power-law function also fits the data equally well with a spectral index of -0.5 ± 0.1 at energies below 300 keV and -4.0 ± 1.0 at higher energies. The apparent dip in the spectrum in channel 3 is only significant at the 2.2σ level below the fitted exponential function. It may result from an error in the value used for the thickness of the dead layer on the CsI central crystal[7]. This dead layer, estimated to be 5 mils thick from measurements of the ratio of the 22 keV to the 88 keV photon fluxes from Cd^{109}, results in a dip in the count rate spectrum at energies above the K edges of cesium and iodine (33 and 36 keV respectively). Consequently, we would expect any inaccuracy in the assumed thickness of this dead layer to result in a dip in channel 2 although such a dip could appear in channel 3 if the incident spectrum had a steep low energy component. No such dip in channel 2 or 3 has been observed in any solar flare spectrum.

Following Mazets et al.[3] and Gilman et al.[8], we have also used the function expected for bremsstrahlung from an optically thin plasma at a temperature, T. This function is of the form

$$\text{photon flux} = B\, E^{-(1+\alpha)} \exp(-E/kT)$$

where k is Boltzman's constant, α results from the temperature-averaged Gaunt factor, and B and T are free parameters determined in the fitting procedure. The value of α changes from 0.48 to 0.148 as kT varies from 10 keV to 1 MeV [9], but for comparison with the results of Mazets et al.[3,4], we have taken α = 0 in all of our analysis. Using the correct value of α would increase the significance of the absorption feature and also increase the least-squares fit temperature. An acceptable fit of this thermal bremsstrahlung function to all 15 data points is not possible since it can never be flatter than $E^{-(1+\alpha)}$. However, an acceptable fit can be obtained to the data for channels 7 to 15 corresponding to the energy range from 151 to 487 keV and this is shown in Figure 3. The best fit value of kT is 330 ± 70 keV. At energies below 151 keV the data points lie considerably below the level of this function, at least a factor of 2 lower at 60 keV, suggesting a broad absorption feature extending down to < 28 keV, the lowest energy measured. For the purposes of investigating spectral changes with time, the event was divided into the eight contiguous intervals indicated in Figure 1. The spectral data shown in Figure 4 was obtained assuming the best-fit exponential spectrum to all the data points in each interval. The thermal bremsstrahlung function was then fitted to as many of the higher energy points as possible while maintaining an acceptable value of χ^2. The resulting curves are plotted in Figure 4.

The spectra for the eight intervals show a general softening with time. The temperature obtained from the fits changes from $\gtrsim$ 400 keV for interval #1 to 70 ± 20 keV for interval #8. The absorption feature appears in all intervals except #8 and possibly #5. In intervals 1, 2 and 4 the absorption feature extends from at least 150 keV down to < 28 keV, the lowest energy measured. In intervals 3, 6 and 7 the absorption appears to extend only to ~ 100 keV or less. The apparent emission features at 330 keV in interval #2 and 260 keV in interval #3 are only significant at the ~ 2σ level and, in any case, they are narrower than the instrument could allow. The spectrum for interval #7 can be interpreted as containing an emission feature at 100 keV with a high temperature continuum. The lower temperature fit (kT = 50 ± 20 keV) with absorption below ~ 100 keV as indicated in Figure 4 appears more likely, however, in view of the normal "cooling" observed by Mazets et al.[4] in many gamma ray bursts, and the low temperature continuum (kT = 70 ± 20 keV) measured in interval #8.
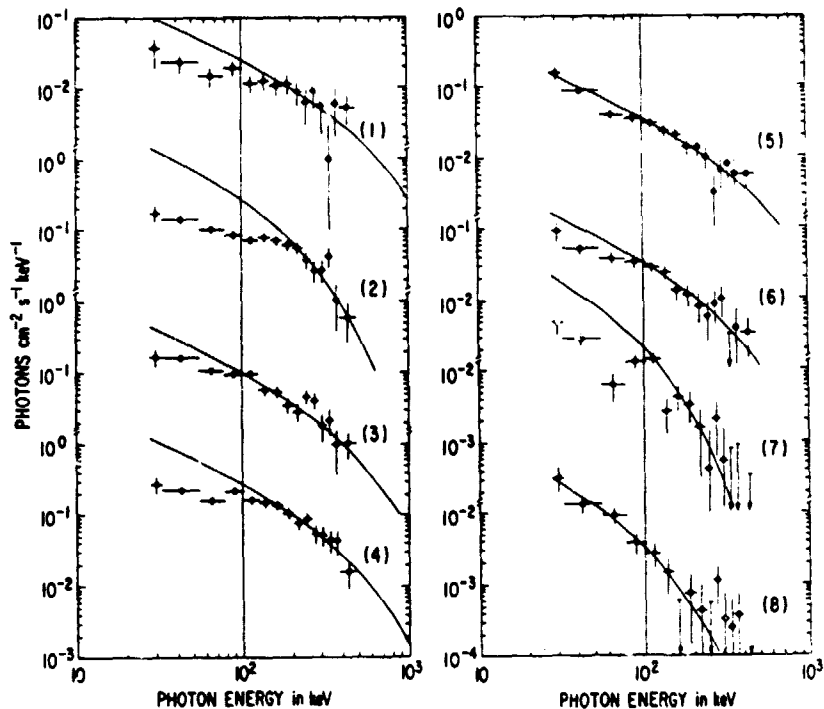
FIGURE 4: Same as Figure 3 but for the individual intervals 1-8 indicated in Figure 1. The curves represent the thermal bremsstrahlung function giving the least-squares fit to as many of the higher energy data points as possible while still obtaining an acceptable value of χ^2. The values of kT in keV for the indicated curves are 406, 229, 510 and 302 for intervals 1, 2, 3 and 4, and 375, 229, 52, and 73 for intervals 5, 6, 7, and 8 respectively.

DISCUSSION

It is now almost certain that the April 19 burst was of nonsolar origin. The timing information from five separate spacecraft gives an error box ∼ 18° from the sun. The rapid flux variations, the short duration of the event, and its extremely hard spectrum are all typical of gamma ray bursts. Furthermore, the sun was very quiet at this time with no reported Hα flares. A small soft X-ray event was in progress at the C2 level as observed by the GOES 2 and GOES 3 satellites (Donnelly, private communication), and a small GRF

radio burst was observed at 3750 MHz from NOAA region #2396 near the east limb at the same time (Enome, private communication). The SMM pointed instruments were observing region #2389 near the west limb and saw nothing. A coronal transient was observed off the N.W. limb by the SMM Coronagraph/Polarimeter in this time frame (Sawyer, private communication) but was probably not connected with the X-ray event. Thus, it is clear that, if the hard X-ray event was of solar or near-solar origin, it would constitute a new type of event never previously detected. Consequently, we prefer to assume that the event is a gamma ray burst and will interpret the data on that basis.

The photon number spectrum obtained for this event cannot be interpreted unambiguously. Observations of gamma rays to energies in excess of 5 MeV in this event[10] show that the simple exponential fit to the HXRBS data alone is probably not correct at higher energies. A two-power-law fit could, however, represent the data. It is unclear at present if the thermal bremsstrahlung function could also fit all the high energy data above ~ 150 keV. In any case, there are many difficulties associated with the assumption that the emission is thermal bremsstrahlung from an optically thin hot plasma[4]. Radiation other than from free-free electron transitions would predominate from the expected nonequilibrium, relativistic and strongly magnetized plasma near the surface of a neutron star. Also, this plasma, while optically thin for free-free transitions, would be optically thick for Compton scattering with consequent strong modification of the spectrum. Nevertheless, the thermal bremsstrahlung function does provide an accurate fit to the spectra of most events detected by Mazets et al.[3,4] in the energy range from 30 keV to 2 MeV and to the spectrum of the one event detected by Gilman et al.[8] from 2 keV to 2 MeV. Thus, this functional form can be considered as representing the source emission, whatever its origin. The deviations from this spectral form observed at low energies in some bursts are then naturally interpreted as resulting from absorption of this source radiation.

The observed absorption feature in the X-ray spectrum and its variation with time strongly support the model of a neutron star as the source of the gamma ray burst. The time variations in the total flux on a scale as short as 20 to 40 ms indicate that the source size is < 10^9 cm. If the burst results from accretion onto a neutron star, then the bulk of the radiation probably originates at or near the magnetic poles, relatively close to the surface. The observations show that the equivalent temperature of the source is of the order of 300 keV. As suggested by Mazets et al[3,4], the flattening of the spectrum at energies below ~ 100 keV may be produced by absorption at the cyclotron frequency by a cooler plasma overlying the source in the presence of a strong magnetic field. The fact that the absorption extends over a broad energy range down to at least 28 keV indicates that the magnetic field strength within the absorbing region must range from <2 x 10^{12} gauss to ~ 10^{13} gauss. The increase in the energy of the upper edge of the absorption feature in intervals 1, 2 and 4 to ≈ 150 keV presumably is a cons-

equence of higher field strengths in the absorbing region suggesting that the source of emission at these times is closer to the surface of the neutron star.

The possibility of an emission feature appearing in interval 7 could indicate that, at this time, the source of emission had moved to a greater altitude above the neutron star, similar to the altitude of the previous absorption. The absence of any spectral feature in the spectrum for interval 8 may result from equal line emission and absorption. Alternatively, the emission region may by this time have moved to an even greater altitude with much lower magnetic fields. Detailed modeling is clearly required before any further understanding of these data can be achieved.

It is interesting to note that two similar though weaker events were detected within two days of the April 19 event. One was detected two days earlier on 1980 April 17 at 1210 UT with the X-ray detector on ISEE-3 and the other two days later on 1980 April 21 at 0308 UT with the HXRBS and the GRE on SMM[10]. The time profiles of all three events show three sharp spikes, and the energy spectra of the April 19 and 21 events are very similar. Unfortunately, neither event has been reported from more than one spacecraft and hence source triangulations have not been possible. Nevertheless, these three events are strongly suggestive of a repetitive nature of the same source.

In conclusion, if we accept the non-solar origin of this event, we have confirmed the results of Mazets et al.[3,4] on the existence of an absorption feature at X-ray energies in the spectrum of a gamma-ray burst. In addition, we have shown variability of the extent of the absorption feature on a time scale of 0.5 s during the event and detected a possible emission feature at ~ 100 keV later in the event. These results combined with the emission line feature observed by Mazets et al.[3] at 45 keV in one burst are strongly suggestive of the quantization of electron energies in intense magnetic fields in the source region. If this interpretation is correct, then the source of most gamma-ray bursts must be in the vicinity of neutron stars within our galaxy. If this event is, however, of solar or near solar origin, then it is a most unusual event and would require reinterpretation on this basis.

REFERENCES

[1] Trumper, J., Pietsh, W., Reppin, C., Voges, W., Staubert, R., and Kendziorra, E., Ap. J.(Letters), 219, L105 (1978).

[2] Goodman, N.B., Spac. Sci. Instr., 2, 425 (1976).

[3] Mazets, E.P., Golenetskii, W.V., Aptekar, R.L., Gur'yan, Yu.A., and Il'inskii, V.N., 1981a, Nature, 290, 378 (1981).

[4] Mazets, E.P., Golenetskii, S.V., Ilinskii, V.N., Gur'yan, Yu.A., Aptekar, R.L., Panov, V.N., Sokolov, I.A., Sokolova, Z.Ya., and Kharitonova, T.V., preprint 719, A.F.IOFFE Physical-Technical Institute, Leningrad, submitted to Astrophysics and Sp. Sci. (1981).

[5] Orwig, L.E., Frost, K.J., and Dennis, B.R., Solar Physics, 65, 25 (1980).

[6] Fenimore, E.E., Laros, J.G., Klebsadal, R.W., Stockdale, R.E., and Lane, S.R., preprint, to be submitted to Ap. J. (1981).

[7] Gruber et al., Ap. J. (Letters), 240, L127 (1980).

[8] Gilman, D., Metzger, A.E., Parker, R.H., Evans, L.G., and Trombka, J.I., Ap. J., 236, 951 (1981).

[9] Matteson, J.L., Ph.D. thesis, University of California at San Diego (1972).

[10] Share, G.H., Strickman, M.S., Kinzer, R.L., Chupp, E.L., Forrest, D.J., Ryan, J.M., Reiger, E., Reppin, C. and Kanbach, G., preprint, to be published in the Late Volumes of the 17th International Cosmic Ray Conference, Paris, France (1981).

ON THE THEORY OF GAMMA RAY AMPLIFICATION
THROUGH STIMULATED ANNIHILATION RADIATION (GRASAR)

R. Ramaty, J. M. McKinley[*], and F. C. Jones
Laboratory for High Energy Astrophysics
NASA/Goddard Space Flight Center, Greenbelt, MD 20771

ABSTRACT

The theory of photon emission, absorption and scattering in a relativistic plasma of positrons, electrons and photons is studied. Expressions for the emissivities and absorption coefficients of pair annihilation, pair production and Compton scattering are given and evaluated numerically. The conditions for negative absorption are investigated. In a system of photons and e^+-e^- pairs, an emission line at ~ 0.43 MeV can be produced by grasar action provided that the pair chemical potential exceeds ~ 1 MeV. At a temperature of $\sim 10^9$K this requires a pair density $\gtrsim 10^{30}$ cm^{-3}, a value much larger than the thermodynamic equilibrium pair density at this temperature. This mechanism could account without a gravitational redshift for the observed lines at this energy from gamma ray bursts.

I. INTRODUCTION

The emission and absorption of photons in cosmic sources are governed by many processes. At temperatures of the order 10^9 to 10^{10}K, typical of gamma ray burst sources, two of the most important ones are pair production and annihilation ($e^+ + e^- \rightleftarrows \gamma + \gamma$) and Compton and inverse Compton scattering ($e + \gamma \rightleftarrows e' + \gamma'$). Arguments based on the observed photon intensities of gamma ray bursts and the likely distances and sizes of their sources, lead to the conclusion that the source regions of some of the bursts are optically thick.[1,2]

Photon absorption in $\gamma\gamma$ pair production has been discussed in the literature,[3] but no calculation has included the effects of the stimulation of annihilation or the suppression of pair production due to large photon or particle occupation numbers. When these stimulation and suppression effects are taken into account, the possibility exists for negative absorption.[4] The condition for this is a population inversion, which in the present context is a pair density that exceeds the thermodynamic equilibrium density.

A recent review of gamma ray burst observations has been given by Cline.[5] Of particular interest for the present paper is the existence of an emission line seen from several gamma ray bursts in the energy range from 0.4 to 0.46 MeV.[6-8] These lines are probably due to e^+-e^- annihilation radiation. If so, e^+-e^- pairs should be present in large numbers in the burst sources, and the sources should be sufficiently hot to produce the pairs, but the source regions should not be in equilibrium because no lines can then be

[*]Also at Oakland University, Rochester, MI 48063

seen. We aim the calculations of the present paper to astrophysical sites where such conditions might exist.

II. EMISSIVITIES AND ABSORPTION COEFFICIENTS IN A RELATIVISTIC PLASMA

We consider systems characterized by temperatures of the order of the electron rest mass energy in which photon-photon collisions can produce much larger pair densities than the ambient electron densities of the astrophysical sites of interest. We therefore consider only cases in which the electrons and positrons have equal densities. As convenient analytical expressions, which allow both equilibrium and non-equilibrium situations, we use Bose-Einstein distributions for the photons and Fermi-Dirac distributions for the pairs.[9]

We assume equal temperatures for the positrons and electrons, $T_+ = T_- = T_\pm$, but allow the photon temperature, T_γ, to differ from $T_\pm$. Since the e^+ and e^- densities are equal, $n_+ = n_- = n_\pm$, these particles must also have equal chemical potentials, $\mu_+ = \mu_- = \mu_\pm$. The photon chemical potential, μ_γ, is zero for a blackbody distribution. We allow non-blackbody photon distributions, but only zero or negative values may be assigned to μ_γ. The pair chemical potential can be positive, zero or negative. If $\mu_\pm = 0$ the pairs are in thermodynamic equilibrium with blackbody photons.

In terms of these temperatures and chemical potentials, the photon and pair densities can be written as[9]

$$n = (4\pi^3 \hbar^3)^{-1} \int d^3p \; \eta, \tag{1}$$

where $\vec{p}$ is the photon or particle momentum and η is the occupation number. These are given by

$$\eta_\gamma = \{\exp[(E_\gamma - \mu_\gamma)/kT_\gamma] - 1\}^{-1} \tag{2}$$

for the photons, and by

$$\eta_\pm = \{\exp[(E_\pm - \mu_\pm)/kT_\pm] + 1\}^{-1} \tag{3}$$

for the particles, where E_γ is the photon energy and $E_\pm$ is the particle total energy (kinetic plus rest mass).

We proceed to define the photon emissivity and absorption coefficient for pair production and annihilation. In particular, we are interested in obtaining a correct expression for stimulated annihilation which has not been taken into account in previous treatments of photon-photon absorption. Stimulated emission has, of course, been taken into account for other processes.[10] But we cannot use the standard expressions for emissitivies and absorption coefficients because pair production and annihilation do not fit the usual pattern in which photons are emitted or absorbed singly and the matter has the same form before and after events. We therefore proceed as follows:

The transition rate in vacuum in either direction between photon states in $d^3p_1 d^3p_2$ and pair states in $d^3p_+ d^3p_-$ can be written as

$$w = (4\pi^3 \hbar^3)^{-2} \, d^3p_1 d^3p_2 d^3p_+ d^3p_- \, \delta^4(p_1+p_2-p_+-p_-)X. \qquad (4)$$

Here $\vec{p}_1$ and $\vec{p}_2$ are photon momenta, $\vec{p}_+$ and $\vec{p}_-$ are momenta of the pair, p_1, p_2, p_+ and p_- are the corresponding 4-momenta, and X is proportional to the squared matrix element of the interaction, summed and averaged over spins and polarization.

To take into account the bath of photons and pairs, we must multiply equation (4) by an appropriate expression in the occupation numbers incorporating the equilibrium conditions $T_\pm = T_\gamma$ and $\mu_\pm = \mu_\gamma$. After doing so and integrating over all four momenta, we obtain

$$\frac{1}{2} \int \frac{n_+ d^3p_+}{4\pi^3\hbar^3} \int \frac{n_- d^3p_-}{4\pi^3\hbar^3} \int d\Omega_1 \, (1+n_1)(1+n_2)[Ic\frac{d\sigma}{d\Omega}]_{ann} = \qquad (5)$$

$$= \frac{1}{2} \int \frac{n_1 d^3p_1}{4\pi^3\hbar^3} \int \frac{n_2 d^3p_2}{4\pi^3\hbar^3} \int d\Omega_+ (1-n_+)(1-n_-)[Ic\frac{d\sigma}{d\Omega}]_{pp}.$$

The left-hand side of equation (5) is the total pair annihilation rate, while the right-hand side is the total pair production rate, both influenced by final state occupation numbers. The invariant product of the flux factor I and differential cross section $d\sigma/d\Omega$ is obtained[11] from X by integration over all final state variables except the angles of one particle:

$$[Ic\frac{d\sigma}{d\Omega}]_{ann} = \int p_1^2 dp_1 \int p_2^2 dp_2 \int d\Omega_2 \, \delta^4(p_1+p_2-p_+-p_-)X \qquad (6)$$

$$[Ic\frac{d\sigma}{d\Omega}]_{pp} = \int p_+^2 dp_+ \int p_-^2 dp_- \int d\Omega_- \, \delta^4(p_1+p_2-p_+-p_-)X. \qquad (7)$$

The factor $\frac{1}{2}$ in equation (5) is introduced so that each pair of photons in either initial or final state is included just once.

To define a photon emissivity and absorption coefficient it is necessary to investigate the balance of reactions involving photons in a chosen increment d^3p_1, rather than integrating over it. It is no longer possible to express the left side in terms of the annihilation cross section, because the necessary integration of equation (6) has not been performed. But we can interchange the order of integration and use equation (7) instead. The required balance is then given by

$$\frac{(1+n_1)d^3p_1}{4\pi^3\hbar^3} \int \frac{d^3p_2}{4\pi^3\hbar^3} \int d\Omega_+ n_+ n_- (1+n_2) \, [Ic\frac{d\sigma}{d\Omega}]_{pp} = \qquad (8)$$

$$= \frac{n_1 d^3p_1}{4\pi^3\hbar^3} \int \frac{d^3p_2}{4\pi^3\hbar^3} \int d\Omega_+ n_2(1-n_+)(1-n_-)[Ic\frac{d\sigma}{d\Omega}]_{pp}.$$

Collecting terms in n_1, we obtain

$$dE_1 d\Omega_1 j_{\gamma\gamma}(E_1) = \frac{cn_1 E_1^2 dE_1 d\Omega_1}{4\pi^3 (\hbar c)^3} K_{\gamma\gamma}(E_1), \tag{9}$$

where the rate of spontaneous emission, $j_{\gamma\gamma}(E_1)$, and coefficient of linear absorption, $K_{\gamma\gamma}(E_1)$, are given by

$$j_{\gamma\gamma}(E_1) = \frac{cE_1^2}{4\pi(\hbar c)^3} \int \frac{d^3 p_2}{4\pi^3 \hbar^3} \int d\Omega_+ n_+ n_- (1+\eta_2) [I \frac{d\sigma}{d\Omega}]_{pp} \tag{10}$$

and

$$K_{\gamma\gamma}(E_1) = \int \frac{d^3 p_2}{4\pi^3 \hbar^3} \int d\Omega_+ [\eta_2 (1-n_+)(1-n_-) - n_+ n_- (1+\eta_2)] [I \frac{d\sigma}{d\Omega}]_{pp} . \tag{11}$$

In equation (10) the annihilation emissivity is expressed in terms of the pair production cross section unlike the approach[12] using the annihilation cross section. In the expression for the absorption coefficient (equation 11), the first term in the brackets is due to absorption by the photon bath while the second term is the contribution of induced annihilation.

Equations (10) and (11) are valid also for nonequilibrium situations provided proper nonequilibrium occupation numbers are used. In terms of equations (2) and (3), the most general nonequilibrium distributions are obtained if $T_\gamma \neq T_\pm$ and $\mu_\gamma \neq \mu_\pm$

With such distributions, the total annihilation and pair production rates are not equal and, moreover, $K_{\gamma\gamma}$ can become negative. This will happen if an appropriate population inversion takes place. By substituting equations (2) and (3) into equation (12) we find that for $T_\pm = T_\gamma$ such an inversion occurs if $2\mu_\pm > \mu_\gamma$. In this

case $K_{\gamma\gamma}$ is negative for $E_1 < 2\mu_\pm - \mu_\gamma$

For the system to exhibit grasar action, however, it is necessary that the total absorption coefficient be negative. For the system of photons and pairs that we consider here, the only important process other than pair production and annihilation is Compton scattering. We ignore the weaker processes of bremsstrahlung and double Compton scattering. We note, however, that synchrotron radiation could potentially be very important, but because we are free to choose an arbitrarily low magnetic field intensity, we ignore synchrotron absorption in the present paper.

For Compton and inverse Compton scatterings $(\gamma_1 + e \rightleftharpoons \gamma_2 + e')$ we

proceed in essentially the same way as for pair production and annihilation. Using E_1 and E_2 for photon energies and $\vec{p}$ and $\vec{p}'$ for electron and positron momenta, we obtain the Compton emissivity and absorption coefficient in the presence of the bath of photons and pairs

$$j_C(E_1) = \frac{cE_1^2}{4\pi^3 (\hbar c)^3} 2 \int \frac{d^3 p}{4\pi^3 \hbar^3} \int d\Omega_2 n_2 n'_\pm (1-n_\pm) [I\frac{d\sigma}{d\Omega}]_C \tag{12}$$

and

$$\kappa_c(E_1) = 2\int\frac{d^3p}{4\pi^3\hbar^3}\int d\Omega_2 \, [n_\pm(1+n_2)(1-n'_\pm)-n_2 n'_\pm(1-n_\pm)] \, [I\frac{d\sigma}{d\Omega}]_c \quad . \quad (13)$$

where the factors of 2 take into account the contributions of both electrons and positrons. The Compton emissivity, equation (12), represents the scatterings of photons 2 into the element $dE_1 d\Omega_1$. For the absorption coefficient, equation (13), the first term in the brackets is due to scattering of photons out of $dE_1 d\Omega_1$, while the second term represents the stimulated scatterings of photons 2 into $dE_1 d\Omega_1$. $K(E_1)$ can become negative and a necessary condition for this is $T_\gamma > T_\pm$. In our subsequent analysis, however, we shall only consider systems with $T_\gamma = T_\pm$ for which κ_c is always positive.

For the numerical evaluations shown below we have used the expressions of Jauch and Rohrlich[11] for the flux factors and differential cross sections. We must also express all quantities in terms of independent variables of integration. The detailed expressions which we used will be published elsewhere.

III. NUMERICAL RESULTS

We have evaluated equations (10) through (13) for various choices of $T_\pm$, T_γ, $\mu_\pm$ and μ_γ. As already indicated, we limit our discussion here to cases with equal pair and photon temperatures, $T_\pm = T_\gamma \equiv T$. We allow, however, arbitrary values for $\mu_\pm$ and μ_γ.

We consider first the case of thermodynamic equilibrium, $\mu_\pm = \mu_\gamma = 0$. The emissivities and absorption coefficients for this
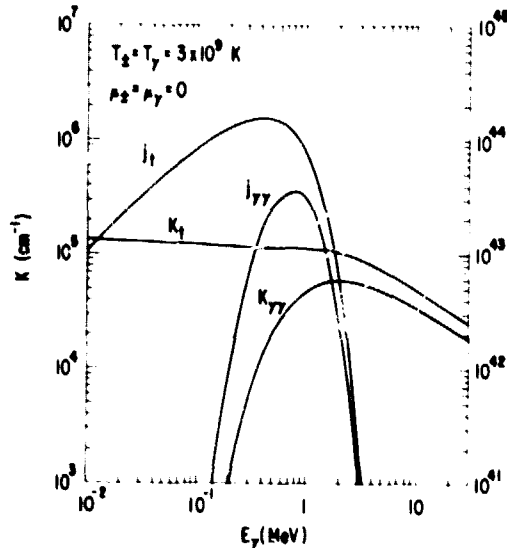

Fig. 1. Emmissivities and absorption coefficients vs. photon energy in a system in thermodynamic equilibrium at 3×10^9K. The Compton emissivity (not shown) is the difference between the total emissivity j_t and the annihilation emissivity $j_{\gamma\gamma}$. The Compton absorption coefficient (not shown) is the difference between the total absorption coefficient κ_t and the pair production-absorption coefficient $\kappa_{\gamma\gamma}$. The photon and pair densities in these conditions are 5.5×10^{29}cm^{-3} and 2.4×10^{29}cm^{-3}, respectively.

case and T = 3×10^9K are shown in Figure 1. As can be seen, the absorption coefficients are positive at all photon energies. The peak of the annihilation emissivity $j_{\gamma\gamma}$ occurs at a higher energy than $mc^2 = 0.511$ MeV, because the annihilation photons must carry away the kinetic energies of the pairs in addition to their rest 9

ass energy.[12-14]

We turn now to the study of cases with inverted populations, $2\mu_\pm > \mu_\gamma$. In this case, $K_{\gamma\gamma}$ is negative for $E_\gamma < 2\mu_\pm - \mu_\gamma$, but since $T_\pm = T_\gamma$, K_C is positive for all E_γ. Grasar action can occur only if $K_t = K_{\gamma\gamma} + K_C < 0$. Since K_C is proportional to $n_\pm$ while the portion

of $K_{\gamma\gamma}$ due to stimulated annihilation varies as $n_\pm^2$, a sufficiently large density is needed for $-K_{\gamma\gamma}$ to exceed K_C. This implies a threshold for $\mu_\pm$ which is higher than the threshold required for just $K_{\gamma\gamma}$ to be negative.

To investigate this threshold we have evaluated $K_t = K_{\gamma\gamma} + K_C$ as a function of $\mu_\pm$ for given temperatures and μ_γ. We have carried out calculations in the temperature range $0 < T < 5 \times 10^9$ K, where the lower limit corresponds to fully degenerate electrons and positrons. We find that the threshold for maser action is close to $\mu_\pm = 1$ MeV and does not depend strongly on μ_γ and T. This corresponds to a pair density threshold of a few times 10^{30} cm^{-3}.

We show numerical results in Figure 2 for $T = 3 \times 10^9$ K, $\mu_\gamma = 0$ and $\mu_\pm = 1.1$ MeV. As can be seen, $K_{\gamma\gamma}$ is negative for $E_\gamma < 2\mu_\pm = $

2.2 MeV and positive at higher energies. K_C is positive at all energies. In the energy range from about 0.25 MeV to 0.7 MeV, $-K_{\gamma\gamma}$
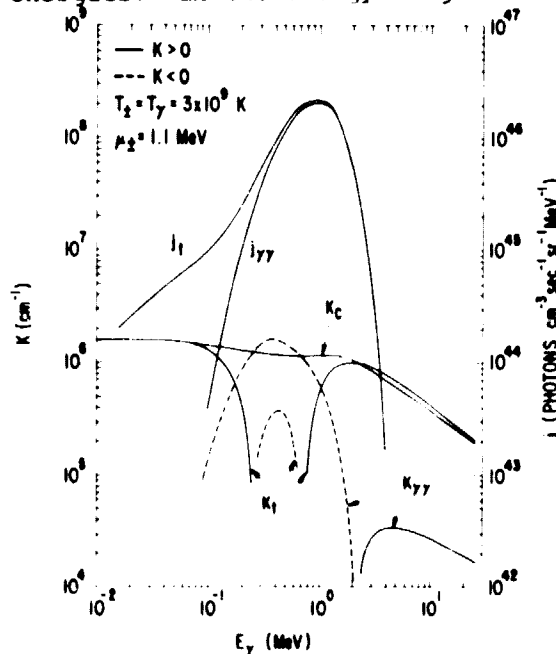

Fig. 2. Emissivities and absorption coefficients vs. photon energy in a system at 3×10^9 K with blackbody photons and an inverted pair population described by pair chemical potential 1.1 MeV. The curves have the same significance as in Fig. 1 except that the Compton absorption coefficient K_C is shown explicitly. Negative values of total and pair production absorption coefficients are represented by dashed curves. The photon and pair densities in these conditions are 5.5×10^{29} cm^{-3} and 7.3×10^{30} cm^{-3}, respectively.

exceeds K_C and hence K_t is negative. If the source is optically thick and K_t is negative over a sufficiently large spatial region, then the radiation intensity has a sharp peak at a photon energy at which $-K_t$ is maximal. The value of this energy, ~ 0.43 MeV from the numerical calculations, is determined primarily from the energy at which $-K_{\gamma\gamma}$ is maximum, shifted somewhat according to the slope of K_C at that energy. From Equation (11) we can also express $K_{\gamma\gamma}$ in the form

$$K_{\gamma\gamma}(E_\gamma) = -\frac{4\pi^3(\hbar c)^3}{cE_\gamma^2} \, j_{\gamma\gamma}(E_\gamma) + \int \frac{d^3p_2}{4\pi^3\hbar^3} \int d\Omega_+ n_2(1-n_+)(1-n_-)[I\frac{d\sigma}{d\Omega}]_{pp} \quad . \quad (14)$$

Above the grasar action threshold, the first term, due to stimulated emission, is much larger in magnitude than the second term which is due to absorption. As discussed above, $j_{\gamma\gamma}(E_\gamma)$ is broadly peaked at an energy greater than mc^2, reflecting the kinetic energy of the annihilating pairs. The division by E_γ^2 (from the factor of density of states) shifts the peak to an energy somewhat less than mc^2.

From the numerical calculations for other values of T and $\mu_\pm$ ($0 < T < 5\times10^9$ K, $0.8 < \mu_\pm < 1.2$ MeV) we find that the peaks of both $-K_{\gamma\gamma}$ and $-K_t$ are in the energy range from about 0.40 to 0.50 MeV.

IV. ASTROPHYSICAL APPLICATIONS

The large photon densities expected[1,2] in gamma ray burst sources should lead to high pair production and Compton opacities. The observation[6-8] of emission lines in the energy range 0.4 to 0.46 MeV, believed to be due to e^+-e^- annihilation radiation, is evidence that e^+-e^- pairs do indeed play an important role in the physics of gamma ray bursts. But it is not immediately obvious how a relatively narrow emission line is produced in a hot and optically thick source region.

Ramaty et al.[15,16] have studied this problem for the transient of March 5, 1979[17-19] from which an emission line was observed[6] at ~ 0.43 MeV.

In their model, the line is formed in the   optical depth of the source region by the annihilation of e^+-e^- pairs that have been cooled by synchrotron radiation prior to their annihilation. The observed[6] upper limit on the width (FWHM $\lesssim$ 0.2 MeV), implies[12] a temperature less than 3×10^8 K. It also implies an upper limit on the density since even at zero temperature the line is broadened by the motions of the degenerate electrons and positrons. Using equation (10) we have evaluated the FWHM of the annihilation emissivity, $j_{\gamma\gamma}$, as a function of $\mu_\pm$ for $T_\pm = T_\gamma = 0$.

We find that if FWHM < 0.2 MeV, then $n_\pm \lesssim 7\times10^{28}$ cm^{-3}.

The density can be independently calculated[16] from the observed line fluence[6] ($\phi \approx 10$ photons cm^{-2}). Let $R/(n\pm)^2 = 7.5\times10^{-15}$

cm^{3}sec^{-1} be the annihilation rate coefficient[12] at 3×10^8 K, A the area of the emitting region, Δt the time interval in which the observed fluence is produced and d = 55kpc the distance to the March 5 source. If the line is formed in a layer of unit optical depth to Compton scattering, then

$$\phi \approx 2R \, K_C^{-1} \, A\Delta t \, (4\pi d^2)^{-1}. \quad (15)$$

Since R varies as $n_\pm^2$ and K_C^{-1} as $n_\pm^{-1}$, ϕ is proportional to $n_\pm$. With the above numerical values, K_C from Figure 1, and $n_\pm$ <

$7 \times 10^{28} \text{cm}^{-3}$, $A\Delta t$ should exceed $1.5 \times 10^9 \text{cm}^2 \text{sec}$. This condition is well satisfied if the annihilation line is produced over the entire surface of a neutron star, $A = 10^{13} \text{cm}^2$, and during the entire impulsive phase[18] of the March 5 event, $\Delta t = 0.15 \text{sec}$. But the model would face considerable difficulties if future measurements should indicate that the line is narrower than 0.2 MeV, or if $A\Delta t$ should turn out, for other reasons, to be smaller than $1.5 \times 10^9 \text{cm}^2 \text{sec}$.

The advantage of producing the annihilation line by grasar action is that a narrow line can form in a hot optically thick region. To illustrate this, we have evaluated the photon intensity perpendicular to a slab of thickness L in which the emissivity and absorption coefficient do not depend on position:

$$ I = (j_t/K_t)\{1 - \exp[-K_t L]\}. \tag{16} $$

Using the j_t's and K_t's of Figure 2, we show in Figure 3 the dependence of I on photon energy E_γ and slab thickness L. As can be seen, grasar action can indeed narrow the line in comparison to the thermal width[12] of ~ 0.8 MeV in an optically thin Maxwell-Boltzmann gas at 3×10^9K.
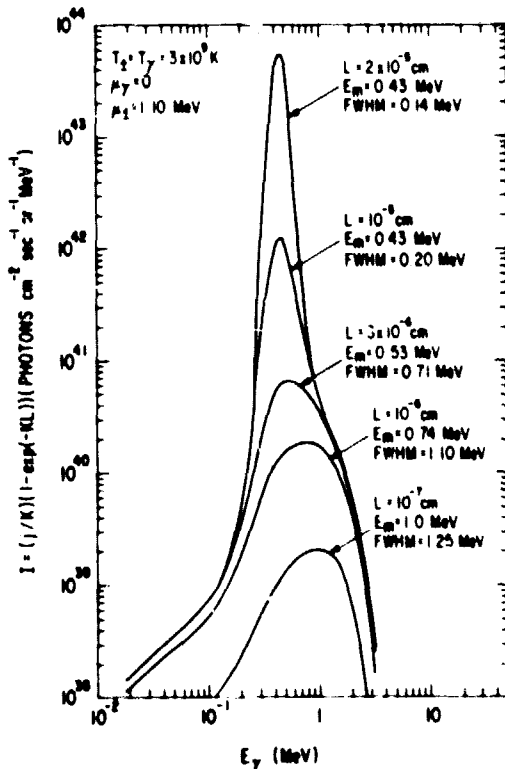
Fig. 3. The development of the annihilation line with increasing thickness of source. The system is the same as that for Fig. 2. The labels on successive maxima indicate the thickness involved, and the peak energy and FWHM of the line.

The peak energy of the annihilation line formed by grasar action, is close to the observed peak energies. Thus, the gravitational redshift of the line due to the compact object which presumably produces the burst should be quite low, $z < 0.1$. This implies that gamma ray burst sources with observed $e^+ - e^-$ emission lines could be objects other than neutron stars, or if they are neutron stars, these stars should have small masses.

Assuming that an inverted layer with parameters as in Figure 3 did exist in the March 5 burst source region, the line fluence φ is

$$\phi = A\Delta t d^{-2} \int I(E_\gamma) dE_\gamma \ . \tag{17}$$

Using the results of Figure 3 with L = 10^{-5}cm and φ = 10 photons cm^{-2}, equation (17) yields AΔt = 1.2 X 10^6 cm^{2}sec. By comparing with the minimum AΔt deduced above for radiation produced in the last optical depth (AΔt > 1.5 x 10^9 cm^2 sec), we see that not only can grasar action produce a narrow line in a hot region, but that the observed line intensity and width are consistent with a much smaller source and/or a much shorter line formation time than required for the optically thin case.

V. CONCLUSIONS

We have carried out a fully relativistic treatment of pair production and annihilation and Compton and inverse Compton scattering in a medium containing photons, positrons, and electrons, with equal e$^+$ and e$^-$ densities. In the calculation of the emissivities and absorption coefficients we have included the stimulation of transitions caused by the Bose-Einstein nature of the photons and the suppression of transitions due to electron and positron degeneracy. We have shown that for systems in thermodynamic equilibrium the calculations lead to an exact balance between pair production and pair annihilation. For systems not in equilibrium, grasar action is possible. We have evaluated, in particular, the absorption coefficient for equal photon and particle temperatures and positive particle chemical potential ($\mu_\pm$>0). For this example of population inversion, the total absorption coefficient can become negative due to the much larger probability for stimulated annihilation than for Compton scattering and pair production. Grasar action produces a narrow emission line peaked at an energy of about 0.43 MeV. This energy is lower than the peak of the spontaneous annihilation emissivity, which occurs at energies greater than 0.511 MeV. In a bath of blackbody photons (μ_γ = 0) and e$^+$-e$^-$ pairs at the photon temperature, the threshold for grasar action is at $\mu_\pm$ = 1 MeV corresponding to a pair densities of ~ 10^{30}

cm^{-3} for T = 10^9K. A temperature of ~ 5x10^9K is needed to produce this density in equilibrium with blackbody photons.

We have applied our results to gamma ray bursts, in particular to the March 5, 1979 transient from which an emission line at ~ 0.43 MeV was observed.[6] While this line could be produced in a cool skin layer,[15,16] grasar action has the advantage of being capable of producing a narrow line from a hot and optically thick source and from a source region of relatively small emitting area and short duration of line formation. But if grasar action is responsible for the observed 0.40 to 0.46 MeV emission lines of gamma ray bursts, then their sources cannot be a neutron stars of mass larger than about 0.6 M$_0$. At the surface of a larger mass neutron star, the

gravitational field would shift the line to an energy lower than observed.

There are several difficulties and shortcomings in our treatment. We have not shown how the inversion ($\mu_* > 0$) is produced. It could in principle result from the cooling of the pairs that is faster than their annihilation, or by a rapid external supply of pairs without heating. Cooling by synchrotron emission has already been proposed,[15,16] but for the high densities that we consider here, the required field ($B > 10^{12}$ gauss) seems to lead to synchrotron self-absorption that could quench the grasar action. We have ignored other effects of a strong magnetic field as well, by limiting our calculations to isotropic distributions and by using plane wave functions instead of Landau functions. This isotropic treatment also does not allow the study of beaming effects which should be present in a gamma ray maser. Finally, we have not made any attempts to study the spatial and temporal development of a system exhibiting grasar action. We expect this development to be highly nonlinear.

As already indicated, gamma ray burst sources are possible astrophysical sites where grasar action could occur. The most obvious observational test for this would be the observation of a narrow (FWHM << 0.1 MeV) emission line at ~ 0.43 MeV.

REFERENCES

1. G. Cavallo and M. J. Rees, MNRAS 183, 359 (1978).
2. W. K. H. Schmidt, Nature 271, 525 (1978).
3. R. J. Gould and G. P. Schreder, Phys. Rev. 155, 1404 (1967).
4. C. M. Varma, Nature 267, 686 (1977).
5. T. L. Cline, Proc. 10th Texas Symp. on Rel. Astrophys. (1981).
6. E. P. Mazets et al., Nature 282, 587 (1979).
7. B. J. Teegarden and T. L. Cline, Ap. J. 236, L67 (1980).
8. E. P. Mazets et al., Nature 290, 378 (1981).
9. L. D. Landau and E. M. Lifshitz, Statistical Physics (Addison-Wesley, Reading, MA 1958).
10. G. Bekefi, Radiation Processes in Plasmas (Wiley, NY 1966).
11. J. M. Jauch and F. Rohrlich, The Theory of Photons and Electrons (Addison-Wesley, Reading, MA 1955).
12. R. Ramaty and P. Mészáros, Ap. J. (in press) (1981).
13. A. A. Zdziarski, Acta Astron. (in press) (1981).
14. F. A. Aharonian, A. M. Atoyan and R. A. Sunyaev, Yerevan Physics Institute Preprint EFI 432(39)-80 (1980).
15. R. Ramaty et al., Nature 287, 122 (1980).
16. R. Ramaty, R. E. Lingenfelter, and R. W. Bussard, Astrophys. Space Sci. 75, 193 (1981).
17. S. Barat et al., Astron. and Astrophys. 79, L24 (1979).
18. T. L. Cline et al., Ap. J. 237, L1 (1980).
19. W. D. Evans et al., Ap. J. 237, L7 (1980).